universität wien

DISSERTATION

Titel der Dissertation

Regulation of Transposable Elements *via* Histone Modifications

angestrebter akademischer Grad

Doktor der Naturwissenschaften (Dr. rer. nat.)

Verfasser:	Mag. rer. nat. Reinhard Brunmeir
Matrikel-Nummer:	9603618
Dissertationsgebiet (lt. Studienblatt):	091 441 Genetik
Betreuerin / Betreuer:	Univ.-Prof. Dr. Seiser / Univ.-Prof. Dr. Baccarini

Wien, am 24. August 2008

DANKE

Diese Arbeit war nur möglich durch die Unterstützung anderer. Mein Dank gilt:

Christian Seiser, meinem Betreuer, der mich durch das Projekt geleitet hat.

Meinen Kollegen und Freunden im Labor: allen voran Lilli und Sabine! Ihr wart immer für mich da! Weiters Gordin, Reinsch, Stefan, Astrid, Jenny, Georg, Tom und Gerald. Es war eine Freude mit euch zu arbeiten.
Den Mitarbeitern und Kollegen am Institut für die Hilfsbereitschaft und das gute Arbeitsklima. Natürlich auch meinen Freunden außerhalb des Labors, die mich durch die vier Jahre begleitet haben.

Schlussendlich möchte ich auch meiner Familie danken, die immer ein Rückhalt für mich war: meinen Eltern, meinen Brüdern Didi und Dominik.

ZUSAMMENFASSUNG

Das Mausgenom besteht ungefähr zu 40% aus repetitiven Elementen (vor allem Transposons), die stillgelegt werden müssen, um die Integrität des Genoms aufrechterhalten zu können. Das wird durch verschiedene Mechanismen gewährleistet, wie zum Beispiel RNA Interferenz, Methylierung der DNA und Modulation der Chromatinstruktur.

Die Fragestellung dieser Arbeit war, aufzuklären, inwieweit die Struktur des Chromatins an diesem Prozess beteiligt ist; im Detail sollte untersucht werden, welche Rolle die Azetylierung von Histonen bei der transkriptionellen Kontrolle von Transposons spielt. Histonazetylierung ist normalerweise mit transkriptionell aktivem Chromatin assoziiert und wird durch zwei antagonistisch wirkender Enzymklassen reguliert: Histonazetyltransferasen, die Azetylreste an die Histone anfügen, und Histondeazetylasen (HDAC), die sie wieder wegnehmen. Im Rahmen dieser Arbeit verwendeten wir HDAC-Hemmer bzw. Zellen ohne funktionelles Gen für das Enzym Histondeazetylase 1, um Histonazetylierungsmuster in der Zelle zu verändern. Anschließend wurden die transkriptionelle Aktivität von Transposons, Histonmodifikationsmuster auf Gesamthistonextrakten und Transposon-assoziiertem Chromatin überprüft. Dabei stellten wir eine erhöhte Histonazetylierung von transkriptionell aktivierten Transposons fest. Interessanterweise konnten wir mit dem LTR Retrotransposon VL30 (Virus-like 30S element) ein Transposon identifizieren, das nach Hemmung von Histondeazetylasen ein starke Expression aufwies. Eine Analyse von VL30 Transkripten ergab, dass sich für die erhöhte Transkription eine spezifische Untergruppe der VL30 Elemente verantwortlich zeigte, die durch spezielle Merkmale in der regulatorischen Region gekennzeichnet war. Weiters wurde die transkriptionelle Aktivierung mithilfe von Stimuli (wie Serum oder Anisomycin), die zu einer Aktivierung von MAK Kinasen und zur Phosphorylierung von Histonen führen können, noch verstärkt. Tatsächlich konnten wir nach kombinatorischer Behandlung doppelt modifizierte (azetylierte und phosphorylierte) Histone Proteine am LTR von VL30 Elementen detektieren.

Es wird ein Modell vorgeschlagen, wonach bestimmte Histonmodifikationen kooperieren, um ein volle transkriptionelle Aktivierung von VL30 Retrotransposons zu erreichen.

ABSTRACT

A large portion of the mouse genome (~40%) consists of repetitive elements which have to be silenced in order to maintain the integrity of the genome. This task is accomplished by different mechanisms, including RNA interference, DNA methylation and the modulation of chromatin structure.

The aim of this work was to gain insight in how far the modulation of chromatin structure contributes to this process; in detail we wanted to clarify the role of histone acetylation in transcriptional control of transposable elements. Acetylation of histones is a post translational modification usually associated with open chromatin and transcriptionally active genes. It is regulated *via* the action of two antagonising enzyme families: histone acetyltransferases, which add acetyl-moieties to histone proteins and histone deacetylases (HDACs) which remove them. In the course of this work we took advantage of chemical inhibitors of HDACs and a cell system where a major histone deacetylase, HDAC1, was inactivated, to change histone acetylation patterns in the cell. Subsequently we analysed transcriptional activity of transposable elements, global histone modification patterns as well as histone acetylation of transposon-associated chromatin. We could detect increased histone acetylation levels of transcriptionally active transposable elements. Most interestingly we identified the LTR retrotransposon VL30 (Virus-like 30S element) to be highly inducible upon HDAC inhibition. Further analysis of VL30 transcripts revealed, that a distinct subgroup of VL30 elements, associated with a characteristic regulatory region, is mainly responsible for increased transcription. Moreover transcriptional activation was further increased by stimuli (such as serum and anisomycin) which lead to the activation of MAK kinase pathways and can cause phosphorylation of histones. Indeed we could detect double-modified (acetylated and phosphorylated) histone proteins at the LTR of VL30 elements upon combinatorial treatment with HDAC inhibitors and MAK kinase activators.

A model is proposed, where two histone modifications cooperate to gain full transcriptional activity of VL30 retrotransposons.

TABLE OF CONTENTS

1. Introduction

During the 19th century major advances in microscopy techniques permitted novel insights into the architecture of the cell. It led to the discovery and description of cellular organelles, including the nucleus and structures therein i.e. the chromosomes. After the rediscovery of G. Mendel's work on the laws of inheritance and T.H. Morgan's experiments with flies in the beginning of the 20th century, chromosomes were recognised as the carrier of genetic information. A few decades later O. Avery established DNA (and not proteins) as "transforming principle" in bacteria and in 1953 J. Watson and F. Crick were able to solve the structure of the double helix, positioning the DNA molecule in the centre of genetics. Together with the development of techniques allowing the manipulation of DNA such as the discovery of restriction enzymes by W. Arber or the sequencing of DNA by F. Sanger, these discoveries were the basis for decades of fruitful research culminating in the creation of transgenic organisms and the sequencing of complete genomes.

At the same time, it became clear that many biological phenomena cannot be fully understood and explained by the plain analysis of the DNA sequence. Phenotypic variation among genetically identical individuals and heritable changes without alterations in the DNA including phenomena such as genomic imprinting and paramutation required the development of novel concepts, summarised as "epigenetics".

Epigenetics postulates the existence of mechanisms that induce and maintain transgenerational changes (in gene expression) without affecting the DNA sequence, which is the primary carrier of genetic information. Only during the last years we learned what these mechanisms are and how they interact with each other to fulfil complex regulatory tasks. We begin to understand the impact of chromatin structure in the regulation and maintenance of gene expression patterns and how small RNA molecules contribute to epigenetic mechanisms.

1.1. Chromatin

The packaging of DNA with proteins into a higher order structure called chromatin is on the one hand a necessity to store almost two meters of linear DNA in an organelle of only 10µm diameter; on the other hand it is a means to organise the accessibility of DNA which is crucial for many biological processes such as replication, recombination, DNA repair and transcription.

The basic unit of chromatin is the nucleosome, which consisting of 146bp of DNA wrapped around a histone octamer core particle containing one H3-H4 tetramer and two H2A-H2B dimers. 10-60bp of linker DNA connect thousands of nucleosomes on a continuous DNA

molecule constituting the famous beads-on-a-string structure (Butler, 1980; Allen, 1981). Higher levels of compaction are achieved by the binding of the linker histone H1 leading to the formation of the so-called 30nm fibre (Ramakrishnan, 1997).
The core histone octamer builds a compact structure comprised of the C-terminal portions of the histone proteins, which are responsible for the assembly of nucleosomes by mediating histone-histone and histone-DNA interactions. In contrast, N-terminal tails of core histones are less structured protrude from the core and therefore can make secondary contacts with DNA, adjacent nucleosomes or proteins (Luger, 1997). They are also targets for a variety of site-specific posttranslational modifications, which will be discussed in detail the following sections.

1.2. Chromatin Remodelling

Compaction and close association with histone proteins conflict with many of the fundamental functions of DNA, where it has to be accessible as e.g. during recombination, transcription and replication. In the course of such processes nucleosomes have to be repositioned or even ejected in order to allow the binding of DNA binding factor, the recruitment of the transcription machinery or the passing of the replication machinery. Up to now we are aware of three distinct but interconnected mechanisms to control the accessibility of the DNA template. This task is mainly achieved by (1) the action of ATP-dependent chromatin remodelling complexes, (2) posttranslational modifications of histone tails and (3) incorporation of histone variants. (Winter, 2007).

1.2.1. Chromatin Remodelling Complexes

Due to the numerous histone-DNA contacts (14 hydrogen bonds and salt linkers) nucleosomes are very stable protein-DNA complexes. Therefore their displacement requires a net-energy input, which is supplied by ATP-hydrolysis. Together with histone chaperones and DNA-binding transcription factors, ATP-dependent chromatin remodelling complexes facilitate the displacement of nucleosomes either by “sliding” of the DNA (Becker, 2002) or by nucleosome transfer (Korber, 2004; Lorch, 1999). Up to now five different classes of multi-subunit ATP-dependent remodelling complexes have been identified, involved in distinct biological tasks. Specificity of the complexes is achieved *via* binding of sequence specific transcription factors as well as chromatin binding factors harbouring motifs, which favour the binding to chromatin associated with distinct protein modifications. Therefore it is not surprising that remodelling complexes act in concert with histone modifying complexes, like

histone acetyltransferase complexes (SAGA, NuA3, NuA4) or histone deacetylase complexes (Winter, 2007).

All known ATP-dependent chromatin remodelling enzymes belong to the helicase superfamily 2 (SF2). The identity of the catalytic ATPase subunit, together with the composition of associated proteins and functional aspects led to the establishment of the following families: (1) the SWI/SNF (switch 2/sucrose-non-fermenting) complexes, comprising the yeast SWI2/SNF2 and RSC (remodels the structure of chromatin), the *Drosophila* BAP and PBAP and the mammalian BRM and BRG1 complexes. (2) The ISWI (imitation switch) family complexes, which are smaller and have fewer subunits, consisting of the Drosophila ACF (ATP-utilising chromatin assembly and remodelling factor), NURF (nucleosome remodelling factor) and CHRAC (chromatin accessibility complex) complexes. (3) The Mi-2 or CHD family complexes combine remodelling and histone modification activities as they contain the ATPase CHD4 (also known as Mi-2) as well as the histone deacetylases HDAC1 and HDAC2. The mammalian NURD (nucleosome remodelling and deacetylase) complex represents the most prominent member of this family. (4 and 5) The SWR1 as well as the INO80 complex were initially characterised in yeast but recently mammalian orthologues have been identified which are associated with proteins also found in histone acetyltransferase (HAT) complexes.

Biological functions fulfilled by the different complexes include transcriptional activation, elongation, termination, repression, DNA repair, replication and chaperone activity (Winter, 2007).

1.3. Histone Modifications

As already mentioned above, the N-terminal tails of histone proteins protrude from the nucleosomal surface. They are subjected to numerous posttranslational modifications (PTMs) like lysine acetylation, serine and threonine phosphorylation, lysine and arginine methylation, lysine ubiquitination, lysine sumoylation, lysine biotinylation, glutamatic acid ADP-ribosylation and others. These modifications may directly influence chromatin structure by changing the electrostatic constitution of histone tails: lysine acetylation leads to the neutralisation of positive charges and therefore may loosen the interaction between histone tails and the negatively charged DNA; serine and threonine phosphorylation may result in decondensation of the chromatin fibre *via* addition of negative charges (Turner, 2000). Alternatively they may serve as recognition sites for binding factors able to modulate chromatin structure (e.g. *via* ATP-dependent chromatin remodelling).

Different modifications are thought to act in a combinatorial or sequential fashion on one or more histone tails to specify downstream functions, strongly interrelating different modifications with each other.
The modification patterns associated with defined regions exerting distinct biological functions can be interpreted as an additional layer of information on top of the genetic information stored within the DNA sequence. This idea was brought forward by the "epigenetic code" hypothesis (Strahl, 2000; Jeunuwein, 2001).

1.3.1. Histone Acetylation

Histone acetylation has already been described and linked to transcription in the 1960ies by V.G. Allfrey (Allfrey, 1964). However, only after the establishment of appropriate tools in the 1980ies – the creation of antibodies specifically recognising acetylated histones – and the identification of enzymes responsible for acetylation and deacetylation of histones in the 1990ies, major insights into the role of histone acetylation were rendered possible. The isolation of the first HAT (histone acetyltransferase) by J.E. Brownell (Brownell, 1996) and the first HDAC (histone deacetylase) by J. Taunton (Taunton, 1996) immediately re-linked histone acetylation to transcription since the isolated enzymes have already been described as transcriptional regulators.
Since then, countless reports clearly demonstrated that hyperacetylation of histones is associated with transcriptional competent chromatin, while hypoacetylation is associated with transcriptional repression.
On histone H3, acetylation sites include lysines 9, 14, 18 and 23 (Thorne, 1990), on histone H4, acetylation occurs on lysine residues 5, 8, 12 and 16 (Turner, 1993; Grunstein, 1997). Several reports suggest that various specific cellular processes are dependent on the acetylation state of distinct lysine residues. In yeast, acetylation of H3K14, H4K8 and H4K16 correlates with transcriptional activation whereas acetylation of H3K9, H4K5 and H4K12 plays a role in histone deposition (Allis, 1985; Sobel, 1995). In Drosophila, H4K5 and H4K8 acetylation is observed in euchromatic, H4K12 in heterochromatic regions. Acetylation of H4K16 is associated with different biological functions, depending on the organism: in yeast it is involved in the formation of boundary elements at telomeres preventing Sir2 spreading (Suka, 2002), in Drosophila it is important for dosage compensation (Akhtar, 2000) and in mammals it is has a function in normal transcriptional control (Lee, 2007).
Recently, reports based on high resolution mapping of histone modification patterns somehow challenge the aforementioned model, that distinct acetylation events are highly specific for certain biological functions, as they find many acetylation marks co-occurring and therefore emphasise the cooperativity and interdependency of acetylation events (Liu, 2005).

1.3.1.1. Histone Acetyltransferases

Histone acetyltransferases are grouped in two major families, the GNAT (GCN5-related N-acetyltransferase) and the MYST (MOZ, YBF2/SAS3, SAS2, Tip60) family. A common feature of all HATs is a highly conserved acetyl-CoA binding site and the fact that they are all part of large multiprotein complexes *in vivo* (Narlikar, 2002; Kimura, 2005; Lee, 2007)). Association with other proteins seems to be crucial for substrate specificity. That way distinct complexes with specificity for certain lysines/histones can fulfil different biological functions (see chapter above).

Data coming from *in vitro* studies, recently also from *in vivo* studies, report that there is a directionality in the acetylation process. For instance histone H4 is acetylated in the following C- to N-terminal order: H4K16 → H4K12 → H4K8 → H4K5 (Sarg, 2004; Jiang, 2007). However, both substrate specificity and the acetylation sequence are far from being completely understood and additional analyses are needed to dissect the exact modes of action as well as their biological functions.

Another important feature of many HATs is a protein domain, which is able to preferentially bind to chromatin carrying certain histone modifications. For instance HATs, but also the ATPase subunit of certain chromatin remodelling complexes can contain a bromodomain (binds preferentially to acetylated lysine residues), a chromodomain (recognising histones tri-methylated at lysine 4), WD40 repeats, PHD fingers (binding other methylated lysine residues) or tudordomains (recognising methylated lysine and arginine residues) (Winter, 2007). This links histone acetylation to several other histone modifications and sets the playground for a variety of cross-regulatory mechanisms.

1.3.1.2. Histone Deacetylases

Deacetylation of histone proteins is accomplished by members of two different enzyme families: (1) the NAD^+-dependent Sir2-like proteins (sirtuins) and (2) the Rpd3/Hda1-like lysine deacetylases. Ad (1) The founding member of this class of deacetylases is the yeast Sir2 (Silent information regulator protein 2) protein which is involved in the transcriptional silencing of several loci, including the mating type locus, telomeres and the rDNA locus. Sir2 activity is dependent on the ratio of NAD^+/NADH, therefore it is suggested that Sir2 might be a sensor of the cellular metabolic and energy rate. Strikingly it is involved in lifespan expansion upon caloric restriction in a wide range of organisms. In mammals seven Sir2 homologues (SIRT1-7) have been identified so far. The proteins display differential specificity toward acetylated substrates (including histones but also other proteins), diverse cellular locations, affect a broad range of cellular functions and appear to divide the functions

originally fulfilled by the common ancestor (Haigis, 2006; Inoue, 2007). Ad (2) The Rpd3/Hda1-like deacetylases utilise a zinc-catalysed mechanism (Finnin, 1999) to deacetylase histones and other proteins. Mammalian HDACs are grouped into 3 subfamilies according to their homology to yeast proteins: class I enzymes comprise HDAC1, 2, 3 and 8 and show homology to the yeast RPD3 (Reduced potassium dependency 3) protein. They are ubiquitously expressed, therefore thought to fulfil general cellular functions and are crucial for basic cellular processes such as transcription, replication and DNA repair. Its prime substrates seem to be histones; however they also can deacetylase other proteins as for example p53, E2F1 and YY1. HDAC1 and HDAC2 are close homologues originating from a gene duplication event in vertebrates. They share more than 80% sequence identity and are found in the multiprotein complexes SIN3, NuRD and CoREST. HDAC1 and HDAC2 have overlapping functions, but knock out studies revealed that they also have distinct and non-redundant biological functions (Lagger, 2002; Montgomery, 2007; Yang, 2008; Brunmeir, 2008). In a wide range of organisms HDAC1 and HDAC2 are important co-regulators of development, differentiation and cell cycle progression. In contrast to HDAC1 and HDAC2, which are located exclusively in the nucleus, HDAC3 has the ability to shuttle between nucleus and cytoplasm. HDAC3 is also found in multiprotein complexes where it delivers the enzymatic activity for the N-CoR / SMRT complex. It is involved in numerous biological processes including differentiation, cell cycle progression and DNA repair (Knutson, 2008; Bhaskara, 2008). HDAC8 is the evolutionary youngest member of the class I HDAC family. It is only found in vertebrates and its function is largely unknown. Class II HDACs are distinguished by a large C-terminal (yeast) or N-terminal (mammals) extension in addition to the deacetylase domain homologous to the corresponding domain of its yeast ancestor Hda1. The N-terminus of HDAC4, 5, 7 and 9 contains multiple MEF and 14-3-3 binding sites crucial for regulation of subcellular localisation and nucleo-cytoplasmic shuttling. Interestingly, enzymatic activity of HDAC4 and HDAC7 is dependent on the class I enzyme HDAC3, linking class I and class II HDAC function. Biological functions of HDAC4, 5, 7, and 9 include tightly regulated differentiation processes such as muscle differentiation and cardiac development. Another member of class II HDACs is HDAC6, which is unusual in its architecture as it carries two deacetylase domains. It is mainly localised in the cytoplasm and regulates multiple cytoplasmic processes such as cytoskeleton dynamics (*via* α-tubulin deacetylation), heat shock response (*via* HSP90 deacetylation) and ubiquitin-dependent pathways. The last member of class II HDACs, HDAC10 seems to be vertebrate specific; little is known about its function. Finally there is one more class of HDACs, class IV (class III is constituted by the sirtuins in this classification system), which consists of a single protein exhibiting equidistance to Rpd3 and Hda1: HDAC11. It is highly conserved, found from

bacteria to mammals and therefore thought to play a fundamental role in diverse organisms. However, little is known about its function so far (Yang, 2008).

1.3.2. Histone Phosphorylation

Phosphorylation of histones, especially on serine 10 and 28 of histone H3, plays an important role in two opposing biological processes. On the one hand, phosphorylation is crucial for chromosome condensation during mitosis (mitotic histone H3 phosphorylation), on the other hand it is involved in chromosome decondensation during transcriptional induction (stimulus-induced histone H3 phosphorylation). Thus, the same mark serves as a signal for antithetic functions. A functional discrimination is possible through the different contexts where the identical histone mark occurs and the action of different signalling cascades.

1.3.2.1. Mitotic Histone H3 Phosphorylation

During the entry into mitosis, chromatin becomes condensed and phosphorylated at serine 10 and 28 of histone H3. Histone phosphorylation starts at pericentric heterochromatin in early prophase and subsequently spreads throughout the whole chromosome, peaking at metaphase (Bradbury, 1992; Koshland, 1996; Goto, 1999). It is suggested, that phosphorylation is required for proper recruitment of the condensin complex and the mitotic spindle (Giet, 2001). The enzymes controlling reversible H3 phosphorylation are Ipl1/AIR-2 kinases (mammalian homologue: AuroraB) and type 1 phosphatases (PP1), respectively.

1.3.2.2. Stimulus-induced Histone H3 Phosphorylation

In contrast to mitotic phosphorylation, which occurs throughout the whole genome, serine 10 phosphorylation during interphase is associated with a minute fraction of the genome. It is restricted to a limited number of genomic loci including intergenic and genic regions (E. Simboeck, PhD thesis, 2008) and appears only transiently. Histone phosphorylation is the result of signalling cascades triggered by external or internal stimuli. It is conferred by signal transduction pathways, which involve phosphorylation cascades, perfectly suited to rapidly propagate and amplify signals. This ensures that the cell can quickly respond to changed conditions and adapt its gene expression patterns accordingly.
The best-studied example of genes regulated by histone phosphorylation is the so-called “nucleosomal response”, where immediate early (IE) genes such as c-fos and c-jun are transcriptionally activated upon mitogen treatment (Mahadevan, 1991). Recently also other genes have been found to be regulated by a mechanism involving phosphorylation of H3S10

(Hauser, 2002). A common feature for all genes identified so far is the phosphorylation of H3S10 *via* the Rsk2 (ribosomal S6-kinase) or the MSK1/2 (mitogen- and stress-activated protein kinase) effector kinase (Thomson, 1999). Rsk2 is activated by the ERK (extra-cellular signal-regulated kinase) MAP kinase signalling pathway which responds to growth signals such as EGF (epidermal growth factor), bFGF (basic fibroblast growth factor) and TPA (12-O-tetradecanoylphorbol 13-acetate). Activation of this pathway results in p42/p44 (ERK1/ERK2) signalling through Ras and Raf, usually linked to proliferation. In contrast, MSK1/2 can be activated through the p38 as well as the ERK signalling pathway (Soloaga, 2003). The p38 signalling pathway is a sensor of external and internal stress signals and is activated by toxins such as anisomycin or UV. Notably, another MAP kinase cascade, the JNK (c-Jun aminoterminal kinase) pathway is not involved in phosphorylation of chromatin, but histone acetylation (Cano, 1995). In addition to MAP kinase cascades, other pathways were also shown to induce H3 phosphorylation in mammals. Viral infection induces upregulation of the INFβ gene (Agalioti, 2002); cytokine induction leads to the activation of NFκB responsive genes (Yamamoto, 2003); both events are accompanied with serine 10 phosphorylation. Finally, induction of progesterone target genes requires MSK1 mediated histone H3 phosphorylation.

Up to now, it is not completely understood, how H3 phosphorylation affects gene expression. It could act similarly as histone acetylation, i.e. weaken the interaction between the N-terminal histone tails and the DNA backbone, thereby rendering the DNA more accessible for interacting factors. Moreover, phosphorylated histones could serve as recognition sites for factors activating transcription. *In vitro* experiments showed that the HAT Gcn5 exhibits a preference for histones phosphorylated at serine 10 (Cheung, 2000). More recently 14-3-3 proteins have been identified to specifically bind to histones modified in such a way (Macdonald, 2005) and influence the phosphorylation-dependent activation of target genes (Winter, 2008; Walter, 2008). Another interesting feature of phosphorylated histones is their special susceptibility for additional histone modifications. It was shown that especially the neighbouring lysines 9 and 14 are highly likely to become acetylated (Cheung, 2000; Clayton, 2000) leading to double modified (“phosphoacetylated”) histones. The “synergistic coupled phosphoacetylation” model considers phosphorylation as facilitator for sequential acetylation events. This is in opposition to another model, the “independent dynamic phosphoacetylation” model, which suggests an independent regulation of phosphorylation and acetylation. There are examples for genes regulated according to the predictions of both models; therefore it might be that different genes are regulated by distinct mechanisms, with the emergence of phosphoacetylation as a common feature.

1.3.3. Histone Methylation

Another histone modification extensively studied is histone methylation. It occurs at lysines, where carboxyl groups become methylated or at arginines where methyl groups are covalently bound to nitrogen atoms. This difference in the chemistry accounts for several distinctions in lysine and arginine methylation. Whereas lysines can be mono-, di- or tri-methylated, arginine is mono- or di-methylated (symmetrically or asymmetrically). Lysines are methylated by histone methyltransferases (HMTs), arginines by protein arginine methyltransferases (PRMTs) (Bannister, 2005).

Methylation of histones bears some specific features distinguishing this epigenetic mark from acetylation and phosphorylation: (1) methylation of histones does not influence the charge of lysine and arginine residues. Therefore it is unlikely that histone methylation does significantly affect the interaction between DNA and the histone protein and directly alter chromatin structure. It rather creates binding epitopes for regulatory proteins that specifically recognise the methylated histone tail by distinct binding domains such as chromo- and tudordomain (Fischle, 2003; Dormann, 2006). (2) Histone methylation is considered to be a rather stable mark. For a long time no lysine specific demethylases were known and lysine methylation was thought to be a real epigenetic mark responsible for the propagation of epigenetic information over generations. This view has been put into perspective by the recent identification of several demethylases (Shi, 2004; Trewick, 2005). However, compared to other posttranslational modifications (e.g. acetylation) the half-life of histone methylation is significantly longer (Fodor, 2006). (3) PRMTs and HMTs are strictly site specific and act on distinct arginine and lysine residues (see Table 1). (4) Several proteins can be necessary to act in a defined order to fully methylate lysine residues; e.g. Suvar3-9 proteins only convert di-methylated into tri-methylated lysine 9. The first two methyl-groups have to be delivered by other HMTs. (5) Methylation of distinct residues is clearly associated with distinct biological functions. The scope of the epigenetic information is further refined by the association of different biological functions with mono- di- or tri-methylated residues.

The biological processes, where histone methylation plays a role, range from transcriptional regulation to epigenetic silencing *via* heterochromatin assembly. Methylation of lysine 4 on histone H3 is correlated with transcription and strongly enriched at active promoters. Remarkably LSD1, an H3K4 specific demethylase is found in the HDAC containing CoREST complex (Lee, 2005) and HDAC inhibition not only leads to enhanced histone acetylation but also increased lysine 4 methylation (Lee, 2006; Jiang, 2007), functionally linking histone acetylation and lysine 4 methylation. Histone 3 lysine 9 methylation is linked with heterochromatin maintenance, especially H3K9met3, which is a hallmark of constitutive

Histone/residue	Methyltransferase	Demethylase	Function
H3 R2	CARM1 (Hs, Mm)		
		PADI4 (Hs)	
H3 K4	SET1 (Sc)		Activator
	SET7/9 (Hs)		Activator
	MLL (Hs)		Activator
	Smyd3 (Hs)		Repressor
	Ash1 (Dm)		Activator
		LSD1 (Hs)	Repressor
		JMJD2A	Repressor ??
H3 R8	PRMT5		Repressor
		PADI4 (Hs)	
H3 K9	SUV39h1 (Hs, Mm)		DNA methylation, Heterochromatin,
	SUV39h2 (Hs)		Repressor
	Clr4 (Sp)		DNA methylation, Heterochromatin
	Dim5 (Nc)		Heterochromatin, Repressor
	Kryptonite (At)		DNA methylation
	G9a (Hs, Mm)		DNA methylation
	Eu-HMTase1 (Hs)		Imprinting, Repressor
	ESET/SETDB1 (Hs, Mm)		Repressor
	E(z)/EZH2 (Hs, Dm)		DNA methylation, Repressor
	Ash1 (Dm)		Repressor
		LSD1 (Hs)	Activator
		JHDM2 (Hs)	Activator
		JMJD2A-D (Hs)	Activator
			Activator, Repressor
H3 R17	CARM1 (Hs, Mm)		Activator
		PADI4 (Hs)	
H3 R26	CARM1 (Hs, Mm)		
		PADI4 (Hs)	
H3 K27	E(z)/EZH2 (Hs, Dm)		Heterochromatin, Repressor
	Ezh2 (Mm)		X-Chromosome inactivation,
			Heterochromatin, Repressor
H3 K36	Set2 (Sc)		Activator
	NSD1 (Mm)		
		JHDM1 (Hs)	Repressor
		JMJD2A/C (Hs)	Activator, Repressor
H3 K79	Dot1/DOT1L (Sc, Hs)		Repressor, DNA damage, Activator
H4 R3	PRMT1		Activator
		PADI4 (Hs)	
H4 K20	SET9 (Sp)		DNA damage
	SET7/8 (Hs, Dm)		Repressor
	SUV4-20 (Hs)		Heterochromatin
	Ash1 (Dm)		Activator
	NSD1 (Mm)		
H1 K26	EZH2 (Hs)		

Table 1. Methylation sites and responsible enzymes (adapted from (Bannister and Kouzarides, 2005))
Hs – Homo sapiens, Mm – Mus musculus, Dm – Drosophila melanogaster, Sc – S. cerevisiae, Nc – Neurospora crassa; H3, H4, H1 – histones, K – lysine, R – arginine

heterochromatin (Peters, 2001). In contrast, mono- or di-methylated lysine 9 residues are found predominantly in euchromatic regions, where they serve as marks for transcriptional silenced genes. Lysine 27 methylation is a repressive mark associated with defined forms of facultative heterochromatin: it is highly enriched at the silenced X chromosome as well as genes targeted by the Polycomb silencing machinery (Rougeulle, 2004; Ringrose, 2004). Methylation at lysine 20 of histone H4 is another repressive mark (Schotta, 2004) and the tri-methylated species of histone H4 lysine K20 is associated with constitutive heterochromatin.

Interestingly, hyperacetylation of H4 is able to prevent efficient lysine 20 tri-methylation (Sarg, 2004), again linking two different epigenetic marks.

1.4. Transposable Elements

One of the most stunning features of genomes of higher eukaryotes is the fact that only a tiny fraction of the DNA sequence is containing coding information. In mammals about 3% of the genome encodes translated sequences, whereas the rest contains intronic, intergenic or interspersed repetitive sequences. The latter ones contribute about 46% of the human and 39% of the murine genome (Lander, 2001; Waterston, 2002). The bulk of interspersed repeats are remnants of once active transposable elements (TEs) having accumulated numerous sequence alterations.

Some time ago, TEs were considered as “junk DNA” without any benefit for the host; they were regarded as paradigmatic example for “selfish genes”, using the host as a parasite solely for the propagation of itself. Nowadays this one-sided view has been modified and the prevailing view is much more ambiguous since recent findings disclosed numerous instances where the host profits from the presence of TE or TE-derived sequences.

1.4.1. Dangers and Benefits

The dangers arising from the presence of TE are obvious: *via* transposition into genes or into the proximity of genes they can act as a mutagen. When inserted into exons, the reading frame might get interrupted leading to premature termination of the transcript. Insertion in intronic or neighbouring regions can cause incorrect splicing events resulting in termination of the transcript or in the creation of fusion transcripts. In some cases the regulatory cassettes of nearby TEs stimulate ectopic expression of genes. LINE elements have the ability to transduce 3’ genomic sequences, thereby bringing coding or regulatory sequences into novel genomic contexts resulting in changes in gene expression patterns or exon shuffling. Based on observations in human and mouse, there are estimations that 0.1% and 10-15%, respectively, of all spontaneous mutations are caused by such events (Maksakova, 2006). Another source of potential harm comes from an intrinsic feature of dispersed repeats: their repetitive nature makes them a susceptible target for homologous recombination events (Prak, 2000) causing deletions or inversions.

All those TE-induced changes may have fatal consequences for the affected individual, however from an evolutionary point of view, TE-mediated alterations are an important source of variation. Only a fraction of TE-induced changes causes phenotypic consequences, the majority is phenotypically neutral. Therefore it is not surprising that there is significant

variability between populations (Xing, 2007) and strains (Takabatake, 2008). Recently, Muotri and colleagues (Muotri, 2005) could show that during neuronal development LINE elements are actively transposing, leading to genetic variation between neurons within the brain of a single individual, possibly contributing to its uniqueness.

Differences in TE localisation patterns clearly can have consequences for the regulation of host genes. Peaston and colleagues identified numerous fusion-transcripts in the murine oocyte driven by TE-derived regulatory sequences and a recent publication demonstrated that strain specific TEs can be the source of strain specific fusion-transcripts (Peaston, 2004; Horie, 2008). This suggests that novel regulatory sequences – as delivered by TEs – are readily incorporated into the arsenal of the host to control endogenous genes.

Not only regulatory sequences are co-opted by the host: there are several examples of host genes descending from TEs now fulfilling essential functions (a process, called “molecular domestication”). For instance, the RAG proteins, similar to DNA transposons, mediate the site-directed DNA rearrangement of immunoglobulin gene segments (V(D)J recombination) and telomerase, the enzyme crucial for telomere length maintenance, might also originate from a TE (Eickbush, 1997; Miller, 1999).

In summary TEs are one of the driving forces of genome evolution; they shape the genome by introducing a range different alterations; from large genome rearrangements to subtle modulation of gene expression patterns.

1.4.2. Classification

Generally, TEs can be divided into two classes, with major differences in their mode of propagation: DNA transposons move as pieces of DNA, cutting and pasting themselves into new genomic locations. In contrast, the genomic expansion of retrotransposons occurs by a replicative mechanism, where a RNA transcript is reversely transcribed into DNA and integrates into a new genomic location (“copy and paste” mechanism) (Prak, 2000). In mammals no active DNA transposons have been identified so far; they are only present as remnants of once active elements, occupying 0.8% (mouse) or 3.0% (human) of the genome. The bulk of TEs comprise retrotransposons, covering 37.3% of the genome in mice and 43.1% in humans (Lander, 2001; Waterston, 2002). They are subdivided into 3 major classes: (1) long interspersed nucleotide elements (LINEs), (2) short interspersed nucleotide elements (SINEs) and long terminal repeat (LTR) elements. For the structure of TEs, please see Figure A.

(1) More than half a million LINE elements, covering roughly 20%, reside in the murine and human genome. Most of them are 5’ truncated or rearranged (Smit, 1999). Several thousands are full length (roughly 7kb), and of these an estimated 50 (human) or 3,000

(mouse) are active. In humans, LINE elements are the most active autonomous TEs in the present day genome. Several instances of LINE insertions causing diseases have been reported (Kazazian, 1998).

(2) SINEs are non-autonomous, non-coding transposable elements with the length of only a few hundred basepairs. They are derived from the 7SL RNA or tRNAs and represent the most abundant class of TEs. In humans, SINEs are represented by Alu elements (1.1 million copies, 13.6% of the genome), in mice by B1, B2, ID and B4 elements (1.4 million copies, 8.2% of the genome) (Waterston, 2002). As they do not contain an ORF, SINEs entirely depend on other mobile elements for their mobility. Transposition occurs by utilisation of the LINE L1 enzymatic machinery *in trans*.

(3) The third class of retrotransposons, LTR elements, is structurally similar to retroviruses. According to the current view, the earliest infectious retrovirus originated from endogenous retroviral-like (ERV) elements that acquired mechanisms for horizontal transfer. In turn, many current endogenous retroviral elements have probably arisen from infectious retroviruses which have lost their capability for horizontal transfer due to mutations in the env gene. Therefore, the classification into three sub-classes is based on their similarity to retroviruses. Interestingly, the different sub-classes show a markedly dissimilar evolutionary history in human and mouse. Whereas ERVs are nearly extinct in human, all three sub-classes have active members in the mouse (Waterston, 2002). Insertional mutagenesis caused by LTR element is responsible for ~10% of all spontaneous mutations in the mouse. Prominent members of the three subclasses in mice are VL30, MuRVY, MuRRS elements (Class I / MLV-like / typeC / gammaretroviruses), IAP, ETn, MusD elements (Class II / MMTV-like / typeB / betaretrovirus) and MERVL, MT, ORR1 elements (Class III). Altogether LTR elements occupy 9.9% and 8.6% of the genome in mouse and human, respectively, of which a considerable number is internally deleted.

1.4.3. Intracisternal A-type Particle

Intracisternal A-type Particle (IAP) retrotransposons are among the best-studied LTR retroelements in the mouse. The name comes from their ability to assemble virus like particles into the cisternae of the endoplasmatic reticulum, which can not leave the cell because the lack of a functional env protein. Recently, an infectious progenitor (IAP-E) with an intact env gene that can pass through a complete retroviral life cycle has been identified (Ribet, 2008). Whereas this extracellular variant is at the edge of extinction with only a single active copy left, the intracellular variant is highly active with around 300 functional and 700 non-functional copies. A full length IAP element is about 7.2kb in length, but several subfamilies exist which carry characteristic internal deletions exist. The most prominent

subfamily is the IAP IΔ1 with a 1.9kb deletion in the gag-pol region (Kuff, 1988). As already mentioned, IAP elements are highly active; they are responsible for numerous germ line as well as somatic mutations (Ishihara, 2004; Howard, 2008). Interestingly the IΔ1 subtype is the predominant variant expressed in myeloid leukaemia cells and IΔ1 elements are responsible for virtually all germ line mutations. Loss of silencing (see next chapter) also leads to preferential expression of this subtype. Recent models suggest a role for the truncated translation product in binding the IΔ1 RNA and recruiting the full length IAP protein for efficient transposition (Saito, 2008).

1.4.4. Virus-like 30S Elements

The Virus-like 30S (VL30) retrotransposon has been identified at the end of the 1970ies. During the propagation of MLV virus particles on mouse cells it was noticed that in addition to the 35-38S MLV RNA, virus particles contained a smaller RNA species sedimenting at around 30S. In subsequent studies this RNA was recognised as derived from genomic VL30 retrotransposons, packed into MLV particles for transmission into heterologous cells (French, 1997). Estimations of genomic copy numbers predict the existence of 150-200 VL30 elements, but so far no element with intact open reading frames has been reported. Therefore VL30 elements are regarded as non-autonomous retrotransposons relying on the enzymatic machinery of other elements for successful retrotransposition. An unusual feature of this class of LTR elements is that its transcription can be efficiently induced by a wide range of agents and stimuli, among them oncogenic (SV40, Ha-ras, N-ras, TPA), growth (FCS, EGF), hormone (progesterone, estradiol) stress (ionising radiation, ischemia, vanadium) and differentiation (retinoic acid) signals (French, 1997; Tzavaras, 2003; Nousopoulos, 2007). Furthermore the regulation seems to be cell line specific and also depend on the enhancer design of individual elements. So far four different subtypes of VL30 elements have been characterised with marked differences in the U3 region of the LTR, which seem to determine differential responsiveness to signals (Nilsson, 1994).

The physiological role of VL30s is largely unknown. Recent findings showed that their expression enhanced the metastatic potential of human melanoma cells (Song, 2002) and VL30 RNA formed a complex with PSF (Song, 2004), a class of repressor proteins, thereby de-repressing the expression of multiple oncogenic genes in human cells (Song, 2005). In mouse, cerebral ischemia induced neuronal expression of VL30 RNA bound to polyribosomes (Costain, 2006). Thus, VL30s seem to play an important regulatory role in reverse gene expression and translation (Nousopoulos, 2007).

1.4.5. Silencing of transposable elements

It has been a long-standing enigma what the mechanisms are that keep TEs in check. The way, how the host recognises TEs and how it mechanistically achieves comprehensive silencing of a multitude of TEs during different stages of development is only recently becoming clearer.

The initial observation that genomic DNA associated with TEs is heavily methylated was one of the most important findings, raising the idea that DNA methylation might restrict the activity of TEs. The use of inhibitors of DNA methylation (Jaenisch, 1985; Davis, 1989) and finally the genetic inactivation of DNA methyltransferases indeed demonstrated the crucial role of DNA methylation in TE silencing (Li, 1992; Walsh, 1998; Okano, 1999; Liang, 2002; Bourc'his, 2004; Gaudet, 2004). Also other proteins involved in the establishment, maintenance or the read-out of DNA methylation patterns have been identified to be involved in transcriptional repression of TEs (Yu, 2001; Huang, 2004; Sharif, 2007). The mode of action how DNA methylation represses TE expression seems to involve the binding of proteins recognising methylated DNA (MBDs, methyl binding domain proteins) and the subsequent recruitment of enzymes and complexes converting the associated chromatin into heterochromatin. Alternatively the DNA methyltransferases can directly interact with histone modifying enzymes. Deacetylation as well as methylation of histones *via* HDAC complexes and HMTs is thought to be essential for the process of heterochromatinisation; this is supported by the finding that loss of the lysine 9 specific HMT Suvar3(9) is sufficient to partly release TE repression in murine ES cells (Martens, 2005). Interestingly silencing *via* DNA methylation is not a strictly hierarchical process, starting with DNA methylation and followed by changes on the chromatin level; heterochromatinisation rather seems a self amplifying process, due to the numerous interactions and feedback loops between the different proteins involved. DNA methylation appears to be the top layer of a multilayered silencing process. In accordance to this, de novo silencing of retroviruses can also occur in the absence of de novo DNA methyltransferases (Pannell, 2000).

Loss of DNA methylation was demonstrated to be sufficient to release the repression of IAP elements in germ cells as well as in somatic cells and LINE elements in germ cells (Walsh, 1998; Bourc'his, 2004). However, reports about transcriptional reactivation of other TEs have been elusive so far. Therefore it is not clear to which degree other TEs can also be reactivated by the loss of DNA methylation. Relieving one layer of repression might not be sufficient to induce transcription. Furthermore many TE intrinsic promoters only act in a cell type or stage specific manner (Branciforte, 1994; Dupressoir, 1996; Seifarth, 2005).

Whereas the mechanisms necessary to repress TE expression – heterochromatinisation *via* DNA methylation, histone deacetylation and methylation – have been disclosed throughout

the last two decades, it has been unclear how silencing is specifically directed to TEs. Only recently, with the discovery of small interfering RNAs (siRNAs) and RNA interference (RNAi), this problem started getting solved; the observation that the introduction of double stranded RNA (dsRNA) leads to the silencing of homologous genomic sequences, sparked the idea that nucleic acid pathogens (viruses, viroids) and parasites (TEs) might distinguish themselves by producing dsRNA. The latter could be detected by a specialised machinery to trigger silencing. Although it turned out that different organisms have developed slightly varying pathways and the initial model has undergone some adaptations, the major concept proved to be correct: small RNAs trigger the silencing of TEs, either by cleavage of the transcript, translational inhibition or by transcriptional repression with the mechanisms described above.

The current model for RNAi dependent TE silencing in animals (Figure B) distinguishes between two pathways: the piRNA pathway (Girard, 2008), where 24-27 nucleotide long so-called piRNAs (because of their association with Piwi-like proteins) are processed from long RNA precursors transcribed from defined loci called piRNA clusters. These clusters are rich in TE-derived sequences, with a bias for TEs oriented in the antisense orientation. Thus, antisense piRNAs are loaded onto Piwi proteins, which target transposon transcripts. This complex can be either targeted to genomic transposons and trigger silencing *via* DNA methylation and histone modifications, or the transposon transcript is sliced by the PIWI protein initiating an amplification cycle (Figure B). The alternative pathway is the short interference RNA (siRNA) pathway (Birchler, 2008), where TE-derived dsRNAs are processed by a Dicer protein into 21-23 siRNAs and loaded into Argonaute proteins. The RNA directs the complex to transposon mRNA which is cleaved or targeted to genomic DNA where it initiates silencing. An amplification step as for the piRNA pathway has not been described in animals (although it exists in plants and yeast) (Figure B).

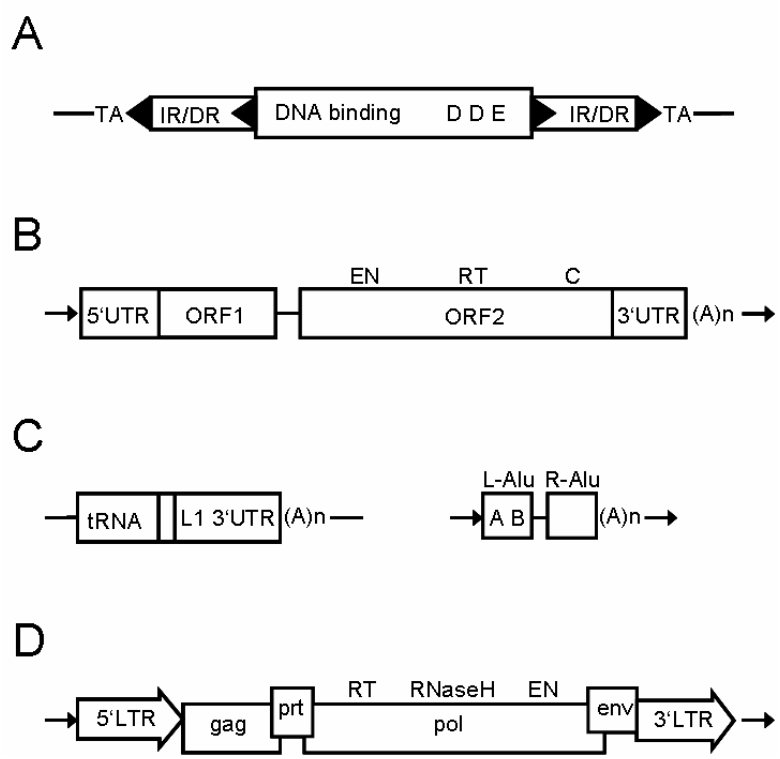

Figure A. Structures of transposable element types. (A) DNA transposons consist of a single ORF that encodes the transposase. The transposase has a DNA-binding domain and conserved DDE motif, the catalytic core, resembling a retroviral integrase. The ORF is flanked by inverted repeats (IR), sometimes also with direct repeats (DR). (B) Full length LINE elements consist of a 5' untranslated region (5'UTR) that has promoter activity; two open reading frames (ORF1 and ORF2) that are separated by an intergenic spacer; followed by a 3'UTR and a poly A tail ((A)n). ORF1 encodes a 40kDa protein that binds nucleic acids, whereas ORF2 contains reverse transcriptase (RT), an endonuclease domain (EN) and a cysteine-rich region. (C) SINEs derived from tRNAs (such as B2, B3, ID, B4) consist of a tRNA-related region (tRNA), a non-tRNA region (L1 3'UTR) often resembling the 3'UTR of LINE elements, and a poly A tail ((A)n). SINEs derived from 7SL RNA (such as Alu, B1) are 300bp intron-less sequences that consist of two GC-rich fragments, the left (L-Alu) and right (R-Alu) monomer, connected by an A-rich linker, and that end in a poly A tail ((A)n). Transcription is driven by an internal Pol III promoter. (D) Full length LTR retrotransposons consist of partly overlapping coding regions for group-specific antigen (gag), protease (prt), polymerase (pol) and envelope genes, flanked on both ends with long terminal repeats (LTRs) with promoter activity. The pol gene contains domains for reverse transcriptase (RT), RNaseH and endonuclease (EN). → … target site duplication. Adapted from Prak, 2000.

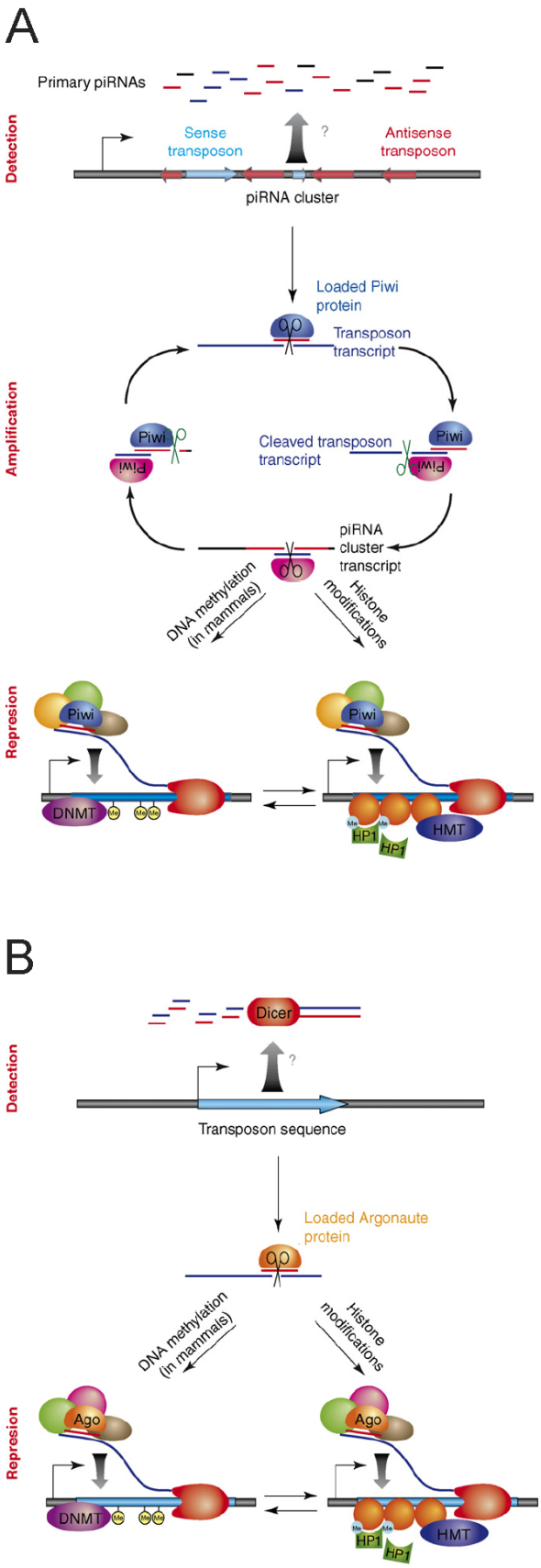

Figure B. RNAi mediated silencing of animal TEs. (A) The piRNA pathway in animals involves the generation of piRNAs from a piRNA cluster, association of the RNA with Piwi proteins and slicing of the transposon transcript. Alternatively genomic loci containing TEs are turned into heterochromatin. (B) The siRNA pathway in animals. Here, dsRNAs serve as substrate for Dicer which processes the dsRNA into short siRNAs. Subsequent loading of the antisense siRNA onto Argonaute proteins leads to cleavage of the transposon transcript or silencing of genomic TEs. Adapted from Girard, 2008.

2. Materials and Methods

2.1. Work with DNA

Plasmid DNA preparation from bacteria

Plasmid DNA from E.coli was prepared using the Wizard® Plus SV Minipreps DNA Purification System from *Promega* or the *QIAGAN*® Plasmid Midi Kit.

Isolation of genomic DNA eukaryotic cells

Genomic DNA from eukaryotic cells was isolated with the help of the PUREGENE® DNA Isolation Kit from *Gentra*™.

Agarose gel electrophoresis

50x TAE:

Tris/acetate pH 5.2	2M
EDTA	100mM

DNA Loading buffer:

Urea	4M
Sucrose	50% (w/v)
EDTA pH 8.0	1mM
Bromphenol blue	0.1%
Storage at -20°C	

TAE Agarose gels:

	2% Agarose Gel	0.8% Agarose Gel
Agarose	1g	0.4g
1x TAE	50ml	50ml
Ethidiumbromid	0.5mg/l	0.5mg/l

For separation and characterisation DNA fragments were loaded with DNA loading buffer on agarose gels and separated according to their size by electrophoresis. Gels were run with 1x TAE, 2-8 V/cm and the DNA was visualised on an UV screen.

λ DNA digested with *Hind*III and different DNA ladders were used as size markers.

Elution of DNA fragments from agarose gels

To isolate DNA fragments for agarose gels the Wizard® Plus SV Gel and PCR Clean up System from *Promega* was used.

Cloning of PCR amplified DNA fragments

To clone DNA fragments amplified with PCR, the pGEM®-T Vector System from *Promega* was utilised following the manufacturers instructions.

PCR analysis

For conventional PCR analysis we used the GoTaq® Colorless/Green Master Mix from *Promega*. For semi-quantitative analysis of ChIP experiments, the linear range of the PCR reaction was determined empirically by using increasing amount of DNA template and adapting the number of cycles for each primer pair. PCR products were resolved on 2% agarose-TAE gels.

Reaction mix per sample:

2x Master Mix	12.5µl
Primer F (10pmol/µl)	0.5µl
Primer R (10pmol/µl)	0.5µl
DNA template	xµl
H_2O	xµl
Total volume	25.0µl

PCR conditions:

Temp	Time	
95°C AT* 72°C	4’ 4’ 45’’	
95°C AT 72°C	60’’ 45’’ 45’’	C#
72°C	4’	
4°C	∞	

AT: annealing temperature (see primer table); C#: number of cycles

Real Time PCR analysis

SYBER green Real Time PCR was performed with the *Bio-rad* iCycler iQ system and *Taq* DNA Polymerase (recombinant) from *Fermentas* to quantify PCR assays. Reactions were always performed in doublets or triplicates and quantified according to a dilution series included within the run.

Reaction mix per sample:

10x taq buffer	2.5µl
10mM dNTP each	0.5µl
25mM $MgCl_2$	2.5µl
TaqDNA polymerase (5U/µl)	0.2µl
Primer F (10pmol/µl)	0.25µl
Primer R (10pmol/µl)	0.25µl
FITC Flourescein Calibration Dye (1µM)	0.9375µl
10x Syber Green	1
H_2O	11.8625µl
Template	5.0µl
total volume	25.0µl

Real Time PCR conditions

Temp	Time	
95°C	3’	
95°C AT 72°C	20’’ 25’’ 25’	40x
95°C 60°C	MC	
20°C	∞	

MC: melting curve; AT: annealing temperature

2.2. Work with RNA

Total RNA isolation

For the isolation of total RNA from tissue culture cells the TRIzol® Reagent (*Invitrogen*) was used according the manufacture's protocol. To avoid degradation of RNA, RNAse Inhibitor was added to isolatied RNA (1u RiboLock™ RNAse Inhibitor / µl sample; *Fermentas*). Remaining DNA contamination was removed by DNAse treatment. Therefore 1-2u of Turbo™ DNase from *Ambion* was added to each sample followed by incubation for 15min at 37°C and 15min at 85°C to inactivate the enzyme.

RNA concentration was determined by absorbance at 260nm.

E_{260nm} x $(dilution)^{-1}$ x e^{-1} = concentration µg/ml

e^{-1} = 40 for single stranded RNA

To ensure equal loading and integrity of the RNA, aliquots (1µg) were diluted in RNA sample buffer containing ethidium bromide and run on MOPS/EDTA agarose gels. The amount of loaded RNA was controlled by visualisation on an UV screen.

RNA separation on MOPS/EDTA agarose gels

10x MOPS/EDTA:

MOPS	200mM
Na-acetate	50mM
EDTA	10mM
adjust to pH 7.0	

RNA sample buffer:

Formamide	15ml
10x MOPS	3ml
37% Formaldehyde	4.8ml
H_2O, RNAse free	2ml
Glycerol	2ml
10% (w/v) Bromphenol blue	1.6ml
Optional: 5µl ethidium bromide (1mg/ml)	
Storage at -20°C	

MOPS/EDTA gel:

	50ml	100 ml
Agarose	0.6g	1.2g
H_2O	42.5ml	85ml
10x MOPS	5ml	10ml
37% Formaldehyde	2.5ml	5ml

To resolve secondary structures in the RNA, the RNA samples supplemented with sample buffer were heated up to 65°C for 5 min, cooled on ice and loaded on a 1.2% MOPS/EDTA gel.

cDNA Synthesis

For preparation of cDNA from total RNA, the iScript^{TM} cDNA Synthesis Kit (*Bio-rad*) containing a mixture of oligo d(T) primers and random hexamer nucleotides was used.

Reaction mix per sample:

5x iScript reaction mix	4µl
iScript reverse transcriptase	1µl
Nuclease free H_2O	xµl
RNA template 1µg of total RNA	xµl
total volume	20µl

Reaction condition:

Temp	Time
25°C 42°C 85°C	5' 30' 5'
4°C	∞

2.3. Work with Proteins

Isolation of whole cell extracts

Cells were harvested by trypsination and resuspended in complete DMEM. After centrifugation (1000 rpm, five minutes), the cell pellet was washed in 5ml 1x PBS and transferred to an *Eppendorf* tube. Alternatively, cells were washed with 1x PBS, scratched from the petri-dish with a rubber policeman in 5ml 1x PBS, collected in a *Falcon* tube, pelleted by centrifugation (1000rpm, five minutes) and transferred to an *Eppendorf* tube. Then, cells were pelleted again by centrifugation at full speed for 10 seconds and the resulting pellet (without supernatant) was frozen in liquid nitrogen and thawed again at RT. Cells were resuspended in 2x pellet volume extraction buffer and again immediately frozen in liquid nitrogen. The extracts were thawed at 37°C for five minutes and refrozen in liquid nitrogen. Slow thawing on ice for 15 minutes, followed by centrifugation at full speed at 4°C for 10 minutes, resulted in a supernatant, which directly could be used for Western blot analysis. If cells were pretreated with chemical inhibitors, 1xPBS and extraction buffer was supplemented with appropriate HDAC or phosphatase inhibitors.

Extraction buffer (Hunt Buffer):

Tris-HCl pH 8.0	20mM
NaCl	100mM
EDTA pH 8.0	1mM
NP-40	0.5%

Protease inhibitors (Complete; *Roche*)

Deacetylase inhibitors

Na-Butyrate 100 × Stock	1M
10mM final concentration	

Phosphatase inhibitors

Inhibitor	Stock	Final conc.
NaF	-	0.21g/100ml lysis buffer
Tetra-Sodium-pyrophosphate	-	0.9g/100ml lysis buffer
Na-orthovanadate	100×	0.184g/10ml 50mM Tris pH7.5
B-glycerphosphate	100×	2.16g/100ml H2O

Histone isolation

Cells were harvested, washed and pelleted as described above. After washing with cold PBS and repeated centrifugation (full speed, 10 seconds) the pellet was resuspended in 1ml ice-cold lysis buffer by vortexing or pipetting and then centrifuged. Three further wash steps with lysis buffer and one with Tris/ EDTA wash buffer, each followed by centrifugation, resulted in a nuclear pellet, which was incubated with 100 µl ice cold H_2O supplemented with H_2SO_4 to a final concentration of 0.4 N for at least 1 hour on ice. Then the samples were centrifuged

(4°C, full speed, 10 minutes). The supernatant was mixed with 10x volume acetone and the histones were precipitated from 1h to overnight at -20°C. Precipitates were collected by centrifugation (4°C, full speed, 10 minutes). The pellet was air-dried and resuspended in a suitable volume of H_2O. If cells were pretreated with chemical inhibitors, 1xPBS, lysis and wash buffer was additionally supplemented with appropriate HDAC or phosphatase inhibitors.

Lysis buffer:

Tris	10mM
Na-bisulfite	50mM
$MgCl_2$	10mM
Na-butyrate	10mM
Triton X-100	1%
Sucrose	8.6%
adjust to pH 6.5	

Wash buffer:

Tris	10 mM
Na_3EDTA	13 mM
adjust to pH 7.4	

Determination of protein concentration

The concentration of total protein was determined using a *Biorad Protein Assay* reagent. The extract was diluted 1:1000 in a 1:5 dilution of the reagent, mixed well and the spectroscopic absorption was measured at 595nm. Total protein concentration was estimated with help of standard curve built for known concentrations of protein vs. OD_{595} values.

SDS-Gel-Electrophoresis

Acrylamide stock:

acrylamide	30%
N,N´-methylene-bisacrylamide	0.8%

Separating gel buffer:

Tris-HCl pH 8.8	1.5M
SDS	0.4%

Stacking gel buffer:

Tris-HCl pH 6.8	0.5M
SDS	0.4%

SDS Sample buffer:

Tris-HCl pH 8.8	100mM
glycerol	20%
bromphenol blue	0.01%
DTT	200mM
SDS	4%

10x Running buffer:

Tris	50mM
glycine	500mM
SDS	0.2%

Western blot analysis

After proteins were separated on an SDS-gel, the stacking gel was removed and the separation gel was transferred to distilled water. *3MM* filter paper and a nitro-cellulose membrane (*Schleicher & Schuell*, Nr. BA 83) were cut to the size of the gel and soaked in Harlow buffer. The support pads of the transfer unit were also soaked in Harlow buffer. The sandwich was assembled in the following order: support pad, 2 sheets of *3MM* paper, gel, nitrocellulose membrane, 2 sheets of *3MM* paper and again support pad. The sandwich was placed in the electrotransfer unit (*Hoefer*), filled with transfer buffer. The transfer was performed at a constant current of 200mA (1 or 2 gels) in a cold room for 1.5 hours under stirring with a magnet bar. The quality of the transfer was checked by staining the membrane with 1x Ponceau for one minute. The excess Ponceau was removed by rinsing the membrane with distilled water.

Harlow 2 transfer buffer:

Tris	25mM
glycine	190mM
methanol	20%

10x Ponceau S:

Ponceau S	2%
trichloroacetic acid	30%
sulfosalicylic acid	30%

Antibody Incubation

In order to block any unspecific reactions of the antibodies, the membrane was incubated with blocking solution for one hour at RT under gentle agitation.

The incubation with the primary antibody (diluted in blocking solution) was carried out at 4°C overnight or at room temperature for at least one hour.

After three washing setps with 1x PBS, containing 0.1% Tween-20, 15 minutes each, the blot was incubated with the secondary (peroxidase-coupled) antibody, diluted in 1x PBS, 0.1% Tween 20, for one hour at RT followed by another three washes.

Western blocking solution:

PBS	1x
PVP	1%
non fatty dried milk	1%
Tween 20	0.1%
NaN_3	0.01%

Immunodetection by ECL (Enhanced Chemo-Luminescence)

Equal amounts of ECL solution 1 and 2 (*Amersham*) were mixed, poured over the blot and incubated for one minute. The excess of ECL solution was removed and the membrane was packed into saran wrap and exposed to X-ray films.

Western blot stripping

Western blots that have been used for ECL could be re-used after stripping. The blot was washed three times in PBS, 0.1% Tween 20. After incubation with stripping buffer at 50°C for 30 minutes, the blot was washed again three times with PBS, 0.1% Tween 20 and was then ready for a new incubation with a different antibody.

Stripping buffer (100 ml):

20% SDS	10ml
1 M Tris-HCl pH 6.7	6.25ml
ß-mercaptoethanol	700µl
H_2O	83.05ml

The following antibodies were used in this study:

Antibody	Name	Dilution	Source	Company	Cat. Nr.
histone H3	c-H3	1:50000	r	*Abcam*	ab1791
pan-acetyl-histone H3	H3ac	1:5000	r	*Upstate*	06-599
pan-acetyl-histone H4	H4ac	1:5000	r	*Upstate*	06-598
acetyl (lys9)-histone H3	H3K9ac	1:5000	r	*Upstate*	07-352
acetyl (lys14)-histone H3	H3K14ac	1:5000	r	*Upstate*	06-911
acetyl (lys5)-histone H4	H4K5ac SAT247	1:5000	r	*Upstate*	06-759
acetyl (lys8)-histone H3	H4K8ac SAT198	1:5000	r	*C. Seiser*	
acetyl (lys12)-histone H3	H4K12ac SAT44	1:5000	r	*C. Seiser*	
acetyl (lys16)-histone H3	H4K16ac SAT53	1:5000	r	*C. Seiser*	
mono-methyl-(lys9)-histone H3	H3K9met1	1:5000	r	*T. Jenuwein*	
di-methyl-(lys9)-histone H3	H3K9met2	1:5000	r	*T. Jenuwein*	
tri-methyl-(lys9)-histone H3	H3K9met3	1:5000	r	*T. Jenuwein*	
mono-methyl-(lys27)-histone H3	H3K27met1	1:5000	r	*T. Jenuwein*	
di-methyl-(lys27)-histone H3	H3K27met2	1:5000	r	*T. Jenuwein*	
tri-methyl-(lys27)-histone H3	H3K27met3	1:5000	r	*T. Jenuwein*	
mono-methyl-(lys20)-histone H4	H4K20met1	1:5000	r	*T. Jenuwein*	
di-methyl-(lys20)-histone H4	H4K20met2	1:5000	r	*T. Jenuwein*	
tri-methyl-(lys20)-histone H4	H4K20met3	1:5000	r	*T. Jenuwein*	
di-methyl-(arg17)-histone H3	H3R17met2	1:2000	r	*Upstate*	07-214
di-methyl-(arg3)-histone H4	H4R3met2	1:2000	r	*Upstate*	07-213
tri-methyl-(lys4)-histone H3	H3K4met3	1:5000	r	*Upsate*	07-473
tri-methyl-(lys4)-histone H3	H3K4met3	1:5000	r	*Abcam*	ab8580
histone deacetylase 1	HDAC1 10E2	1:2000	m	*C. Seiser*	
histone deacetylase 2	HDAC2 3F3	1:100	m	*C. Seiser*	

histone deacetylase 3	HDAC3	1:10000	r	*Abcam*	ab16047
DNA methyltransferase 1	DNMT1	1:2000	m	*Abcam*	ab13537
ß-actin	ACTIN	1:5000	m	*Sigma*	A5316

2.4. Work with Bacteria

Solutions and media

Antibiotic stock solutions

Ampicillin	100 mg/ml
Kanamycin	50 µg/ml

Luria-Bertani liquid medium (LB-medium)

Bacto-Trypton (*Difco*)	10 g/l
Bacto-Yeast Extract (*Difco*)	5 g/l
NaCl	5 g/l

Top agarose

Bacto-Trypton (*Difco*)	10 g/l
NaCl	8 g/l
Agarose	6 g/l

All media were sterilized by autoclaving and stored at 4°C. For the selection of transformed bacteria the autoclaved media were supplemented with the appropriate antibiotics.
Solid bacteria media were prepared by adding 1.5% w/v Bacto-Agar (*Difco*) to liquid media before autoclaving. After cooling the medium to 50°C, antibiotic stock solutions were added to the proper final concentrations and poured into petri dishes. LB plates were stored at 4°C. For blue/white selection of bacteria, LB plates were supplemented with IPTG (5.5mM) and X-Gal (= 5-bromo-4-chloro-3-indyl-β-D-galactoside) 80µg/ml.

Growth of bacteria

Liquid cultures were inoculated either with frozen bacterial stocks or with bacterial colonies from agar plates stored at 4°C. Single colonies were picked with sterile toothpicks, transferred into the appropriate liquid medium and incubated at 37°C under agitation overnight.

Freezing of bacteria

For long-term storage, 2x freezing buffer and overnight bacteria culture were mixed 1:1 and stored at -80°C.

2x Freezing buffer

K_2HPO_4	12.60 g/l
KH_2PO_4	3.60 g/l
Na citrate	0.90 g/l
$MgSO_4$ •7 H_2O	0.18 g/l
$(NH4)_2SO4$	1.80 g/l
Glycerol	88.00 g/l
storage at 4°C	

Transformation of bacteria

Heat shock competent bacteria (DH5α) were thawed on ice, DNA (~5ng) was added and bacteria were incubated for another 20min on ice. After a heat shock of 45sec at 42°C, 500µl of SOC medium was added and bacteria were rotated for ½ - 1h at 37°C before they were plated on appropriate LB plates and incubated O/N at 37°C.

SOC medium

Bacto-Trypton	2%
Bacto-Yeast Extract	0.5%
NaCl	10 mM
Kcl	2.5 mM
MgSO4	10 mM
MgCl2	10 mM
Glucose	20 mM
storage at -20°C	

2.5. Cell Culture

Solutions and media

10x Phosphate buffered saline (PBS):

NaCl	80g/l
KCl	2g/l
Na2HPO4	16.5g/l
KH2PO4	2g/l
Adjust pH to 7.4	

100x Antibiotic stock solution (AB):

Penicillin G potassium salt	6g/l
Streptomycin sulfate	10g/l
Dissolved in 1x PBS	

100x Antibiotic stock solution plus glutamine (AB + G):

Glutamine	5.8g/l
Dissolved in 100x AB	

Trypsine/EDTA solution (TE):

Trypsine 2.2U/mg	700mg
10x PBS	25ml
1% Na-EDTA, pH 7.4	5ml
Add water to a final volume of 250ml	

Dulbecco's modified eagle medium (DMEM)

DMEM (*Sormed)* powder was dissolved in bidestilled water, supplemented with 3.7g/l $NaHCO_3$ and sterilised by filtration (pore size 0.2µm). The DMEM was stored at 4°C. Before use 450ml DMEM were supplemented with 5ml AB and fetal calf serum (FCS, *Gibco BRL*) stored in 50ml aliquots at -20°C.

Medium for murine embryonic stem cell (ESC) cultivation (M15)

ES cell qualified high-glucose DMEM containing 4500 mg/l glucose (*Sigma*) was supplemented with 15% FCS (*HyClone*), 1x AB + G, 1x ß-mercaptoethanol and ESGRO LIF (10^3 units / ml medium). The medium was stored at 4°C and prewarmed at 37°C before use.

100x ß-Mercaptoethanol stock solution (0.01M)

72µl of 14M ß-mercaptoethanol were added to 100ml 1x PBS, the solution was sterilized by filtration, aliquoted and stored at – 20°C. Once in use, the solution was stored at 4°C.

0.1% (w/v) Gelatine solution

10g gelatine were added to 1l dH_2O, the solution was mixed on a rotator and autoclaved for 30 minutes at 120°C. After cooling down to room temperature, the working solution was prepared by diluting the 1% gelatin in sterile water. Gelatine solution was stored at 4°C.

2x Freezing medium for ESCs

2x Freezing Medium for ESCs contained 20% DMSO, 20% FCS (*HyClone*) in high-glucose DMEM (*GibcoBRL*).

Cell culture and splitting of fibroblast and osteosarcoma cells

Cells were cultured in petri-dishes with DMEM medium at 37°C and in an atmosphere of 7.5% CO_2. After reaching a critical density (sub-confluent), the cells were split and supplied with fresh medium. Therefore, cells were washed twice with 1x PBS and incubated with TE at 37°C for several minutes. When cells detached from the surface they were taken up with an appropriate amount of medium, resuspended carefully and split to fresh petri-dishes in adequate dilutions.

Cell culture and splitting of ESCs

ES cells were cultured on pre-gelatinised tissue culture dishes: therefore petri-dishes were covered with 0.1% gelatine solution and incubated for at least 10min at room temperature. Prior to use excess of gelatine was removed. Cells were incubated at 37°C in a 5% CO_2-atmosphere.

Established ES cell lines required to be subcultured every third day. When reaching confluence, ES cells were split 1:3 - 1:5. For this purpose, cells were washed twice with 1x PBS and trypsinised with TE in HBBS w/o Ca&Mg (*Gibco*) twenty minutes at 37°C. Trypsinisation was stopped by adding at least two volumes of M15. Cells were disaggregated by carefully pipetting up and down with a glass or a Gilson pipette to generate a single-cell suspension, before being replated at optimal density onto fresh gelatinised petri-dishes. Medium had to be changed every day.

Freezing of fibroblast and osteosarcoma cells

Logarithmically growing cells were trypsinised, taken up with 10ml medium and collected by centrifugation at 1200 rpm for 5 minutes. The resulting cell pellet was dissolved in 90% FCS and 10% DMSO, mixed well and transferred into a freezing-ampoule (*cryo tube, Nunc*). After 30 minutes of incubation on ice, the freezing-ampoule was cooled to -80°C for one day and finally transferred to liquid nitrogen for long time storage.

Thawing of fibroblast and osteosarcoma cells

Cells stored in liquid nitrogen were quickly thawed at 37°C in a water bath for 2-3 minutes. Then cells were transferred in a fresh petri-dish containing a 10 ml CO_2 saturated DMEM medium. When cells attached to the surface, fresh medium was supplied to remove the DMSO contained in the freezing medium.

Freezing of ESCs

After 2x washing with 1x PBS, trypsinisation and neutralization with the appropriate medium, one volume of 2x freezing medium was added to the cells, drop by drop, under gentle agitation.

If the cell suspension to be frozen had a volume larger than 0.9-1 ml, cells were collected by centrifugation and resuspended in 0.5 ml cell culture medium before dropwise addition of the same volume of freezing medium. Freezing vials were stored at –80°C at least overnight before being transferred into liquid nitrogen for long-term storage.

Thawing of ESCs

After quick thawing in a 37°C waterbath, cells were transferred into a Falcon tube. 10 to 15 ml of appropriate cell culture medium was added dropwise under gentle shaking. To avoid any contamination by DMSO, cells were collected by centrifugation at 1000 rpm for 7 minutes. The supernatant was discarded, cells were resuspended in a suitable volume of medium and seeded onto tissue culture dishes.

Cell lines used in this study

Mouse fibroblasts 3T3 Swiss (ATCC: CCL-92)

The mouse fibroblast cell line 3T3 Swiss was cultured by G. Todaro and H. Green and derived from Swiss Albino mouse embryos. This hypotetraploid cell line was cultured in DMEM + AB + 10% FCS and was arrested in G_0 by reducing FCS to 0.2% for 48-72 hours.

Mouse fibroblasts NIH/3T3 (ATCC: CRL-1658)

NIH/3T3 is a fibroblast cell line established from NIH Swiss mouse embryo cultures. Culture conditions are similar to 3T3 Swiss cells.

Mouse fibroblasts PM

This mouse fibroblast cell line was established by Y. Zhang from the laboratory of P. Matthias at the FMI, Basel. Cells were derived from E13.5 129SV/BL6 mouse embryos carrying two floxed alleles of the HDAC1 gene and immortalised *via* the 3T3 protocol. Cells are aneuploid and carry a mutation in the p53 tumour suppressor gene (see J. Jurkin,

Diploma thesis, 2006). Cultivation conditions are similar to 3T3 Swiss cells. Several subclones of this cell line have been established: PM1/1, PM1/2, PM1/3 and PM1/4 subclones were transiently transfected with an EGFP carrying plasmid, GFP^+ cells were FACS sorted into 96-well plates and raised for further use as wildtype control cell lines. PM4/1, PM4/2, PM4/3 and PM4/4 subclones were transfected with a plasmid carrying EGFP and the cre recombinase gene. GFP^+ cells were FACS sorted into 96-well plates, raised, and served as HDAC1 knock out fibroblast cell lines (Deletion of exon 6 of the HDAC1 gene was verified *via* PCR, Western Blot and Immunoflourescence).

Mouse embryonic stem cells 3A1R

This embryonic stem cell line was created by blastocyst outgrowth experiments from G. Weitzer at the MFPL, Vienna in collaboration with our laboratory. The ES cell line carries one wildtype and one floxed allele of the HDAC1 gene, corresponding to a wildtype genotype; the genetic background is 129SV/BL6. Cells are cultivated on gelatinised petri-dishes in M15 ES cell medium with LIF.

Human osteosarcoma cells U2OS (ATCC: HTB-96)

This cell line was derived from a moderately differentiated sarcoma of the tibia of a 15 year old girl in 1964 by J. Ponten and E. Saksela. Cells are hypertriploid and are maintained in medium containing DMEM + AB + 10% FCS.

Drugs, inhibitors and reagents

The following drugs were used in this study:
Trichostatin A (TSA) (66nN or 166nM; *Wako Pure Chemical Industries*)
5'-Aza-2'-deoxycytidine (Aza-dC) (1µM or 100µM; *Sigma*)
Anisomycin (Aniso) (189nM; *Sigma*)
Okadaic acid (OA) (50nM; *Sigma*)
all-trans-Retinoic acid (RA) (10nM; *Sigma*)
H89 (10µM; *Alexis Biochemicals*)
G-418 (500µg/ml; *Sigma*)

Transfection of U2OS cells

To transfect U2OS cells with plasmid DNA, the Lipofectamine™ reagent from *Invitrogen* was used according the manufactorers instruction. Shortly, 1µg and 5µl of Lipofectamine™ was incubated in 250µl OptiMEM® (*Invitrogen*) each for 5min at RT. Then the content of both eppis was joined, incubated for another 15min at RT and put on a 6well plate which contained logarithmically growing U2OS cells in 2ml DMEM + AB + 10% FCS. Therefore, the

cells were split 24h prior to the transfection procedure and 100,000 cells were seeded per 6well. 5-6h after transfection the medium was removed and replaced by 2.5ml DMEM + AB + 10% FCS. If desired, 66nM of TSA was added for 24h after transfection. To monitor expression levels of the transfected DNA constructs, cells were lysed 24h after transfection with 500µl TRIzol® reagent from *Invitrogen* and RNA was isolated as described above. For quantification of RNA levels, cDNA was prepared as described earlier and subjected to Real Time PCR analysis. For analysis of transposition frequency, cells were trypsinesed 24h post transfection and transferred to a 10cm dish where they were grown till ~80% confluency (~6days). Then, cells were again trypsinesed, cell numbers were determined using the CASY®1 cell counter and 500,000 cells were seeded per 10cm dishes. Selection for neo^+ cells was started 24h later by adding 500µg/nl G418 to the medium and maintained for 10-14days till all neo^- cells detached from the surface and neo^+ positive cells were growing in visible clones of at least 1mm diameter. To quantify the number of neo^+ positive clones, cells were washed with 1x PBS prior to fixation with 70% EtOH for 10min, washed again with 1x PBS, stained with Methylenblue-Solution for 10min to visualise the colonies and finally the plates were rinsed with H_2O to remove the remaining background staining.

Methylenblue-solution:

Methylenblue	0.1% w/v
NaAc	0.5M

2.6. Chromatin Immunoprecipitation (ChIP)

Buffers

Wash buffer I

Triton X-100	0.25%
EDTA pH 8.0	10mM
EGTA pH 7.5	0.5mM
Hepes pH 7.5	10mM

Wash buffer II

NaCl	0.2M
EDTA pH 8.0	1mM
EGTA pH 7.5	0.5mM
Hepes pH 7.5	10mM

SDS lysis buffer

SDS	1%
EDTA	10mM
Tris-HCl pH 8.1	50mM

Dilution buffer

SDS	0.01%
Triton X-100	1.1%
EDTA	1.2mM
Tris-HCl pH 8.1	16.7mM
NaCl	167mM

RIPA wash

NaCl	150mM
Tris-HCl pH 8.0	50mM
SDS	0.1%
NaDoc	0.5%
NP-40	1%

High salt wash

NaCl	500mM
Tris-HCl pH 8.0	50mM
SDS	0.1%
NP-40	1%

LiCl wash

LiCl	250mM
Tris-HCl pH 8.0	50mM
NaDoc	0.5%
NP-40	1%

TE

Tris-HCl pH 8.0	10mM
EDTA pH 7.5	1mM

Elution Buffer

SDS	2%
$NaHCO_3$	0.1M
DTT	10mM

Preparation of sepharose bead suspension

Solid A-beads were pre-swollen in TE on ice for 30 minutes. A-beads were then washed three times with TE. G-beads, which are provided by the manufacturer as a suspension, were re-buffered in TE by washing the beads three times with TE. Then the beads were blocked by adding the following solutions per ml swollen beads:

sonicated Salmon Sperm DNA (10mg/ml)	20µl
BSA (10mg/ml)	100µl
NaAzid 2%	50µl
TE	830µl

Finally the beads were rolled for one hour at 4°C. Beads were stored at 4°C.

Formaldehyde fixation and preparation of soluble chromatin

Chemical cross-link of chromatin was performed by addition of formaldehyde for 10 minutes at 37°C directly to the medium in the culture-dish at a final concentration of 1%. A subsequent incubation with glycine at a final concentration of 125mM for 5 minutes at room temperature stopped the formaldehyde fixation. After washing the cells twice with 1x PBS they were scraped with a rubber policeman in PBS containing 1mM PMSF. The cells were then pelleted at 1200 rpm at 4°C for five minutes. The cell pellet was washed with wash buffer I containing 1mM PMSF, protease inhibitors (Complete; *Roche*) and when desired 10mM sodium butyrate, 10mM β-glycerophosphate and 10mM orthovanadate. After 10 minutes incubation on ice, nuclear extracts were pelleted at 1200 rpm at 4°C for five minutes. The nuclear pellet was washed with wash buffer II containing the same inhibitors and incubated on ice of 10 minutes. Finally, washed nuclear extracts were pelleted at 1200 rpm at 4°C for five minutes and the washed nuclear pellet was resuspended in lysis buffer at a concentration of 10^7 cells/ml containing inhibitors as indicated above. The lysate was incubated 30 minutes on ice or stored up to two months at 4°C. Chromatin was sheared to an appropriate size for ChIP (approximately 500bp) by sonication of the nuclear lysate. The *Bandelin* UW 70 sonotrode, which was equipped with a 2mm tip, was used setting the output signal to 40% and the duty cycle to 90%. After each sonication step for 15 seconds the lysate

was kept on ice for two minutes. Sonication steps were repeated up to 6 times. To pellet cellular debris, the cell lysate was centrifuged for 10 minutes at 4°C at full speed.

Chromatin immunoprecipitation and isolation of precipitated DNA

The remaining supernatant, which comprises the soluble chromatin fraction, was then aliquoted for different chromatin immunoprecipitations using approximately 10^6 cells in 100µl per IP and diluted 10-fold in dilution buffer containing the specific inhibitors as mentioned above. One aliquot was kept for isolation of DNA fragments and is referred to as input DNA. The chromatin samples were pre-cleared by addition of 20µl of protein A/G Sepharose beads and rocked at 4°C for at least one hour. After centrifugation for three minutes at 4°C at 1500 rpm the supernatant was combined with the antibody of interest (2-8µg, depending on the antibody) or with an unspecific IgG (1µg) and immuno-complexes were formed while rocking over night at 4°C.

Chromatin antibody complexes were isolated by incubation with 30µl of protein A/G Sepharose beads and rocked at 4°C for at least one hour. The beads were harvested by centrifugation at 4°C for three minutes at 1500 rpm and were then washed one to two times with 900µl of each RIPA, high salt and LiCl buffer and two to four times with 900 µl TE buffer by rocking for 10 minutes at 4°C. Immuno-complexes were eluted from the Sepharose beads by addition of 400µl elution buffer and vigorous rocking at room temperature for 30 minutes. Cross-link of immunoprecipitated chromatin and input aliquots was reversed by addition of 0.05 volume of 4M NaCl to the eluted samples and incubation at 65°C over night. Next day Proteinase K digestion was performed (0.025 volume of 0.5M EDTA pH 7.5, 0.05 volume of 1M Tris pH 6.5 and proteinase K (final concentration 0.1mg/ml)). DNA was recovered by a phenol-chloroform-isoamylalcohol (PCI) extraction and precipitated by addition of 0.1 volume of 1M sodium acetate pH 5.2, 20µg glycogen and 2.5 volumes of ethanol. Immunoprecipitated and input DNA was dissolved in 200µl water. For quantification *via* Real Time PCR or semi-quantitative conventional PCR, 5µl of the DNA or 5µl of a 1:40 dilution of input DNA was used as template.

Antibodies

The following antibodies were used in this study:

Antibody	Name	µl	Source	Company	Cat. Nr.
unspecific IgG	UN	1	r	*Ch. Seiser*	-
histone H3	c-H3	6	r	*Abcam*	ab1791
pan-acetyl-histone H3	H3ac	5	r	*Upstate*	06-599
pan-acetyl-histone H4	H4ac	5	r	*Upstate*	06-598
phospho (ser10)-acetyl (lys14)-histone H3	H3S10p/H3K14ac	10	r	*Upstate*	07-081
phospho (ser10)-acetyl (lys14)-histone H3	H3S10p/H3K14ac GP3	2	r	*Ch. Seiser*	-

2.7. Primers used in the study

Primers for ChIP analysis

Gene	Name	Sequence	Temp.
ß-actin	actb_prom_f	GCCAGCACCCATCGCCAAAACTC	59°
	actb_prom_r	TTGGCTCCGCGTCGCTCACTCA	
	PL: promoter		
Prss11 / HtrA1	mPrss11 (-500) F	CAAGTTCACAGCCACAGTCC	59°
	mPrss11 (-500) R	GGCACTTAACAGAGGGAAACC	
	PL: mPrss11 (-500) F: -401 of 1exon1; mPrss11 (-500) R: -256 of exon1; **PS:** 146bp		
LINE1	L1-ORF2-for	TTTGGGACACAATGAAAGCA	59°
	L1-ORF2-rev2	CTGCCGTCTACTCCTCTTGG	
	PL: ORF2; **PS**: ~200bp; **RE:** Martens, 2006		
SINE B1	Sine_B1_for	GTGGCGCACGCCTTTAATC	59°
	Sine_B1_rev	GACAGGGTTTCTCTGTGTAG	
	PS: 122bp; **RE: :** Martens, 2006		
SINE B2	Sine_B2_for	GAGATGGCTCAGTGGTTAAG	59°
	Sine_B2_rev	CTGTCTTCAGACACTCCAG	
	PS: 132bp; **RE: :** Martens, 2006		
VL30 int	mVL30-for	CCTTTGTTGCCCAGGTAAGTC	59°
	mVL30-rev	CACTGTAGCCAGTTGTGACCAG	
	PL: pol; **PS**: ~380bp; **RE:** Puschendorf, 2006		
VL30 LTR	VL30_LTR/UTR_for	ACAGCGCGACCACCCAGAGG	59°
	VL30_UTR_rev	GTCCCTGATCCTCCCCTGTTCCT	
	PL: 5'LTR/UTR; **PS**: ~240bp		
IAP int	IAPgagIDI_for	GAGATTGGACTTTTGACTTGT	59°
	IAPasen	TGTGGCTTGCTCATAGATTAG	
	PL: gag region; **PS**: ~270bp		
IAP LTR	IAP_LTR_chip_I/III_for	AC AAG ATG GCG CTG ACA GCT	59°
	IAP_LTR_chip_I/II_rev	G AGC ATT CTC CTT CGC CTC	
	PL: LTR; **PS**: ~170bp		
ETn	ETn-for	CAGGCTTTGGAGACAATAGGG	59°
	ETn-rev	TCTCTCAGGGAACTCAGAAACG	
	PS: ~280bp; **RE:** Puschendorf, 2006		
MERVL	MuERVL-for	CCCATCATGAGCTGGGTACT	59°
	MuERVL-rev	CGTGCAGATCCATCAGTAAA	
	PS: ~280bp; **RE:** Puschendorf, 2006		
MT	MT-for	ATGTCTTGGGGAGGACTGTG	59°
	MT-rev	AGCCCCAGCTAACCAGAACT	
	PS: ~250bp; **RE:** Puschendorf, 2006		
ORR	ORR1-for	CTTTAGTTGATGGCCCAGGA	59°
	ORR1-rev	CCAACTCTGCCCTCTGTAGC	
	PS: ~250bp; **RE:** Puschendorf, 2006		
Tigger	Tigger_for	GTGTCAGGAGGTTTCAAAGGCTC	59°
	Tigger_rev	CGCTCTCTTGAAGGCAAGGACTC	
	PS: 352bp; **RE:** based on homology to human Tigger; Martens, 2006		

Primers for gene expression analysis

Gene	Name	Sequence	Temp.	Org.
HPRT	RT-HPRT-fo	GCTGGTGAAAAGGACCTCT	59°	m
	RT-HPRT-rev	CACAGGACTAGAACACCTGC		
ß-actin	Actin-for	TGG CAC CAC ACC TTC TAC AAT GAG	59°	m
	Actin-rev	CAA GAA GGA AGG CTG GAA AAG AG		
Prss11 / HtrA1	RT-Prss11for	TCG GAG GAT GGA CTG ATT GT	59°	m
	RT-Prss11rev	GTT TGG CTT TGC TAG ATG TGA G		
LINE1	L1-ORF2-for	TTTGGGACACAATGAAAGCA	59°	m
	L1-ORF2-rev2	CTGCCGTCTACTCCTCTTGG		
	PL: ORF2; **PS**: ~200bp; **RE:** Martens, 2006			
SINE B1	Sine_B1_for	GTGGCGCACGCCTTTAATC	59°	m
	Sine_B1_rev	GACAGGGTTTCTCTGTGTAG		
	PS: 122bp; **RE:** Martens, 2006			
SINE B2	Sine_B2_for	GAGATGGCTCAGTGGTTAAG	59°	m
	Sine_B2_rev	CTGTCTTCAGACACTCCAG		
	PS: 132bp; **RE:** Martens, 2006			
RLTR1b	RLTR1b_for	GAGAGGCGAGAGGCAGAAGAAAG	59°	m
	RLTR1b_rev	GTCGCCAACCTAGGTATCCAGAG		
RLTR6	RLTR6_for	CCCCCTGAGGAGCGGTGT	59°	m
	RLTR6_rev	AGTAAGCATCCCCTGTCGTTTCA		
VL30	mVL30-for	CCTTTGTTGCCCAGGTAAGTC	59°	m
	mVL30-rev	CACTGTAGCCAGTTGTGACCAG		
	PS: ~380bp; **RE:** Puschendorf, 2006			
IAP	IAPsen	ACTAACTCCTGCTGACTGG	59°	m
	IAPasen	TGTGGCTTGCTCATAGATTAG		
	PL: IAPsen: gag region;pos. ~890; IAPasen: gag region; pos. ~1310; **PS**: ~420bp			
ETn	ETn-for	CAGGCTTTGGAGACAATAGGG	59°	m
	ETn-rev	TCTCTCAGGGAACTCAGAAACG		
	PS: ~280bp; **RE:** Puschendorf, 2006			
MERVL	MuERVL-for	CCCATCATGAGCTGGGTACT	59°	m
	MuERVL-rev	CGTGCAGATCCATCAGTAAA		
	PS: ~280bp; **RE:** Puschendorf, 2006			
MT	MT-for	ATGTCTTGGGGAGGACTGTG	59°	m
	MT-rev	AGCCCCAGCTAACCAGAACT		
	PS: ~250bp; **RE:** Puschendorf, 2006			
ORR	ORR1-for	CTTTAGTTGATGGCCCAGGA	59°	m
	ORR1-rev	CCAACTCTGCCCTCTGTAGC		
	PS: ~250bp; **RE:** Puschendorf, 2006			
Tigger	Tigger_for	GTGTCAGGAGGTTTCAAAGGCTC	59°	m
	Tigger_rev	CGCTCTCTTGAAGGCAAGGACTC		
	PS: 352bp; **RE:** based on homology to human Tigger; Martens, 2006			
HDAC1	mHDAC1 RT-F	AAGCAGCAGACG GACATCG	59°	m
	mHDAC1 RT-R	GCCTCTTCCACGCCATCG		
neo	neo_for_N	ATCAGACAGCCGATTGTCTG	59°	h
	neo_rev	CAGTTCCGCCCATTCTCCG		
	PS: ~250bp			
GAPDH	RT_hGAPDH_for	TCTTCTTTTGCGTCGCCAG	61°	h
	RT_hGAPDH_rev	AGCCCCAGCCTTCTCCA		
	RE: Fraga, 2005			

Primers for genotyping

Gene	Name	Sequence	Temp.
HDAC1 wt	WT-fo	GGCCTTGTGTCTTGGAAGAGCACC	54
	WT-rev	GCTGAAGGAAGGTGGAAGAGTGGC	
	PL: WT-fo/rev: exon 5; **PS:** 319bp		
HDAC1 ko	KO-fo	CCTCCCATTGAGTTGGCAGGGCAA	54
	Lac-out	AACCCGTCGGATTCTCCGTGGGAA	
	PL: KO-fo: intron 4; Lac-out: LacZ gene; **PS:** 490bp		
HDAC1 lox	HDAC1-lox-for	GGTAGTTCACAGCATAGTACTT	54
	HDAC1-lox-rev	CTGTGTCATTAGAATCTACTT	
HDAC1 delta	HDAC1-lox-for	GGTAGTTCACAGCATAGTACTT	54
	HDAC1-delta-rev	GTTACGTCAATGACATCGTCTT	
DNMT1	DNMT1-delta-for	AGAGGCTAGGGGGTTGGCATTGG	54
	DNMT1-delta-rev	AAAGGCGTGAAAGCAGCATCGTGT	
cre	Cre-for	TAATCGCCATCTTCCAGCAG	54
	Cre-rev	CAATTTACTGACCGTACA	

Primers for cloning

Gene	Name	Sequence	Temp.
IAP	IAPgagCON_for		56°
	IAPgagCON_rev		
	PL: IAPgagCON_for/rev: gag region; **PS:** ~ 500bp; **ET:** 50sec; **C#:** 40x		
VL30	VL30con_for2		62°
	VL30con_rev2		
	PL: VL30con_for2: 5' of 3' LTR; VL30con_rev2: R region of LTR; **PS:** ~ 500bp; **ET:** 1min; **C#:** 35x		

PL: Primer Location; **PS:** Product Size; **ET:** Extension Time; **C#:** Cycle Number; **RE:** Reference; **Org.:** Organism: human (h), mouse (m); **Temp.:** Annealing Temperature

3. Aims of the Work

Activation of transposable elements (TEs) in somatic cells can potentially lead to mutations resulting in pathological relevant changes of gene expression patterns. Therefore, restriction of transposon activity is crucial for maintaining genomic integrity of a cell.

So far, DNA methylation, RNAi pathways and histone methylation have been implicated in the silencing of TEs in eukaryotic cells. The role of another epigenetic modification known to be involved in the regulation of transcriptional control – histone acetylation – has not been analysed in detail. Therefore we wanted to survey TE expression in murine somatic cells with altered histone acetylation states. This was achieved either by chemical inhibition of all class I and II histone deacetylases (HDACs) or genetic inactivation of the major class I deacetylase HDAC1. That way we tried to identify TEs regulated by histone acetylation and in subsequent experiments to gain further insight into molecular mechanisms relevant for activation of this class of TEs.

4. Results

4.1. Influence of HDAC1 inactivation, HDAC inhibition and reduced DNA methylation on global histone modification patterns and IAP DNA methylation levels in fibroblasts

To monitor the influence of histone acetylation on various biological processes, our lab is on the one hand utilising chemical inhibitors of HDACs, on the other hand we established ESCs and fibroblast cell lines lacking a functional copy of the Hdac1 gene.

In collaboration with the laboratory of P. Matthias (FMI, Basel), a fibroblast cell line derived from a BL6/129Sv mouse carrying two floxed alleles of Hdac1 was established and immortalised following the 3T3 immortalisation protocol. Four subclones were transfected with a vector expressing the cre recombinase leading to the deletion of exon 6 encoding the catalytic core of the HDAC1 protein. Four additional subclones were transfected with a control vector. That way we obtained four cell lines lacking a functional copy of Hdac1 (referred to as $HDAC1^{-/-}$) and four cell lines with a functional copy of the gene serving as wildtype control cell lines ($HDAC1^{+/+}$). Some aspects of proliferation, cell cycle regulation, gene expression profile and HDAC complex formation connected to the loss of Hdac1 in this cell system have been analysed by others (J. Jurkin, diploma thesis, 2006; Y. Zhang, FMI Basel).

To extend the analysis and monitor the influence of other HDACs beside Hdac1, we also treated $HDAC1^{+/+}$ fibroblast cell lines with trichostatin A (TSA), a compound efficiently inhibiting all class I and class II HDACs. Furthermore, $HDAC1^{+/+}$ fibroblast cell lines were treated with 5'-Aza-2'-deoxycytidine (Aza-dC), a compound leading to a reduction in DNA methylation.

In a first step, levels of the class I HDACs HDAC1, HDAC2, HDAC3 and of the maintenance DNA methyltransferase DNMT1 were monitored *via* Western blot analysis using specific antibodies. As visible in Figure 1A, loss of HDAC1 lead to upregulation of its closest homologue, HDAC2. This compensatory mechanism may buffer some of the effects caused by the loss of HDAC1, but still total cellular HDAC activity was diminished by about 30% when HDAC1 was depleted (Figure 1B), underlining its dominant role in this cell type. HDAC3 and DNMT1 protein levels remain unchanged. General HDAC inhibition *via* TSA treatment does not change steady-state levels of HDAC1, 2 and 3, whereas DNMT1 levels are slightly decreased (Figure 1A). Reduction of DNMT1 levels after HDI treatment has previously been reported in Jurkat T and cervix cancer cells and seems to result from reduced mRNA expression (You, 2008) or decreased mRNA stability, respectively (Januchowski, 2007). Treatment of fibroblasts with Aza-dC does not influence HDAC levels,

whereas DNMT1 protein levels are slightly diminished which is consistent with reports that Aza-dC can lead to the proteasomal degradation of DNMT1 (Goshal, 2005).

Having monitored expression levels of proteins directly targeted by chemical or genetic inhibition, we went on to evaluate effects on the biological targets of HDACs and DNMT1, i.e. histone modification patterns and the methylation status of CpG dinucleotides. To examine DNA methylation levels, we employed the Ms-SNuPE technique (Gonzalgo, 1997) and analysed the methylation of CpG sites within the regulatory region of IAP retrotransposons, which are normally highly methylated (collaboration with G. Egger, Norris Comprehensive Cancer Center, University of Southern California, USA). The use of differential primers allowed us the analysis of distinct subgroups of IAP elements; locating both PCR primers within the LTR of the retrotransposon resulted in the amplification of DNA derived from multiple genomic loci and therefore mirrored the average DNA methylation of multiple IAP elements. This approach was used to quantify DNA methylation levels of two subgroups of IAP elements. Figure 1C shows the average methylation of canonical IAP elements including elements which are still capable of retrotransposition (Dewannieux, 2004) and Figure 1D shows average DNA methylation of a heterochromatic Y chromosome specific subgroup of IAP elements (Fennelly, 1996). To investigate DNA methylation of defined single copy elements, one PCR primer was located in the genomic region flanking the 5' LTR and therefore the amplified DNA corresponds to a distinct genomic IAP retroelement. Figure 1E shows the DNA methylation levels of a full length IAP element harbouring all features necessary for autonomous retrotransposition and exhibiting 100% LTR-LTR homology, a signature of recent integration. It served as paradigm for an evolutionary young retroelement. In contrast to this, Figure 1F shows DNA methylation levels of an IAP element representing an evolutionary old member of this retroelement family with only 86% LTR-LTR homology.

Despite the different features of the IAP retrotransposons tested, DNA methylation in all four cases showed a characteristic pattern: loss of HDAC1 did not influence CpG methylation (compare black and grey bars) demonstrating that HDAC1 is not necessary for the maintenance of proper DNA methylation patterns of transposable elements. Inhibition of the enzymatic function of all class I and II HDACs with TSA for 24h also did not change DNA methylation. Only when cells were treated with Aza-dC, which directly targets DNA methyltransferases, CpG methylation levels were reduced to 30-60% of the normal values.

Next we wanted to characterise histone modification patterns upon HDAC1 knock out or TSA and Aza-dC treatment of cells. Therefore logarithmically growing cells were treated with TSA or Aza-dC and histone acetylation and methylation patterns were monitored *via* Western blot analysis. Histone modification patterns in fibroblast cells lacking functional HDAC1 protein were only slightly influenced. Loss of HDAC1 in fibroblasts was selectively enhancing acetylation of lysine 8 at histone H4 (H4K8ac) as compared to wildtype cells (Figure 2A). All

other histone modifications examined, including active marks such as acetylation of H3K9, H3K14, H4K5, H4K12, H4K16, tri-methylation of H3K4, di-methylation of H3R17m2, H4R3m2 and repressive marks such as mono-, di-, and tri-methylation of H3K9, H3K27, H4K20 remained unaffected. When cells were treated with TSA, major changes in the histone modification landscape were induced: as expected all lysine residues examined were hyperacetylated; remarkably lysine residues proximal to the N-terminal end of the histone exhibited a higher increase in acetylation than lysine residues further distal to the N-terminus (Figure 2A). Other histone modifications were also altered in response to HDI treatment: the active mark H3K4m3 was enriched as well as the repressive mark H3K27m3. Decreased signals for H4K20m3 could be due to loss of this repressive mark or originate from the property of the antibody to recognise the epitope less efficiently, when nearby lysine residues are hyperacetylated (see Figure 3). This could also be valid for H3R17m2 and H4R3m2; however we do not know the features of these antibodies concerning or with respect to epitope recognition upon hyperacetylation. Loss of DNA methylation has severe effects on genomic integrity and gene expression patterns (Jackson-Grusby, 2001) and numerous reports showed physical and functional interaction between the DNA methylation machinery and histone modifying enzymes. Therefore we evaluated histone modification patterns after inducing reduced DNA methylation levels. We found two opposing effects caused by Aza-dC treatment: on the one hand, active marks correlating with gene transcription such as H3ac, H3K9ac, H4ac, H4K5ac, H4K8ac, H4K12ac and H3K4m3 were increased, on the other hand histone modifications usually considered as repressive marks and associated with heterochromatin showed marked enrichment, notably H3K9m3, H3K27m3, H4K20m2 and H4K20m3.

The data presented so far, show that interfering with single aspects of epigenetic regulatory pathways also had consequences on several other, not directly targeted pathways.

In detail, genetic inactivation of HDAC1 in fibroblasts lead to a 30% decrease in total HDAC activity, albeit the upregulation of its close homologue and interaction partner, HDAC2. Work from others demonstrated that in immortalised fibroblasts the activity of HDAC1/HDAC2 containing multiprotein-complexes was altered (J. Jurkin, diploma thesis, 2006) and a small number of genes was deregulated (Y. Zhang, FMI, Basel). Here we show that global histone modification patterns were only modestly and specifically changed, i.e. H3K8ac was increased, while all other modifications examined remained equal. This finding is in contrast to recent findings from embryonic stem cells (ESCs), where loss of HDAC1 lead to a more pronounced hyperacetylation detectable with antibodies against pan-acetylated histones H3 and H4 (Lagger, 2002) and a reduction of H3K9m3. Furthermore up to seven percent of all genes were found deregulated (Zupkovitz, 2006), suggesting that in less committed ESCs histone deacetylation may play a more dominant role in gene silencing than in fully

committed fibroblasts, where more stable marks might take over this task. Another finding was that the HDAC1 protein was not necessary for proper maintenance of DNA methylation patterns of transposable elements. This is interesting, since HDAC1 and DNMT1 physically interact (Fuks, 2000) but it is still unclear, whether this interaction is essential for DNMT1 function. Additionally there are reports linking HDAC inhibition with loss of DNA methylation in cancer cells (Ou, 2007; Milutinovic, 2007). However, these reports suggest a mechanism involving active demethylation rather than passive loss of DNA methylation and HDACs acting indirectly. Nevertheless, we did not observe changes in DNA methylation levels of IAP retrotransposons when cells were treated with TSA for 24h. HDAC inhibition caused a global increase of histone acetylation, most prominent at lysine residues within the proximity of the N-terminus. So far we cannot fully explain this phenomenon; possible reasons could be that (i) HDACs preferentially deacetylate lysines proximal to the N-terminus leading to low levels of steady state acetylation near the N-terminus (ii) HATs preferentially acetylate lysine residues distal to the N-terminus, or if different HATs have distinct specificities, those which preferentially acetylate distal lysines are dominant. To answer this question we need more insight into the specificity of HDACs and HATs on native substrates. Data obtained *in vitro* may support a model where HATs deliver specificity and HDACs unspecifically remove acetyl-moieties from lysines and thereby maintain a silenced ground state. Other histone modifications altered upon TSA treatment were increased tri-methylation of H3K4 and H3K27. While H3K4m3 was most likely enriched because the H3K4 specific demethylase LSD1 removes methyl-groups less efficiently from hyperacetylated histones (Shi, 2005; Lee, 2006), the reason for H3K27m3 enrichment remains unclear. Although it is well established that HDAC1 and HDAC2 are components of certain PcG complexes (van der Vlag, 1999), which deliver H3K27 tri-methylation, functional data on the influence of histone acetylation on K27 methylation are lacking. A speculative model may interpret the increase in H3K27m3 as compensatory mechanism counteracting the possible release of PcG target gene expression upon hyperacetylation. An alternative is the involvement of HDACs in H3K27 demethylation by recently discovered JmjC-domain containing proteins.

Aza-dC treatment of fibroblasts had severe and complex consequences on several epigenetic modifications. In accordance with previous work, DNA methylation levels were decreased as exemplified with the analysis of several IAP LTR retrotransposon subtypes. Furthermore there was an increase in histone acetylation; interestingly we detected a preference for lysine residues proximal to the N-terminus what is reminiscent of the changes induced by TSA treatment, although Aza-dC has more subtle effects. The interplay between DNA methylation and histone acetylation is well established and additionally to the physical interaction between HDAC1 and DNMT1, methyl CpG binding domain (MBD) proteins are integral components of the NuRD complex and thought to target HDAC1/HDAC2 containing

complexes to methylated DNA (Denslow, 2007). Therefore the increase in histone acetylation could be a direct consequence of diminished HDAC recruitment to target genes and consequently lead to increased H3K4m3 levels. Explanations for the enrichment of the repressive marks H3K9m3, H3K27m3, H4K20m2 and H4K20m3 are less obvious; one might regard it as a compensatory mechanism for the loss in repression caused by reduced DNA methylation; however this does not throw light on possible mechanisms involved in this process.

In summary we uncovered a combination of direct and indirect effects mediated by the application of chemical inhibitors, some of them already described and analysed, others novel and waiting to be elucidated.

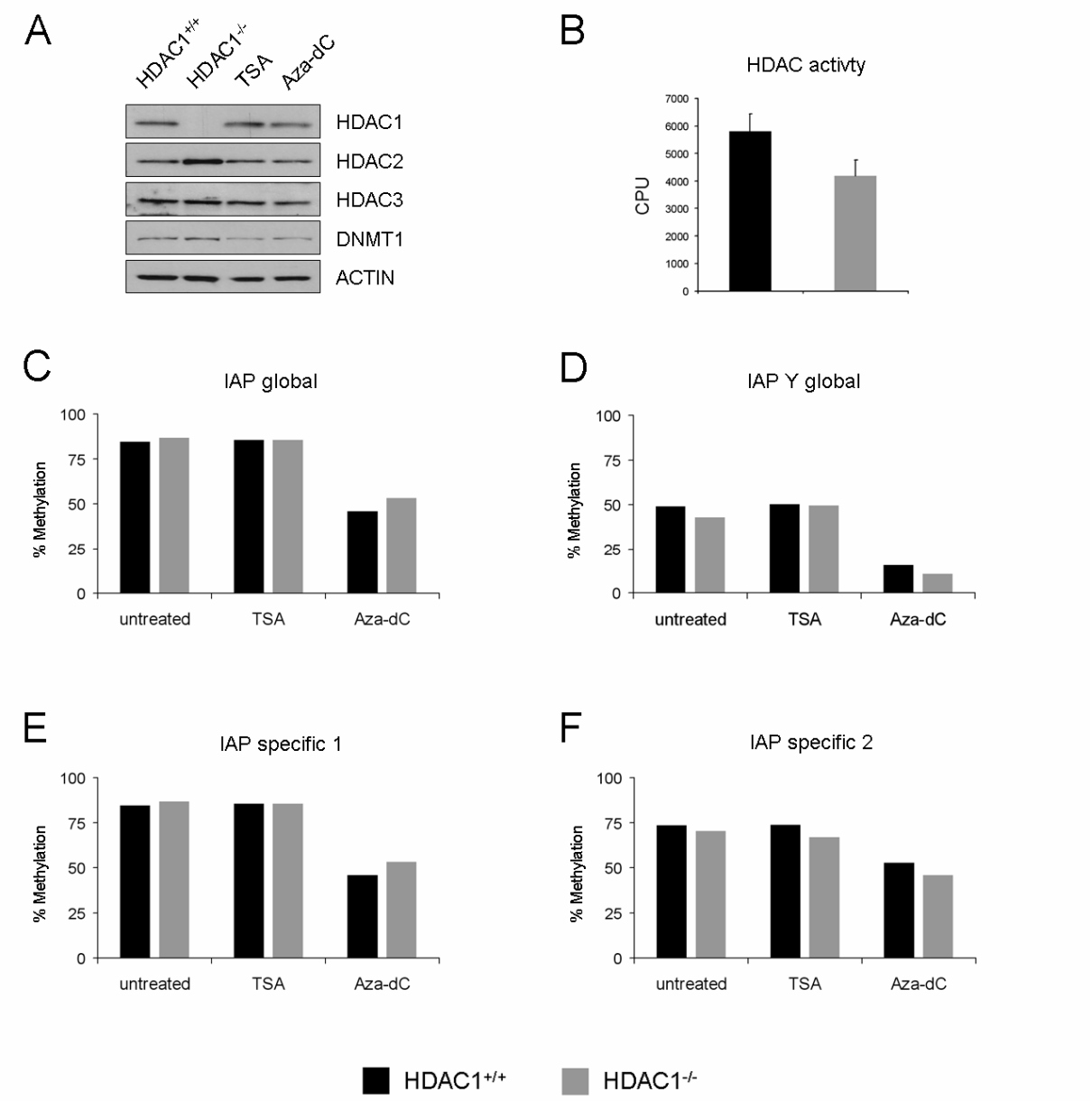

Figure 1. Genetic inactivation of HDAC1, chemical inhibition of class I and II HDACs or DNA methylation leads to changed protein levels of targeted genes, total HDAC activity and DNA methylation of IAP retrotransposons.

(A) Logarithmically growing HDAC1$^{+/+}$ and HDAC1$^{-/-}$ fibroblasts were treated with 166nM TSA for 24h, with 1µM Aza-dC for 24h followed by incubation without inhibitor for another 24h or incubated with vehicle DMSO (untreated), harvested and subjected to Western blot analysis. Protein levels were determined with specific antibodies. Loss of HDAC1 lead to the upregulation of HDAC2; TSA and Aza-dC treatment to a slight reduction in DNMT1 levels. ACTIN served as loading control.

(B) Total histone deacetylase activity was determined from equal amounts of protein extracts isolated from HDAC1$^{+/+}$ (black bar) and HDAC1$^{-/-}$ (grey bar) fibroblasts incubated with [^{3}H]acetate labelled chicken erythrocyte histones. Counted radioactivity corresponds to the amount of released acetyl moieties per hour and 10µg protein and reflects relative deacetylase activity. Values correspond to the average of four independent experiments. Inactivation of HDAC1 resulted in a 30% reduction of total HDAC activity.

(C) – (F) DNA methylation levels of HDAC1$^{+/+}$ (black bars) and HDAC1$^{-/-}$ (grey bars) fibroblast cells, treated as in (A). Methylation of the LTR region of IAP retrotransposons was determined employing the Ms-SNuPE technique as described recently (Gonzalgo, 1997). (C) Average methylation status of two CpG sites within the LTR of multiple copies of retrotransposition competent IAP elements (Dewannieux, 2004). (D) Average methylation of two CpG sites of a multi-copy Y chromosome specific species of IAP elements (Fennelly, 1996). (E) DNA methylation of the LTR region of a retrotransposition competent IAP element exhibiting 100% LTR homology (Dewannieux, 2004). Values correspond to the average methylation of 3 CpG sites. (F) Methylated CpG sites within the LTR of an IAP element, which shows 86% LTR homology and is therefore considered as evolutionary old. Values represent the average methylation of 3 CpG sites. All classes of IAP elements examined in (C) – (F) showed decreased DNA methylation upon Aza-dC treatment, but levels remained constant upon loss of HDAC1 or treatment with TSA.

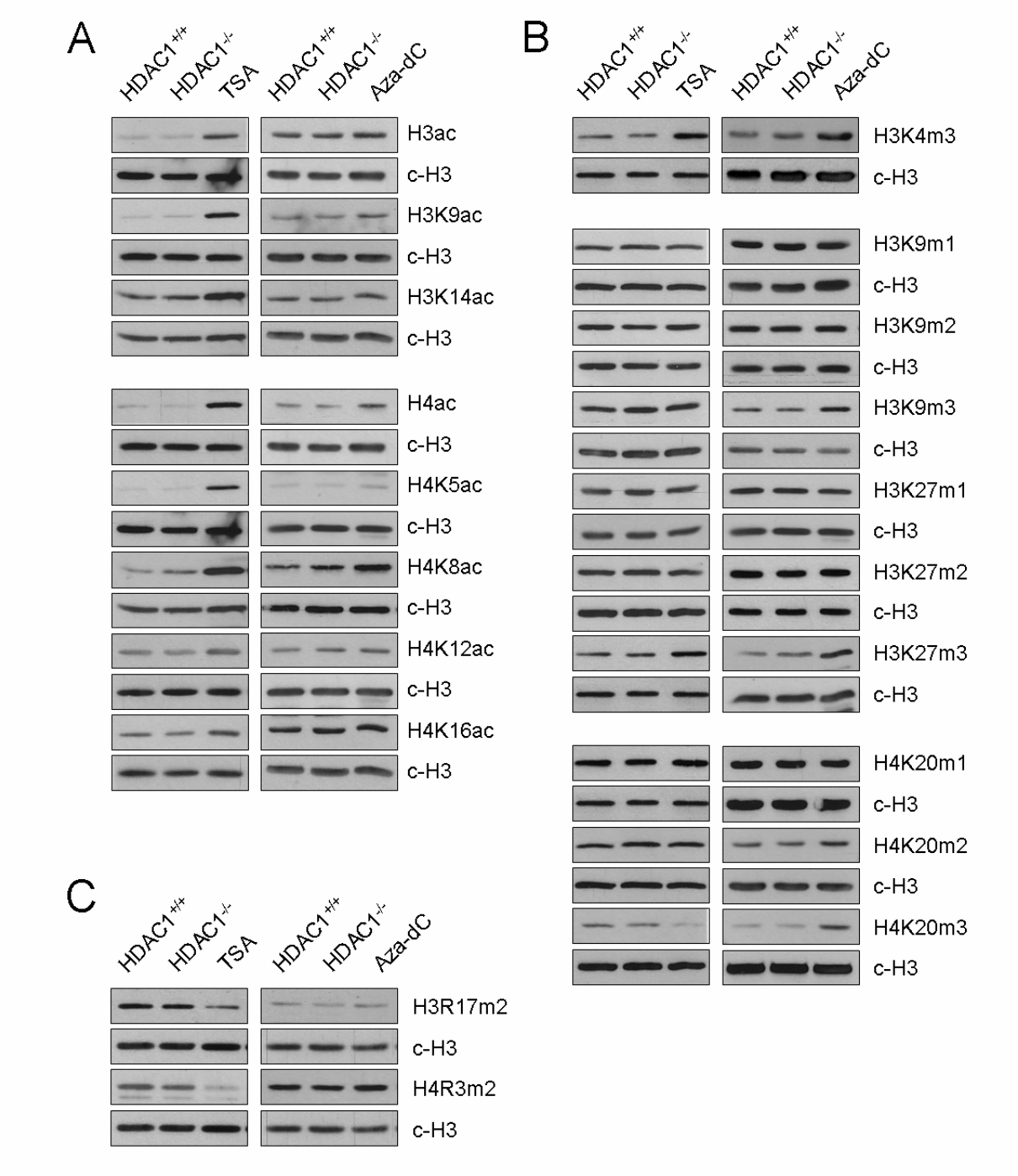

Figure 2. Histone modification patterns are altered upon HDAC1 knock out, HDAC inhibition and decrease in DNA methylation.

(A) Logarithmically growing HDAC1$^{+/+}$ and HDAC1$^{-/-}$ fibroblast cells were treated with 166nM TSA for 3h or with 1µM Aza-dC for 24h followed by incubation without inhibitor for another 24h or incubated with vehicle, harvested, histones were extracted and subjected to Western blot analysis. Antibodies recognising pan-acetylated histone proteins H3 (H3ac) and H4 (H4ac) were used as well as antibodies recognising acetylation marks at defined lysine residues (H3K9ac, H3K14ac, H4K5ac, H4K8ac, H4K12ac, H4K16ac). An antibody directed against the c-terminal part of histone H3 (c-H3) served as loading control.

(B) To monitor histone lysine methylation patterns after HDAC1 knock out, TSA or Aza-dC treatment, cells were treated as in (A) with the exception that TSA was applied for 24h. Antibodies used were directed against either mono-, di- or tri-methylated lysine residues; the antibody against the c-terminus of H3 served as loading control.

(C) Methylation status of arginine residues. Cells were treated as in (B).

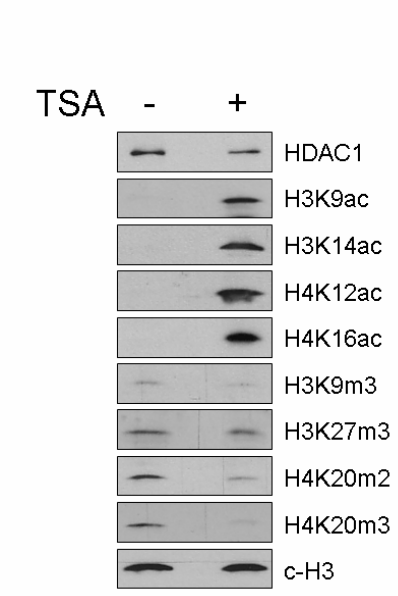

Figure 3. Characterisation of antibodies recognising specifically modified histone proteins.
To test the influence of acetylation of neighbouring lysine residues on epitope recognition, hyperacetylated histone proteins were incubated with recombinant HDAC1 and the cofactor RbAp48 leading to deacetylation of histone proteins at multiple lysine residues as detected with antibodies against H3K9ac, H3K14ac, H4K12ac and H4K16ac. Addition of TSA to the reaction inhibited deacetylation (left lane). While antibodies directed against trimethylated K9 and K27 were not influenced in their ability to recognise their epitopes by differential acetylation state of neighbouring lysine residues, the antibodies against H4K20m2 and H4K20m3 were disturbed in their epitope recognition. To demonstrate equal loading of histones, an antibody recognising the N-terminus of histone H3 was included in the analysis.

4.2. Histone acetylation of transposable elements

Having monitored general changes in chromatin and DNA methylation patterns upon HDAC1 inactivation, HDAC inhibition and reduction in DNA methylation, we went on to specifically address the role of histone acetylation in the regulation of transposable elements. Therefore we wanted to know the acetylation status of chromatin associated with transposable elements. $HDAC1^{+/+}$, $HDAC1^{-/-}$, TSA treated and Aza-dC treated fibroblasts were harvested; chromatin was isolated and subjected to chromatin immunoprecipitation (ChIP) experiments. Antibodies recognising pan-acetylated histones H3 and H4, were used to monitor the acetylation status, antibodies recognising the c-terminal part of histone H3 to survey the nucleosome density and unspecific rabbit IgGs served as controls for the specificity of the immunoprecipitation reaction. Real Time PCR analysis allowed the quantification of histone acetylation levels of the transposable elements listed in Table 1. Additionally two single copy genes were included as examples for not repetitive sequences: Pde10a, encoding phosphodiesterase 10A, located on chromosome 17 and Gsn, encoding gelsolin, located on chromosome 2. Both genes are not or only weakly expressed in untreated fibroblasts and the latter one can be transcriptionally induced by TSA treatment. As seen in Figure 4 HDAC1 deletion in fibroblasts did not change H3ac, H4ac and nucleosome density at any of the loci investigated. In contrast to this, TSA treatment for 3h (Figure 5) or 24h (Figure 6) was perturbing histone acetylation levels associated with transposable elements. As apparent in Figures 5A and 6A, H3ac was enriched at SINE B1, SINE B2 and VL30 transposable elements as well as the promoter of the Gsn gene, whereas H4ac was highly induced at all transposable elements analysed as well as both single copy control regions (Figure 5B and 6B). Thus, hyperacetylation of histone H3 upon HDAC inhibition seems to be restricted to specific sequences while hyperacetylation of H4 seems to be a phenomenon common to all kinds of transposable elements as well as at least some single copy genes. Figure 7 shows H3 and H4 histone acetylation levels upon Aza-dC treatment, which were enriched at specific sequences including SINE B1, SINE B2, VL30 and IAP elements. Noteworthy H3ac and H4ac levels were equally enriched at both histones, with the exception of SINE B2 elements, where only H4ac was increased.

A fact, one should take into consideration when interpreting these data is the restricted specificity when using consensus primers for quantification. This is relevant especially for SINE elements, which are highly abundant short sequences found throughout the genome including intergenic regions, introns and promoters. Therefore the chromatin status of numerous SINEs might closely depend on the genomic environment rather than on SINE specific factors and increased histone acetylation as detected with consensus primers might mirror enriched acetylation of a subgroup of elements located e.g. in the proximity of

promoters and not a general increase in acetylation of SINE elements. When focusing on LTR elements this objection might be less relevant, since LTR retrotransposons are bigger and therefore do not represent integral parts of regulatory regions of other genes to the same degree.

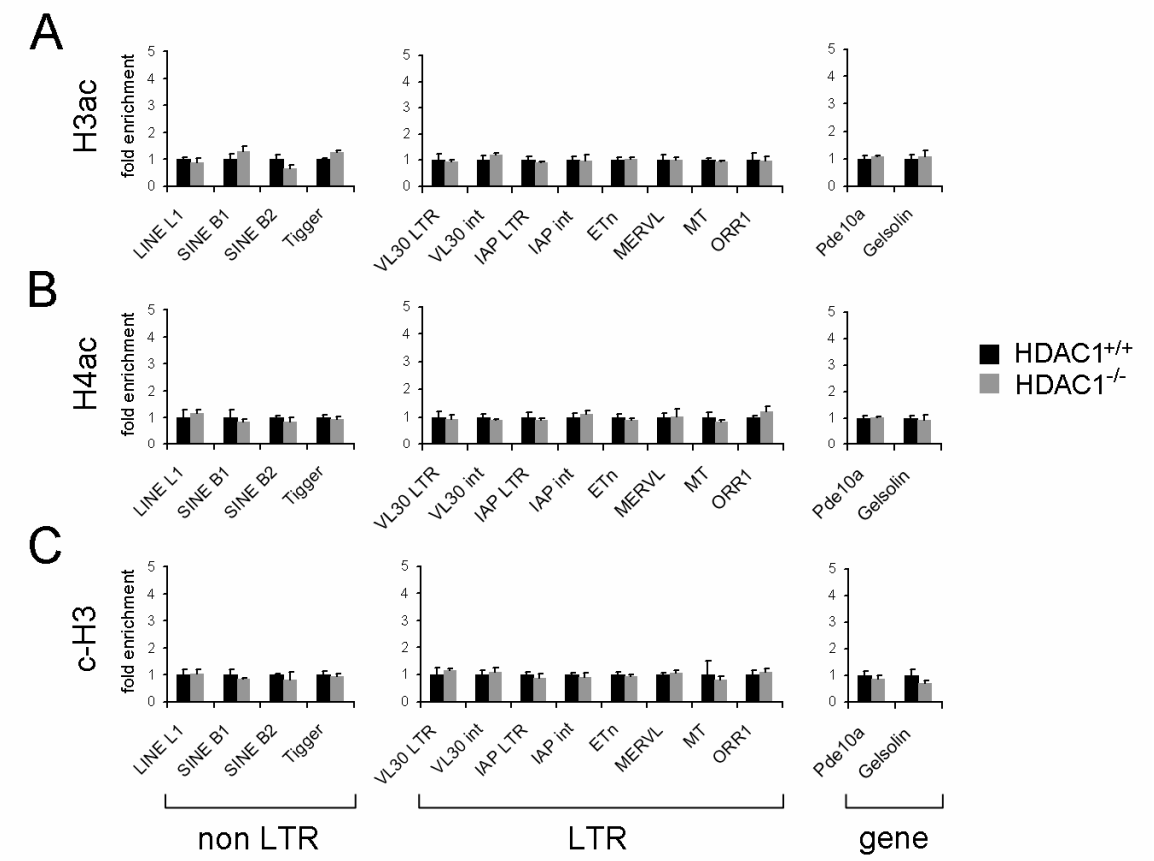

Figure 4. Histone acetylation states of transposable elements in HDAC1$^{+/+}$ and HDAC1$^{-/-}$ fibroblasts.
ChIP experiments with chromatin from HDAC1$^{+/+}$ and HDAC1$^{-/-}$ were performed and acetylation levels were determined *via* Real Time PCR. Values are presented as relative enrichment of acetylation compared to HDAC1$^{+/+}$ cells and each bar represents the average of at least three independent experiments. HDAC1 deletion does not influence H3 and H4 acetylation of chromatin associated with transposable elements (A and B) or nucleosome density (C). ± SEM. n=3.

Figure 5 and 6. Histone acetylation states of transposable elements are altered upon TSA treatment.
HDAC1$^{+/+}$ fibroblasts were treated with 166nM TSA for 3h (Figure 5) or 24h (Figure 6), chromatin was isolated and ChIP experiments were performed. For quantification Real Time PCR was employed. Values represent the average of at least three independent experiments and are given as relative enrichment based on the values obtained in untreated cells. Apart from some minor differences, 3h and 24h TSA treatment leads to similar changes in histone acetylation; H3ac is specifically enriched in SINE B1, SINE B2, VL30 elements and Gsn (Fig. 5A and 6A) while H4ac is enriched at all studied sequences (Fig. 5B and 6B). Nucleosome density is not influenced as assayed *via* ChIP using an antibody against c-term H3 (Fig. 5C and 6C). ± SEM. n=3.

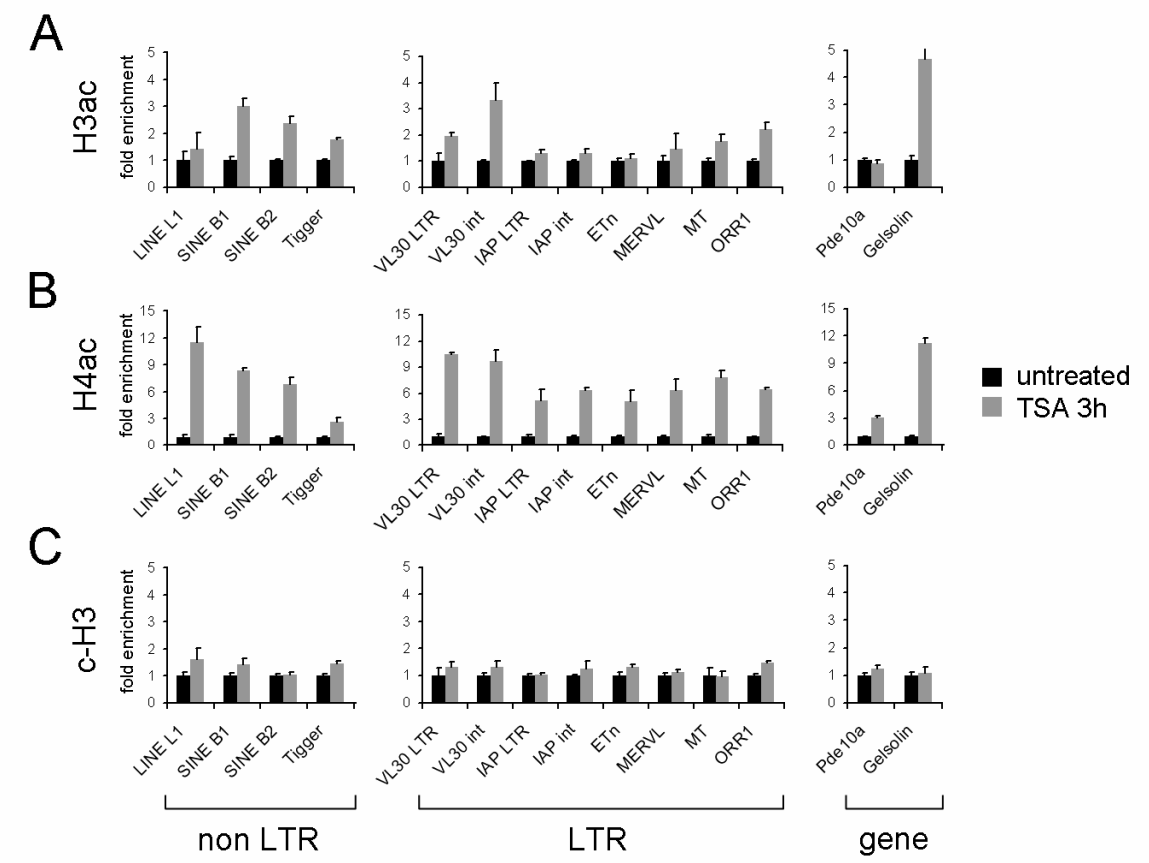
A
H3ac
fold enrichment
B
H4ac
fold enrichment
C
c-H3
fold enrichment
LINE L1
SINE B1
SINE B2
Tigger
VL30 LTR
VL30 int
IAP LTR
IAP int
ETn
MERVL
MT
ORR1
Pde10a
Gelsolin
untreated
TSA 3h
non LTR
LTR
gene

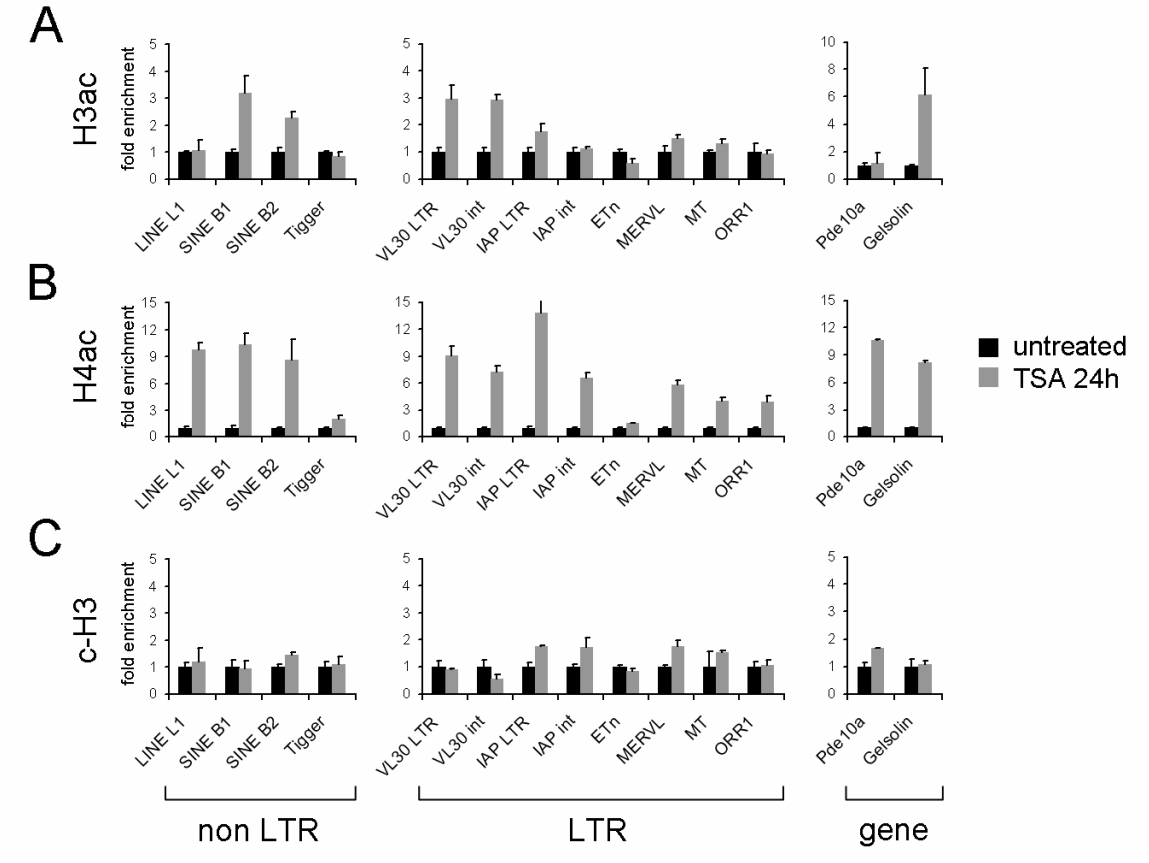
A
H3ac
fold enrichment
B
H4ac
fold enrichment
C
c-H3
fold enrichment
LINE L1
SINE B1
SINE B2
Tigger
VL30 LTR
VL30 int
IAP LTR
IAP int
ETn
MERVL
MT
ORR1
Pde10a
Gelsolin
untreated
TSA 24h
non LTR
LTR
gene

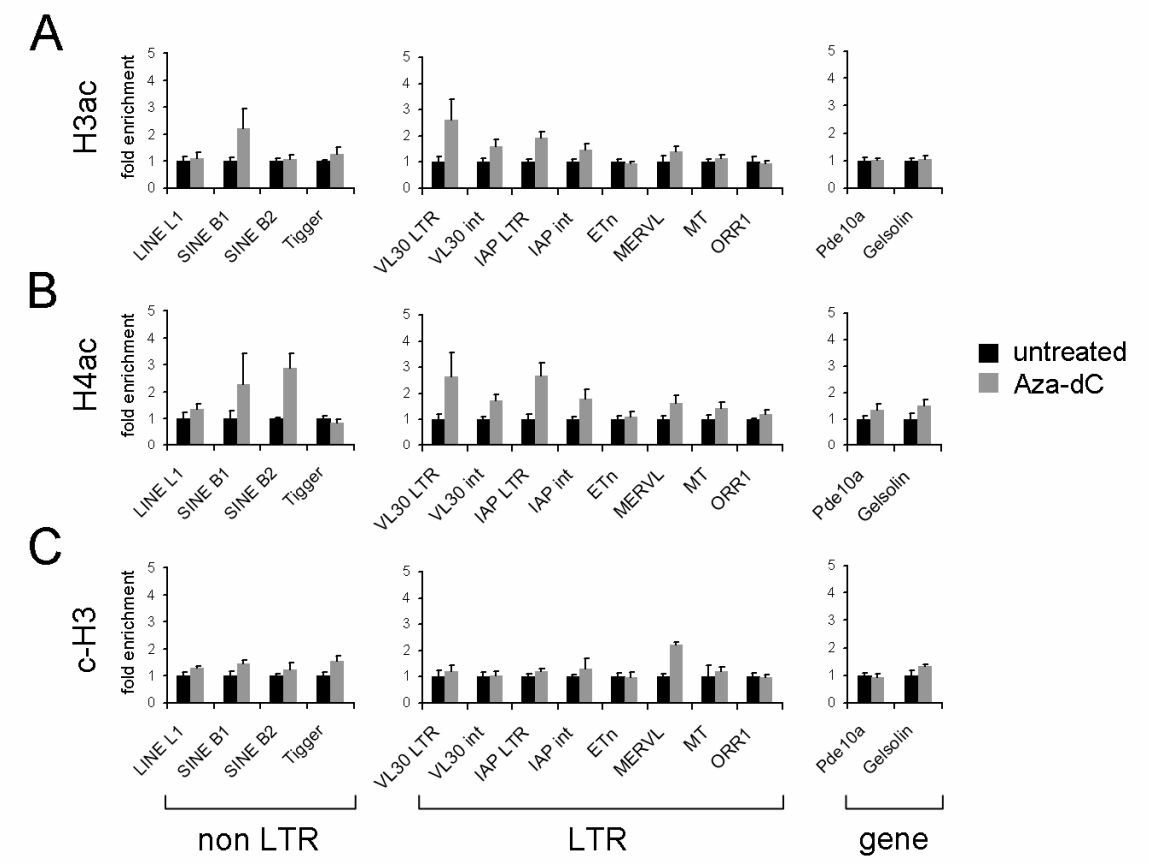

Figure 7. Histone acetylation states of transposable elements are altered upon Aza-dC treatment. HDAC1$^{+/+}$ fibroblasts were treated with 1µM Aza-dC for 24h followed by incubation without inhibitor for another 24h, then chromatin was isolated and ChIP experiments were performed. For quantification Real Time PCR was employed. Values represent the average of at least three independent experiments and are given as relative enrichment based on the values obtained in untreated cells. H3ac and H4ac are similarly enriched at SINEs, VL30 and IAP elements (A and B) whereas nucleosome density shows no major changes (C). ± SEM. n=3.

				PCR Amplicons	
Class	**Sub-Class**	**Element**	**Copy Number**	**Expression**	**ChIP**
LINE		L1	599000*	ORF2 (2400-2600)	ORF2
SINE	7SL RNA	B1	564000*	-	-
	tRNA	B2	348000*	-	-
DNA		Tigger	24000*	internal (250-550)	internal
LTR	ERV Class I	VL30	150-200^{+}	pol (3700-4100)	5'LTR (600-840)/pol
	ERV Class II	IAP	1000^{+}	gag (1000-1300)	5'LTR (30-200)/gag
	ERV Class II	ETn	300-400^{+}	-	-
	ERV Class III	MERVL	200^{+}	pol (3900-4200)	pol
	MaLR (III)	MT	13000-50000°°	internal (450-700)	internal
	MaLR (III)	ORR1	10000-38000°°	internal (1400-1600)	internal

Table 1. List of Transposable elements analysed. Classification of transposable elements, copy number and approximate location of primers used to survey the expression and histone modification status of TEs. *Waterston 2002; $^{+}$Maksakova 2006; °°Smit 1993; note that the last Reference is out-dated and might underestimate the actual number of MT and ORR1 elements.

4.3. Expression of transposable elements

To test whether the changes in histone acetylation mediated by TSA and Aza-dC mirrored changes in the biological activity of the TEs, we monitored expression levels of the elements listed in Table 1. RNA from HDAC1$^{+/+}$, HDAC1$^{-/-}$, TSA treated and Aza-dC treated fibroblasts was isolated, reversely transcribed and subjected to Real Time PCR analysis. Figure 8 summarises the results of HDAC1$^{-/-}$ (Fig. 8A), TSA treated (Fig. 8B) and Aza-dC (Fig. 8C) treated fibroblasts compared to untreated HDAC1$^{+/+}$ cells. Loss of HDAC1 did not influence TE expression, what was not surprising, since acetylation levels of histones associated with TEs in HDAC1$^{-/-}$ fibroblasts were not affected. As shown in Fig. 8A treatment with TSA lead to a modest increase in the expression of some transposable elements (LINE1, SINE B1, SINE B2, IAP, ETn, MERVL). Strikingly, expression levels of VL30 elements were highly induced. Aza-dC treatment strongly enhanced the expression of VL30 as well as IAP elements, corroborating earlier reports (Davis, 1989; Tzavaras, 2003). To confirm that the results obtained do not mirror the behaviour of a particular fibroblast cell line, we additionally tested TE expression levels in the two widely used fibroblast cell lines Swiss 3T3 and NIH/3T3. As summarised in Table 2, TSA and Aza-dC treatment had similar effects on TE expression with a significant enrichment of VL30 transcripts in TSA and Aza-dC treated cells and enrichment of IAP transcripts upon Aza-dC application. Interestingly, in embryonic stem cells VL30 elements could not be induced by TSA or Aza-dC. Instead ETn elements showed elevated mRNA levels, indicating cell type specific regulation of transposable elements. Of further interest was the accumulation of IAP but not VL30 transcripts in DNMT1 knock out brains, although reduction of DNA methylation *via* the chemical inhibitor Aza-dC lead to activation of VL30 elements in fibroblasts (Table 2). This discrepancy could be due to (i) the lack of factors promoting VL30 expression in neuronal cells or (ii) DNMT1 independent activation of VL30 expression in Aza-dC treated cells. We favour the second alternative for the following reasons: first, others could show that VL30 expression could be induced by certain stimuli in neuronal cells (Costain, 2006) and second, Aza-dC might have additional effects besides the reduction of DNA methylation (e.g. DNA damage) which could be the causative reason for VL30 induction.

Having established the regulation of VL30 and IAP retrotransposons *via* histone acetylation and DNA methylation in fibroblasts, we went on to compare TE expression data with the acetylation status upon inhibitor treatment. Thereby, three major points became evident: (i) expression levels of LTR retroelements correlated with the acetylation status of histone H3, when cells were exposed to TSA. As described before, H4 acetylation was increased unspecifically. (ii) Upon Aza-dC treatment H3ac as well as H4ac was specifically enriched at LTR elements showing enhanced expression. (iii) Hyperacetylation of SINEs as induced by

TSA (SINE B1, SINE B2) and Aza-dC (SINE B1) was accompanied by only minor increases in mRNA, if at all. Obviously, there is a discrepancy between the behaviour of LTR elements on the one hand and SINEs on the other hand; the reason for this might be similar to the reason for enriched histone acetylation found at SINEs after TSA treatment: these short sequences are integral parts of numerous genes and therefore the modest increase in transcript abundance might originate from increased transcription of genes harbouring SINE sequences within the gene body rather than from weak induction of SINE expression itself. However, although we favour this model, we cannot rule out the second alternative. In contrast to this, high activation of the LTR elements VL30 and IAP is more likely to originate from activation of the element itself.

In summary, we could not only show a correlation between TE expression and histone acetylation states but also identified a class of LTR elements (VL30) which can be transcriptionally activated by HDAC inhibition.

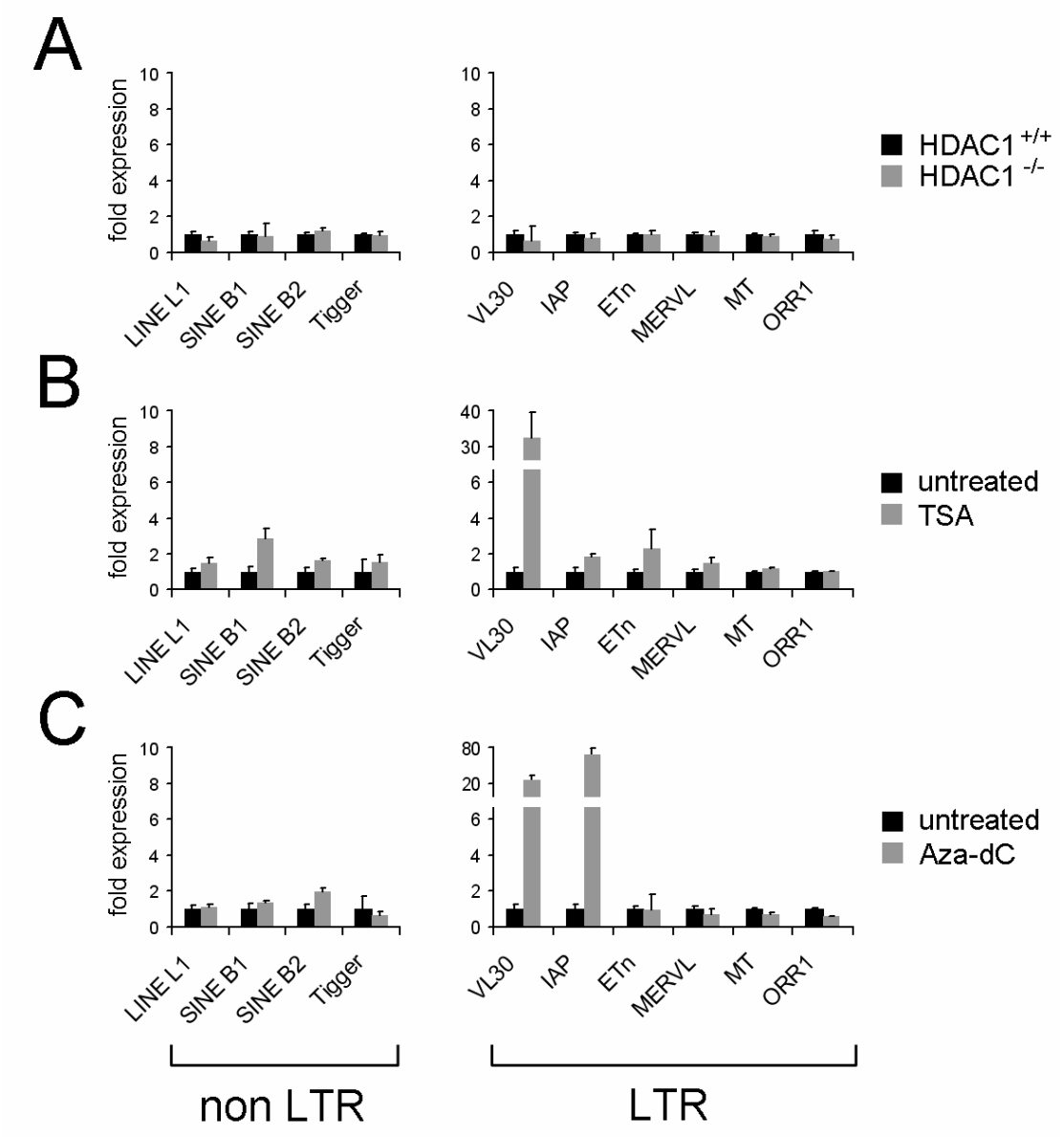

Figure 8. Expression levels of transposable elements are altered upon TSA and Aza-dC treatment.
Cells were left untreated, grown in medium containing 166nM TSA for 24h or supplemented with 1µM Aza-dC for 24h followed by growth for 24h in inhibitor free medium. mRNA levels of different TEs were analysed *via* Real Time PCR. Values were normalised to the housekeeping gene HPRT, and shown as relative values compared to untreated wildtype fibroblasts. Bars represent the average of at least three independent experiments. ± SD. (A) HDAC1 knockout does not influence TE expression. (B) Upon TSA treatment, expression of the LTR retrotransposon VL30 is increased more than thirty times. (C) Aza-dC has the ability to highly induce expression of VL30 as well as IAP retrotransposons.

Table 2

		RNA											DNA
		LINE	SINE		LTR								
					ERV_classI			ERV_classII		ERV_classIII			
		L1	B1	B2	RLTR1b	RLTR6	VL30	IAP	ETn	MERVL	MT	ORR1	Tigger
HDAC1-/-	embryos E9.5	2.2 ± 1.8	1.3 ± 0.9	1.1 ± 0.6	ND	ND	2.0 ± 1.3	1.7 ± 1.5	1.4 ± 1.1	ND	2.1 ± 1.5	1.6 ± 1.1	ND
	brain P11	1.6 ± 1.0	1.3 ± 0.9	1.2 ± 0.8	ND	ND	1.2 ± 0.5	1.2 ± 0.6	ND	1.5 ± 1.1	1.5 ± 0.8	ND	ND
	fibroblasts	0.6 ± 0.4	0.9 ± 0.4	1.2 ± 0.6	0.5 ± 0.5	0.4 ± 0.1	0.6 ± 0.4	0.8 ± 0.1	1.0 ± 0.4	0.9 ± 0.2	0.9 ± 0.3	0.7 ± 0.2	0.9 ± 0.4
TSA	fibroblasts	1.5 ± 0.3	2.9 ± 0.6	1.7 ± 0.1	1.0 ± 0.2	1.8 ± 0.3	31.9 ± 7.2	1.9 ± 0.1	2.3 ± 1.0	1.5 ± 0.2	1.2 ± 0.0	1.0 ± 0.1	1.6 ± 0.4
	3T3 Swiss	0.5 ± 0.1	1.2 ± 0.6	1.3 ± 0.1	ND	ND	13.1 ± 1.9	0.4 ± 0.1	ND	0.3 ± 0.1	0.6 ± 0.1	0.7 ± 0.1	ND
	NIH/3T3	2.7 ± 1.2	1.8 ± 0.8	1.6 ± 0.2	ND	ND	8.3 ± 1.1	1.9 ± 0.7	2.6 ± 1.2	1.7 ± 0.4	1.7 ± 0.3	1.8 ± 0.6	ND
	ESCs	1.8 ± 0.1	1.9 ± 0.3	1.3 ± 0.0	ND	ND	2.1 ± 0.3	2.4 ± 0.4	6.3 ± 0.5	2.2 ± 0.1	1.5 ± 0.2	2.2 ± 0.1	1.8 ± 0.2
DNMT-/-	brain P11	1.1 ± 0.2	1.6 ± 0.3	1.3 ± 0.4	1.1 ± 0.0	1.5 ± 1.2	1.3 ± 0.2	50.0 ± 4.1	0.9 ± 0.2	1.0 ± 0.3	1.2 ± 0.1	1.3 ± 0.4	0.7 ± 0.2
Aza-dC	fibroblasts	1.1 ± 0.2	1.3 ± 0.1	2.0 ± 0.2	1.6 ± 1.2	1.1 ± 0.4	31.1 ± 6.9	69.6 ± 8.6	0.9 ± 0.2	0.7 ± 0.3	0.7 ± 0.6	0.6 ± 0.0	0.6 ± 0.2
	3T3 Swiss	0.9 ± 0.5	2.0 ± 0.7	0.6 ± 0.1	ND	ND	5.4 ± 0.8	5.4 ± 1.3	ND	0.4 ± 0.3	1.5 ± 0.4	0.9 ± 0.3	ND
	NIH/3T3	4.7 ± 0.7	1.4 ± 0.2	2.1 ± 0.3	ND	ND	5.9 ± 1.2	326.5 ± 30	3.4 ± 1.7	2.0 ± 0.6	2.2 ± 0.6	1.5 ± 0.9	ND
	ESCs	2.5 ± 0.3	2.7 ± 0.5	1.2 ± 0.1	ND	ND	1.8 ± 0.1	8.2 ± 0.5	9.0 ± 6.7	3.3 ± 0.6	1.9 ± 0.2	2.3 ± 0.1	1.2 ± 0.1

Expression analysis of transposable elements in different genetic backgrounds (HDAC1-/-; DNMT1-/-) and upon chemical inhibition of HDACs (TSA) and DNMTs (Aza-dC) in different biological systems.

mRNA levels of indicated transposable elements have been monitored in the following systems: murine embryos harvested at day 9.5 of embryonic development (embryos E9.5), whole brain extracts of mice at postnatal day 11 (brain P11), fibroblasts derived from BL6/129Sv mice and immortalised according to the 3T3 immortalisation protcol (fibroblasts), 3T3 Swiss fibroblasts (3T3 Swiss), NIH/3T3 fibroblasts (NIH/3T3) and embryonic stem cells obtained by blastocyst outgrowth experiments (ESCs). HDAC1+/+, +/- and -/- embryos were obtained from intercrosses between BL6/129Sv mice heterozygous for the HDAC1 gene (Lagger, 2002); HDAC1 and DNMT1+/+ and -/- brains were obtained from mice carrying two floxed alleles of the corresponding gene. To delete HDAC1 or DNMT1 specifically in the brain the cre recombinase transgene driven by the neuronal specific Keratin 5 promoter was introduced leading to the deletion of HDAC1 or DNMT1 in neurons; HDAC1+/+ and -/- fibroblasts as well as ESCs were established as described in Materials and Methods. 3T3 Swiss and NIH/3T3 are widely used fibroblasts commonly available. For TSA treatment logarithmically growing cells were supplied with 166nM TSA for 24h (3T3 Swiss fibrobalsts: 332nM; ESCs: 66nM), for Aza-dC treatment logarithmically growing cells were incubated with 1µM Aza-dC for 24h (3T3 Swiss fibroblasts: 100µM) followed by incubation for 24h without inhibitor.
TE expression levles were determined via Real Time PCR and values represent fold expression of TEs normalised to the levels in the corresponding untreated cell line or wildtype tissue. Experiments were at least perfomed twice. For reasons of clarity, values > 5 are highligthed with a grey box, values > 2.5 with an open box.
± SD; ND not determined.

4.4. Single locus *versus* multi copy origin

Whenever working with transposable elements, one should be aware of a specific feature of repetitive elements: they exist in multiple copies distributed all over the genome and therefore individual elements are different in respect of genomic environment influencing chromatin status and potential transcriptional activity. Furthermore, TEs are under high selective pressure and mutation mediated by host or TE-intrinsic factors leads to the generation of a pool of elements with individual sequence specificities. Therefore a class of elements is a collection of similar, but heterogeneous individuals, differing in external and internal features.

Increased transcript levels upon external signals could originate from upregulation of all transposable elements within a class, of a subgroup of elements exhibiting specific features or even a single copy with unique intrinsic or positional properties. In order to distinguish between these different scenarios we analysed VL30 and IAP derived transcripts arising upon TSA and Aza-dC treatment and compared them to transcripts present in untreated cells. mRNA from three independent biological samples each (fibroblasts; TSA, Aza-dC, untreated) was collected, reversely transcribed and subjected to PCR amplification in doublets. To amplify IAP derived transcripts, primers annealing in the highly conserved *gag* region were used, for VL30 transcript amplification primers within the 3' UTR and 3'LTR R region were chosen. The six PCR products derived from each condition were pooled to exclude a bias due to individual PCR reactions, PCR products were cloned and sequenced. As control, the same procedure was also performed with genomic DNA as template for PCR amplification. Each sequenced clone corresponding to an individual transcribed (or genomic) TE was then subjected to further analysis: first, sequences were aligned to scan if the pool of transcripts contained identical sequences emerging repeatedly, what would indicate preferred expression of unique TEs or of a specific subgroup of TEs with high similarity.

This analysis revealed that IAP sequences were heterogeneous, even upon induction of expression with Aza-dC. VL30 sequences lost the heterogeneity existing when left untreated, upon induction of high expression with TSA or Aza-dC. This indicated that IAPs were transcribed from multiple genomic loci, while VL30 elements were transcribed from a limited number of loci when induced. Second, sequences were blasted against the annotated murine genome (http://www.ncbi.nlm.nih.gov/blast/Blast.cgi) to identify genomic TEs serving as potential sources of transcription. Genomic sequences showing at least 98% homology to the cloned sequences were considered to show sufficient homology to be regarded as potential source of transcription. If more genomic sequences showed homology >98%, the sequence with the highest E-value was chosen. That way ~90% of the cloned sequences could be assigned to distinct genomic TEs (IAP: 115 of 127 clones; VL30: 64 of 72 clones).

The complete sequence of these genomic transposons was used to classify the expressed IAP and VL30 elements. As summarised in Table 3, IAP elements expressed under different conditions were full length (44 – 65% of all expressed elements) or belonged to the IΔ1 subgroup (delta I; 12 – 26%), a non autonomous subpopulation of IAP elements carrying a 1.9kb internal deletion and responsible for most of the described insertional mutations. The rest consisted of IAPs carrying miscellaneous other deletions (10 – 30%). Strikingly the proportion in untreated and TSA treated cells was grossly similar to the composition of genomic IAP elements as amplified within the control experiment, when genomic DNA was used as template for the PCR reaction (Figure 11A). This indicates that under those conditions none of the three subtypes is preferentially expressed. Only upon Aza-dC treatment, we noticed a reduced contribution of IAP elements carrying internal deletions to the pool of expressed IAPs, which seemed to be non-random ($X^2 = 0.025$). Next we analysed the regulatory regions of the sequenced IAP elements, the long terminal repeats (LTRs). Comparing the 5' LTR to the 3' LTR of given IAP elements demonstrated that with the primers used, we amplified exclusively evolutionary young IAP elements, as the majority of the 5' LTRs showed 100% identity with the corresponding 3' LTRs (78%), a signature for recent integration. The remaining 22% still exhibited at least 97.8% 5' LTR – 3' LTR homology (Table 3). Alignment and phylogenetic analysis of the LTRs revealed no significant difference between genomic copies, elements expressed under non-inducing conditions (untreated, TSA) and elements expressed upon induction of high expression (Aza-dC) (Tree 1). However, comparison of the LTR length disclosed a marked peculiarity of IAP elements expressed after Aza-dC treatment: the average length of the LTR was 375bp in contrast to 350, 352 or 356bp for genomic IAPs, elements expressed when cells were untreated or TSA treated (Figure 11B, Table 3). This increment in length was caused by the presence of additional nucleotides in the highly variable CT-rich R region. The region encoded of varying numbers of the 17bp or 15bp tandem repeat sequences CTCTCTCTTGCTTCTTG or CTCTCTTGCTTCTTG (identified with the Tandem Repeat Finder Program http://tandem.bu.edu/trf/trf.html using default settings; Benson, 1999), containing a binding site for the CCAAT/enhancer-binding protein alpha (C/EBPalpha) transcription factor (identified with the Alibaba2.1 transcription factor binding site prediction program using the TRANSFAC 4.0 database). IAP elements expressed upon Aza-dC treatment comprised 2 – 3 binding sites, the others 1 – 2, indicating that expression of IAP elements was strongly enhanced by the presence of additional C/EBPalpha binding sites when restricting DNA methylation was lost.

Analysis of VL30 elements revealed that the main fraction of genomic elements was associated with LTRs containing a type III U3 region (Tree 2). It was demonstrated earlier (French, 1997) that the U3 region is crucial for transcriptional regulation and so far, four

subtypes have been classified (Nilsson, 1994). Elements expressed in untreated fibroblasts showed similar characteristics concerning the U3 region, indicating that under those conditions, many of the genomic copies are transcribed and there is no preference towards the expression of specific subtypes. When VL30 expression was induced by HDAC or DNMT inhibitors, the composition of transcribed subtypes exhibited major changes. The majority of the cloned sequences contained U3 regions of the subtype IV, the remaining ones of the subtype I, but no sequences encoding U3 subtype III regions were identified (Figure 11C, Table 4). Phylogenetic analysis of the U3 sequences showed, that the U3 subtype IV regions were almost identical and possibly were derived from a single genomic copy (Tree 2). Screening the murine genome with BLAST identified only one genomic locus with significant similarity supporting the hypothesis that these sequences may stem from a single VL30 element. Detailed analysis of this VL30 element gave rise to a surprising finding: whereas the 3' LTR contained a subtype IV U3 region, the 5' LTR contained a subtype I U3 region. The source of transcription might therefore be a hybrid element whose expression is driven by a 5' LTR subtype I U3 regulatory region. That way, all transcripts cloned upon TSA or Aza-dC treatment might originate from elements driven by a type I U3 region; the majority from a single locus, some additional transcripts from several other U3 subtype I controlled elements (Figure 11D).

In summary we revealed a differential behaviour of two particular LTR elements: whereas loss of DNA methylation leads to high expression of multiple genomic IAP elements (with a preference for IAPs with additional transcription factor binding sites at the R region), HDAC inhibition or loss of DNA methylation is specifically inducing the transcription of VL30 elements associated with LTRs of a specific subtype.

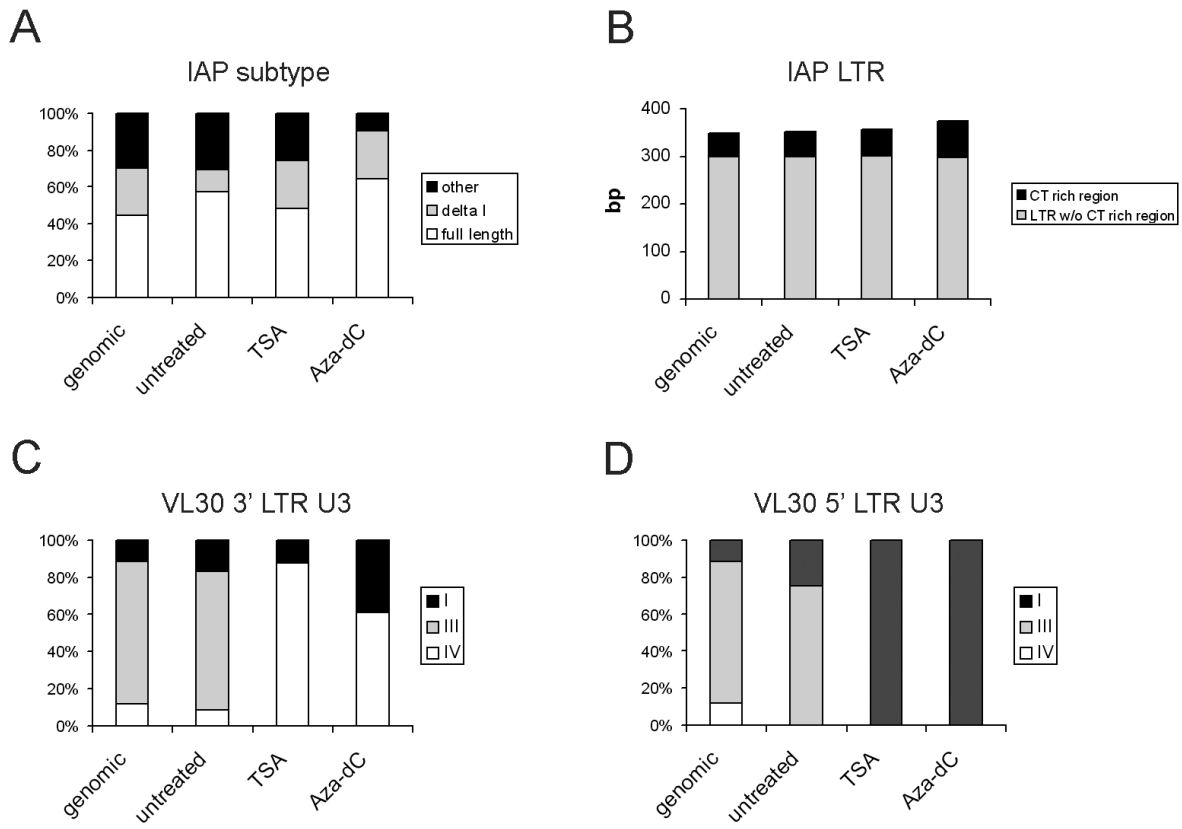

Figure 11. Characterisation of IAP and VL30 elements expressed upon different stimuli in 3T3 fibroblasts.
(A) IAP elements expressed under different conditions were either full length (white bars), belonged to the IΔ1 subgroup (delta I, grey bars) or carried different other internal deletions (other, black bars).
(B) The average length of the LTRs driving IAP expression upon Aza-dC treatment was increased due to an extension of a CT rich stretch within the R region.
(C) When untreated, 3T3 fibroblasts expressed mostly VL30 elements associated with a type III U3 region within the 3' LTR (grey bars); when cells were treated with TSA or Aza-dC, only elements with a type I or IV U3 region were detected.
(D) VL30 elements potentially serving as genomic sources of transcription mainly were associated with a type III subtype 5' LTR in untreated cells, whereas 5' LTRs of VL30 elements induced with TSA and Aza-dC exclusively belonged to the type I subgroup.

	IAP element					LTR		
	Homology	Chromosome	bp	Type	Nested	bp	Homology	CT bp
G 01	99,7	10	5223	IΔ1		374	100,0	75
G 02	99,3	11	4339	other		352	99,7	53
G 03	99,7	3	4427	other	LX	341	100,0	45
G 04	99,6	17	7067	full length		337	98,2	38
G 05	99,9	6	7106	full length	L1	337	100,0	38
G 06	99,9	6	5163	IΔ1		337	100,0	38
G 07	99,9	10	7123	full length		366	100,0	68
G 08	99,6	13	5092	IΔ1		354/389	99,2	55
G 09	98,7	8	7085	full length		352	100,0	53
G 10	99,7	7	6578	other		336	100,0	38
G 11	98,6	14	7146	full length		338	99,7	38
G 12	98,1	6	5168	IΔ1	L1	338	100,0	39
G 13	99,7	3	5212	IΔ1		335	100,0	36
G 14	99,7	X	7119	full length		368	99,7	68
G 15	100,0	4	5337	IΔ1		336	100,0	38
G 16	98,5	11	7092	full length	L1	352	100,0	53
G 17	99,6	17	5369	IΔ1	IAP	419	100,0	121
G 18	100,0	2	7103	full length		354	100,0	55
G 19	100,0	4	7089	full length		350	100,0	51
G 20	99,6	14	7080	full length		352	100,0	53
G 21	99,7	17	7106	full length		338	100,0	40
G 22	99,6	1	5862	other	L1	353	100,0	53
G 23	99,6	7	5019	other		338	99,4	38
G 24	99,9	12	6962	other		352	100,0	53
G 25	99,9	8	5150	other		339	100,0	40
G 26	99,8	8	7160	full length		355	100,0	56
G 27	99,9	17	6864	other		336/-	-	38
0 01	99,0	4	7060	full length	L1	339	100	39
0 02	98,6	12	3979	other		359/357	98,9	61
0 03	99,9	2	6592	other		382	100,0	82
0 04	99,5	1	1551	other		-	-	-
0 05	99,6	7	7091	full length		336	99,7	38
0 06	99,2	9	7076	full length		352	99,7	53
0 07	98,2	14	7192	full length		366	100,0	68
0 08	99,6	18	6575	other		337	99,7	38
0 09	99,7	8	7126	full length		371	100,0	72
0 10	99,6	2	6020	other		338	100,0	40
0 11	100,0	16	7164	full length		381	99,7	81
0 12	99,0	18	4238	other	IAP	338	99,7	38
0 13	98,4	17	7132	full length	L1	352	99,7	54
0 14	99,0	19	7050	full length		322	100,0	38
0 15	99,9	4	4862	other	L1	350/351	99,7	52
0 16	99,3	2	7123	full length	RSINE	371	100,0	70
0 17	99,2	17	7076	full length		336	99,4	38
0 18	99,5	10	5584	IΔ1	LX	337	100,0	38
0 19	99,9	11	4311	other		337	100,0	38
0 20	99,7	3	5313	IΔ1		389	100,0	90
0 21	98,4	14	7192	full length		366	100,0	68
0 22	99,9	12	7079	full length		352	99,7	53
0 23	99,1	14	7107	full length		337	99,7	39
0 24	98,8	X	7071	full length	L1	337	100,0	38
0 25	99,2	12	5212	IΔ1	RMER	368	100,0	70
0 26	99,1	X	7132	full length		351	100,0	53

	IAP element					LTR		
	Homology	Chromosome	bp	Type	Nested	bp	Homology	CT bp
T 01	98,8	X	7071	full length	L1	337	100,0	38
T 02	99,2	17	6015	other		369	100,0	70
T 03	99,3	7	7080	full length		352	100,0	53
T 04	99,3	17	7068	full length		352	100,0	0
T 05	99,1	18	7117	full length		367	100,0	68
T 06	100,0	12	6961	other	charlie	352	100,0	53
T 07	98,6	7	7080	full length		353	99,4	53
T 08	99,9	2	7103	full length		337	100,0	38
T 09	98,6	10	5223	IΔ1		374	100,0	75
T 10	99,9	19	4875	other		337	99,7	38
T 11	98,1	X	7193	full length		365	100,0	67
T 12	99,4	9	5180	IΔ1	L1	353	100,0	54
T 13	99,9	6	5334	IΔ1		376	100,0	77
T 14	99,7	4	4507	other		338	100,0	38
T 15	99,6	6	4701	other		338	100,0	38
T 16	98,7	16	5284	IΔ1		406	100,0	107
T 17	99,5	1	7105	full length		337	100,0	38
T 18	100,0	14	7080	full length		352	100,0	53
T 19	99,9	2	7103	full length		337	100,0	38
T 20	100,0	6	7064	full length	LX	337	100,0	38
T 21	98,6	12	7150	full length		352	100,0	53
T 22	99,9	16	7074	full length		337	99,7	38
T 23	99,5	5	4344	other		352	100,0	53
T 24	99,5	13	7086	full length		352	100,0	53
T 25	98,8	X	5203	IΔ1		382	100,0	83
T 26	99,3	3	5308	IΔ1		366	100,0	67
T 27	99,9	1	7082	full length		354	99,4	55
T 28	98,9	13	5349	IΔ1		398	100,0	118
T 29	99,9	10	5223	IΔ1		374	100,0	75
T 30	100,0	5	4344	other		352	100,0	53
T 31	99,6	11	5790	other		337	100,0	38
A 01	100,0	15	7127	full length		372	100,0	74
A 02	98,4	14	5460	IΔ1		456	100,0	157
A 03	99,5	8	5418	IΔ1	L1	415	100,0	117
A 04	99,5	10	4948	other	L1	337	100,0	38
A 05	99,5	17	7107	full length		367	100,0	68
A 06	99,6	1	7179	full length		367	100,0	68
A 07	100,0	X	7119	full length		368	99,7	53
A 08	99,4	3	7064	full length		351	100,0	53
A 09	99,7	8	7102	full length		353	100,0	106
A 10	98,4	8	5315	IΔ1		405	100,0	106
A 11	99,9	2	7154	full length	L1	399/397	99,6	98
A 12	99,9	19	7201	full length		413	100,0	114
A 13	99,3	17	7068	full length		352	100,0	103
A 14	99,1	10	4308	other		401	100,0	53
A 15	99,9	6	7089	full length		353	100,0	53
A 16	99,7	16	7104	full length		354	100,0	67
A 17	99,9	2	5260	IΔ1		366	100,0	50
A 18	99,7	2	5306	IΔ1	L1	349	100,0	50
A 19	99,6	14	7079	full length		337	99,1	38
A 20	99,0	9	7159	full length		367	100,0	68
A 21	100,0	13	7092	full length		352	100,0	53
A 22	99,5	7	5137	IΔ1		421	100,0	123

	IAP element					LTR		
	Homology	Chromosome	bp	Type	Nested	bp	Homology	CT bp
A 23	99,5	3	7376	full length		416	100,0	118
A 24	100,0	7	5137	IΔ1		421	100,0	123
A 25	99,7	8	4320	other	LX	337	100,0	38
A 26	98,3	7	7329	full length	ORR1	405	97,8	107
A 27	99,7	8	5153	IΔ1		337	100,0	38
A 28	98,8	X	7214	full length		351	100,0	52
A 29	99,2	10	7145	full length		386	100,0	87
A 30	100,0	14	7087	full length		353	100,0	53

	IAP element			LTR		
	bp	Type	Reference	bp	Homology	CT bp
M17551	7096	full length	Mietz, 1987	338	100,0	38
AB099818	7309	full length	Ishihara, 2004	443	100,0	145
AC012382	7084	full length	Dewnnieux, 2004	354	100,0	55
AC087891	7155	full length	Dewnnieux, 2004	353	100,0	55
AC090431	7126	full length	Dewnnieux, 2004	354	100,0	53
AL590616	7070	full length	Dewnnieux, 2004	337	100,0	38
X04120	5059	IΔ1	Ymer, 1985	337	100,0	38
AxinFu	5195	IΔ1	Whitelaw E	338	100,0	38

Table 3. Characterisation of cloned IAP elements. Summary of characteristic features of cloned IAP elements. Clones G 01 to G 27 correspond to IAP elements amplified from genomic material, 0 01 to 0 26 to IAP elements expressed in untreated cells, T 01 to 31 and A 01 to 30 to IAPs expressed upon TSA or Aza-dC treatment, respectively. Given is the homology of the cloned sequence to the most homologous genomic sequence (Homology), genomic location of the corresponding sequence (Chromosome), length of the genomic IAP element (bp), affiliation to one of the three subgroups: full length, IΔ1 deletion type or IAP carrying another deletion (Type). If the genomic IAP is inserted into another TE, the identity of the TE is given as determined with the Repbase TE database (http://www.girinst.org/censor/; Jurka, 2005) (Nested); Finally, the LTR is characterised in terms of length (bp), homology of the 5' LTR to the 3'LTR (Homology), and length of the CT rich hypervariable region in the R region (CT bp). The list is further extended by the characterisation of eight IAP elements published earlier (M17551, AB099818, AC012382, AC087891, AC090431, AL590616, X04120, AxinFu).

	VL30 element				LTR			
	Homology	Chromosome	bp	Nested	bp	Homology	U3 5'	U3 3'
G 01	99	7	5346	IAP	584	100,0	III	III
G 02	99	17	4826	LX	628	100,0	III	III
G 03	100	2	5316	RMER	603	100,0	III	III
G 04	100	9	5208		585	100,0	III	III
G 05	100	13	4237	B2	558	99,8	IV	IV
G 06	99	8	5248	LX	564/565	99,8	IV	IV
G 07	99	15	5468		646	99,8	III	III
G 08	99	10	4610		600	100,0	III	III
G 09	100	18	5310	ORR1	588	100,0	III	III
G 10	100	6	4964		561	100,0	I	I
G 11	99	13	5526	ORR1	568	99,8	I	I
G 12	100	8		IAP / VL30	553	100,0	III	III
G 13	99	2	5495		649	99,7	III	III
G 14	99	8		IAP / VL30	553	100,0	III	III
G 15	98	17	5521		605	100,0	III	III
G 16	99	17	5226	MTA / L1	555	100,0	III	III
G 17	99	18	5130		544	100,0	III	III
0 01	100	8		IAP / VL30	553	100,0	III	III
0 02	99	6	4964		561	100,0	I	I
0 03	100	18	5130		544	100,0	III	III
0 04	99	2	5316	RMER	603	100,0	III	III
0 05	100	2	4843	B3	569/575		I	IV
0 06	100	18	5410		600	100,0	III	III
0 07	100	8	5441		605/606	99,8	III	III
0 08	100	13	5139	MT2A	534	100	I	I
0 09	100	2	5316	RMER	364/645		III	III
0 10	98	8		IAP / VL30	553	100,0	III	III
0 11	99	13	4857		602	100,0	III	III
0 12	99	X	4807		589	100,0	III	III
T 01	99	2	4843	B3	569/575		I	IV
T 02	100	2	4843	B3	569/575		I	IV
T 03	100	2	4843	B3	569/575		I	IV
T 04	100	17	4954	RMER	535	100,0	I	I
T 05	99	2	4843	B3	569/575		I	IV
T 06	100	2	4843	B3	569/575		I	IV
T 07	100	2	4843	B3	569/575		I	IV
T 08	99	2	4843	B3	569/575		I	IV
T 09	100	2	4843	B3	569/575		I	IV
T 10	100	2	4843	B3	569/575		I	IV
T 11	99	2	4843	B3	569/575		I	IV
T 12	99	2	4843	B3	569/575		I	IV
T 13	98	6	4964		561	100,0	I	I
T 14	99	2	4843	B3	569/575		I	IV
T 15	100	2	4843	B3	569/575		I	IV
T 16	99	2	4843	B3	569/575		I	IV
A 01	100	2	4843	B3	569/575		I	IV
A 02	99	2	4843	B3	569/575		I	IV
A 03	100	2	4843	B3	569/575		I	IV
A 04	100	2	4843	B3	569/575		I	IV
A 05	99	2	4843	B3	569/575		I	IV
A 06	99	2	4843	B3	569/575		I	IV
A 07	99	6	4964		561	100,0	I	I
A 08	98	6	4964		561	100,0	I	I
A 09	98	6	4964		561	100,0	I	I
A 10	98	6	4964		561	100,0	I	I
A 11	100	2	4843	B3	569/575		I	IV

	VL30 element				LTR			
	Homology	Chromosome	bp	Nested	bp	Homology	U3 5'	U3 3'
A 12	98	6	4964		561	100,0	I	I
A 13	98	6	4964		561	100,0	I	I
A 14	100	2	4843	B3	569/575		I	IV
A 15	100	2	4843	B3	569/575		I	IV
A 16	99	6	4964		561	100,0	I	I
A 17	100	2	4843	B3	569/575		I	IV
A 18	100	2	4843	B3	569/575		I	IV

Table 4. Characterisation of cloned VL30 elements. Summary of characteristic features of cloned VL30 elements. Clones G 01 to G 17 correspond to VL30 elements amplified from genomic material, 0 01 to 0 12 to VL30 elements expressed in untreated cells, T 01 to 16 and A 01 to 18 to elements expressed upon TSA or Aza-dC treatment, respectively. Given is the homology of the cloned sequence to the most homologous genomic sequence (Homology), genomic location of the corresponding sequence (Chromosome) and length of the genomic VL30 element (bp). If the genomic VL30 is inserted into another TE, the identity of the TE is given as determined with the Repbase TE database (http://www.girinst.org/censor/; Jurka, 2005) (Nested); The LTR is characterised in terms of length (bp) and homology between 5' LTR and 3'LTR (Homology). Finally, the affiliation of the 5' and 3' U3 region to one of the four described subgroups (I-IV) is specified.

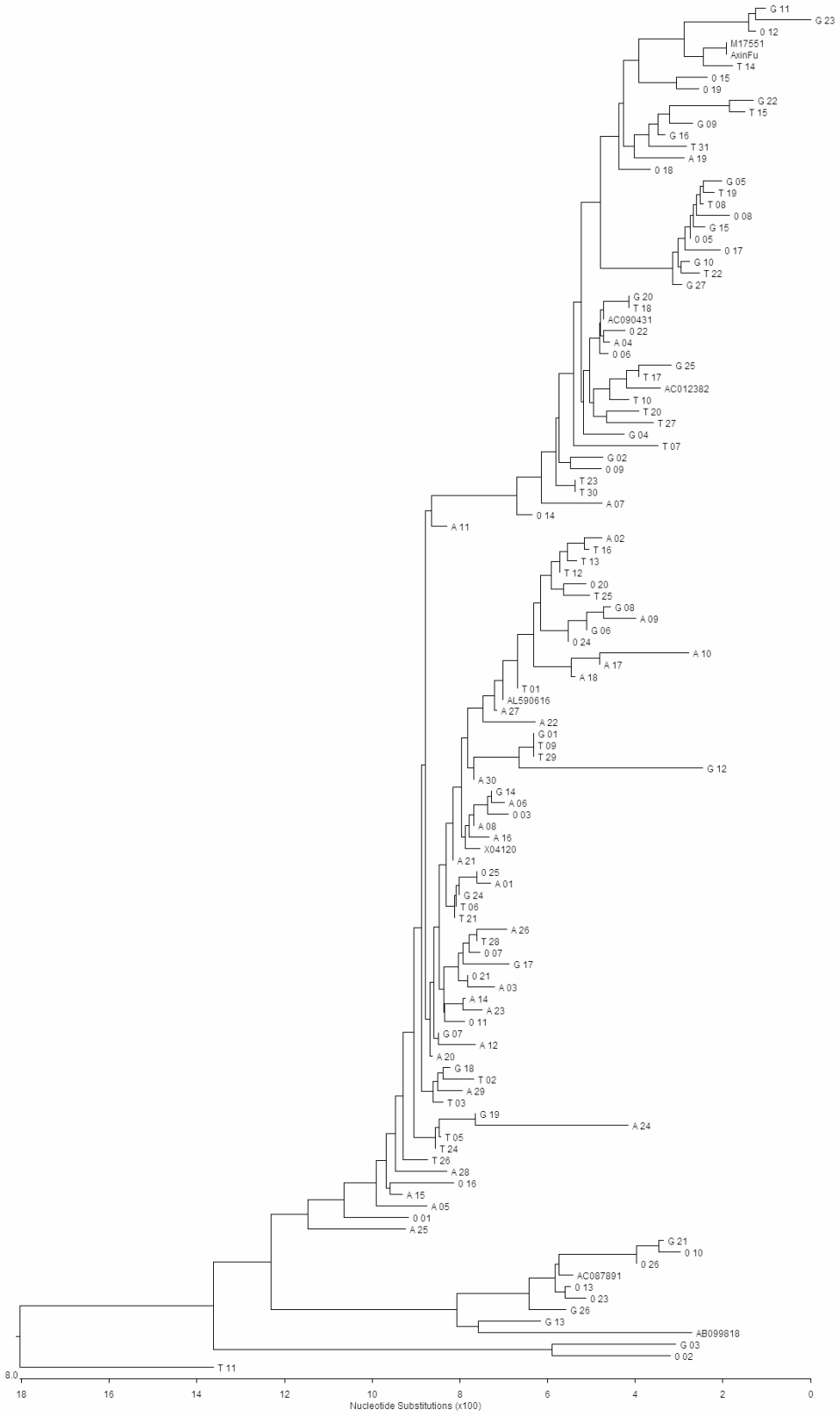

Tree 1. Phylogenetic Relationship between the LTR regions of IAP elements. LTR sequences of IAPs showing high similarity to cloned IAP fragments, together with previously characterised IAPs (see Table 3) were aligned with ClustalV using default settings. If necessary, the alignment was manually adjusted. Construction of a neighbour-joining tree was performed in Megalign.

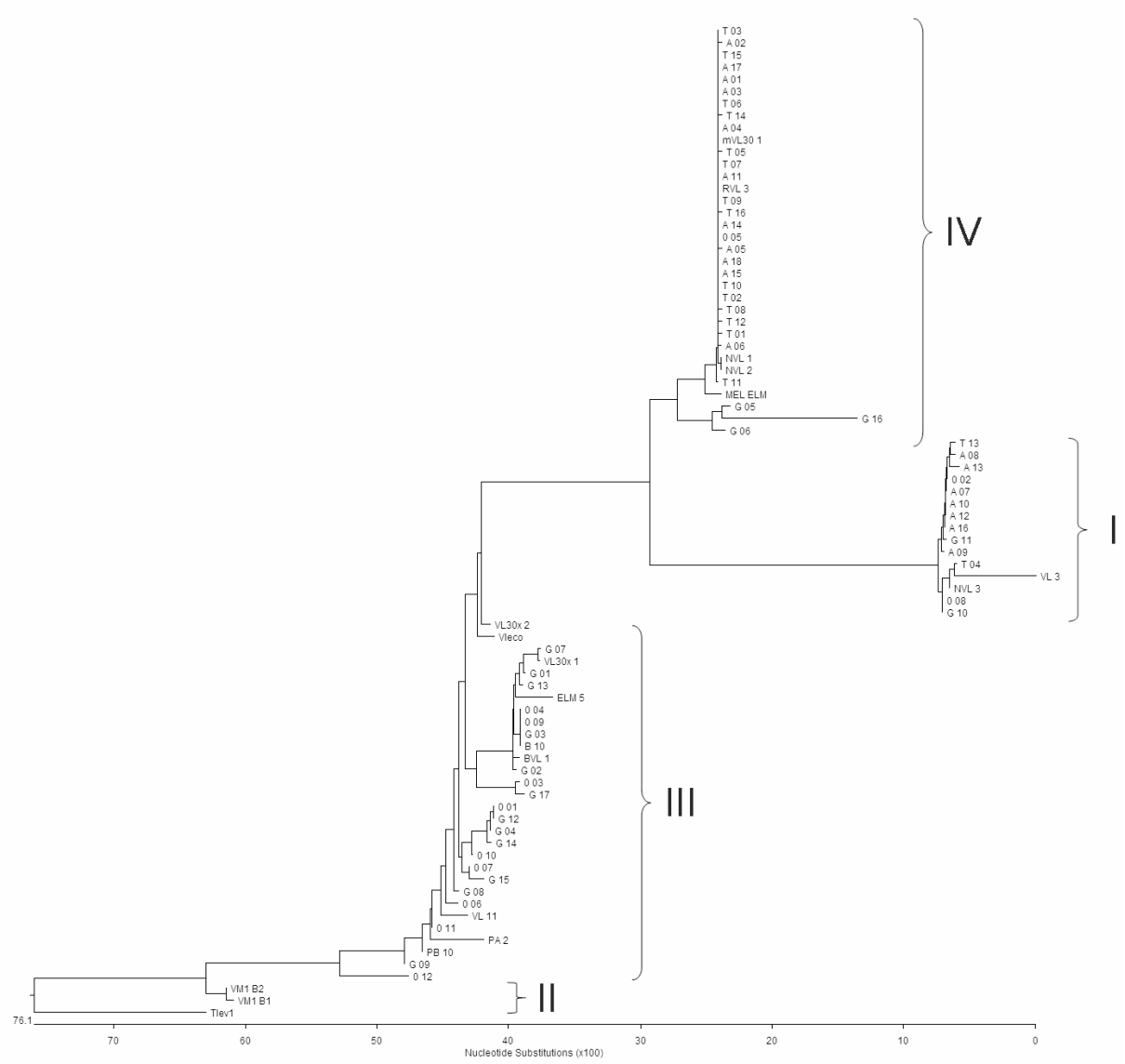

Tree 2. Phylogenetic Relationship between U3 LTR regions of VL30 elements. Sequences of the 3' U3 regions of genomic and expressed VL30 elements were aligned with ClustalW. Additionally U3 sequences of elements described earlier (French, 1997; Nilsson, 1994; Costain, 2006) were included. VL3 and NVL3 are representatives of the subgroup I, Tlev1, VM1 B1 and VM1 B2 constitute the subgroup II, VL30x1, ELM5, BVL1 VL11 PA2 and PB10 are members of the subgroup III, and finally mVL30 1, RVL3, NVL1, NVL2 and MEL ELM were included as representatives of the subgroup IV. Cloned U3 regions from genomic and expressed VL30 elements could be clearly assigned to three of the four subgroups (I, III and IV). Note that all U3 sequences derived from cells treated with TSA or Aza-dC within subgroup IV are nearly identical, indicating a single genomic copy as source of transcription.

4.5. A dual histone modification mark regulates the expression of VL30 elements

Transcriptional regulation of VL30 elements has already been in the focus of research since the 1990s. Contributions from numerous laboratories showed that VL30 elements could be activated by a plethora of stimuli (French, 1997; Tzavaras, 2003; Noutsopoulos, 2007). Interestingly, many of the stimuli can be summarised as internal or external stress in the broadest sense and a considerable number among them is able to trigger signalling cascades such as the ERK or p38 pathways. Signalling *via* these pathways ultimately leads to activation of several transcription factors but also to phosphorylation of histone proteins.

Phosphorylation of serine 10 at histone H3 (H3S10p) during interphase is a rare event that correlates with the activation of specific target genes (Mahadevan, 1991; Thompson, 1999). The presence of S10-phosphorylated histone H3 (H3S10p) marks at promoter-associated chromatin coincides with acetylation of neighbouring lysines K9 and K14 leading to a dual histone modification termed phosphoacetylation (Cheung, 2000; Clayton, 2000; Li, 2001). Histone H3 phosphoacetylation correlates with the activation of the so called “immediate early” genes c-fos and jun-B as well as late inducible genes such as HDAC1 (Hauser, 2002). Recently, it was shown that the dual histone modification mark H3S10pK14ac serves as a binding epitope for 14-3-3 proteins (Winter, 2008; Walter, 2008).

The finding that the HDAC inhibitor TSA was sufficient to highly induce VL30 expression in logarithmically growing fibroblasts (where ERK pathways are activated through the action of growth factors) prompted us to ask if both stimuli, histone acetylation and histone phosphorylation were required for full VL30 activation. To test this model, we had to switch the cell system from proliferating to serum-arrested fibroblasts (3T3 Swiss). Arrest in G_0 upon serum withdrawal eliminates mitotic H3 phosphorylation, a modification that targets the majority of histone H3 molecules associated with chromatin condensation during mitosis. This system also allows to selectively activate specific signalling cascades in the absence of serum-dependent activity of different kinase pathways. Cells arrested for 48–72h were treated with TSA, serum (FCS) to activate the ERK pathway, anisomycin (Aniso) to activate the p38 stress pathway or retinoic acid (RA) as a compound able to induce VL30 expression without direct link to histone phosphorylation. Figure 12A shows the effect of the different compounds on histone H4 acetylation and histone H3 phosphoacetylation as detected with an antibody directed against H3S10p/K14ac in G_0 arrested 3T3 Swiss fibroblast. As expected TSA lead to the accumulation of hyperacetylated histones; phosphoacetylation was absent in untreated arrested cells, upon TSA, RA and RA/TSA treatment, detectable in very low abundance upon Aniso treatment, clearly detectable in logarithmically growing cells and cells incubated with FCS. Combined treatment with Aniso/TSA or FCS/TSA finally lead to the efficient formation of phosphoacetylated histones.

Earlier reports demonstrated that the fraction of phosphoacetylated histone H3 is only minute, even upon Aniso/TSA treatment (Winter, 2008) and the mark is localised to a restricted number of genomic loci (Simboeck, PhD thesis, 2008). Therefore we were interested, if phosphoacetylated histones were associated with VL30 elements. We performed ChIP experiments with untreated, TSA, Aniso and Aniso/TSA treated resting 3T3 Swiss fibroblasts using an antibody against H3S10ph/K14ac double modified histones and surveyed phosphoacetylation levels *via* semi-quantitative PCR of the VL30 5'LTR regulatory region. Strikingly, we could detect phosphoacetylated histones at VL30 elements, when cells were treated with Aniso/TSA, but not upon single treatment with Aniso or TSA (Figure 12B). Additional ChIP experiments from cells treated with FCS/TSA demonstrated the presence of phosphoacetylation also upon activation of the ERK pathway together with induction of hyperacetylation. Retinoic acid together with TSA did not lead to the formation of such a histone mark (Figure 12C). In summary, activation of the p38 or ERK pathway together with induction of hyperacetylation results in the establishment of a phosphoacetylation mark at VL30 LTRs. Next we were interested in the influence of the different stimuli on VL30 expression. We isolated mRNA from arrested 3T3 Swiss fibroblasts exposed to the aforementioned chemicals, reversely transcribed them and quantified VL30 levels with Real Time PCR. Whereas single treatment of cells with TSA, Aniso, FCS or RA lead to a modest increase in expression, combined treatment of Aniso, FCS or RA with TSA revealed a synergistic effect between p38, ERK, retinoic acid receptor activation and histone acetylation (Figure 13). As presented above, Aniso/TSA and FCS/TSA create phosphoacetylated histones at the VL30 promoter, RA/TSA does not. Nevertheless, RA/TSA treatment is equally efficient in boosting expression, suggesting that binding of the retinoic acid receptor to the RAR-RXR binding site is an independent mechanism to induce VL30 element expression. Previous studies clearly demonstrated that the DNA sequence serving as the retinoic acid response element is distinct from the response elements important for VL30 induction upon numerous other stimuli such as transformation, epidermal growth factor (EGF), TPA, cAMP, and anoxic stress which are all activating either the p38 or the ERK pathway. Two DNA sequence cassettes have been identified to be involved in the transmission of those stimuli: the first encodes an AP1 transcription factor binding site followed by a CREB/JUN binding site (French, 1997), the second consists of a 36bp long stretch referred to as VLTRE containing a CREB/JUN and a REL/NFκb binding site. These cassettes are good candidates for binding sites for transcription factors recruiting the kinase necessary for H3S10 phosphorylation. So far, two possible kinases have been identified as histone H3 kinases, Rsk2 which is activated through the ERK pathway and MSK1/2 which is activated through the ERK and p38 pathway, making it the prime candidate for mediating H3S10ph of VL30 associated chromatin. To test if MSK1/2 is indeed involved in VL30 promoter phosphorylation

we took advantage of the protein kinase inhibitor H89. This compound was used at a concentration (10μM) that was shown to efficiently block histone H3 phosphorylation without affecting transcription factor phosphorylation (Thompson, 1999). However, others could demonstrate that H89 also inhibited other protein kinases such as PKA, S6K1 and ROCK-II (Davies, 2000).

As shown in Figure 14A, inhibition of MSK1/2 *via* H89 abolished the formation of a phosphoacetylation mark upon Aniso/TSA treatment in arrested Swiss 3T3 fibroblasts, suggesting that MSK1/2 is the responsible kinase for H3 phosphorylation of VL30 elements. Equally important, H89 treatment also prevented transcriptional induction upon Aniso/TSA treatment (14B), indicating that H3S10p/K14ac does not only correlate with transcriptional induction mediated by Aniso/TSA treatment, but is necessary for proper VL30 expression.

As phosphorylation is a reversible process, one or more specific phosphatases must exist to counteract kinase activity. So far, only one phosphatase has been identified to play a role in the removal of H3S10 phosphorylation: PP2A has been shown to be the responsible phosphatase to counteract MSK1/2 kinase activity in the context of p21 regulation, another recently discovered phosphoacetylation target gene (Simboeck 2008, PhD thesis). However, PP2A was found to specifically regulate p21 expression, not other phosphoacetylation target genes, demonstrating that PP2A is not the only phosphatase involved in the dephosphorylation of H3S10. We were curious, if VL30 elements were also regulated by PP2A, therefore we treated logarithmically growing Swiss 3T3 cells with ocadaic acid alone or together with TSA or Anisomycin. Ocadaic acid is a phosphatase inhibitor specifically inhibiting PP2A, but not PP1, when used at low concentrations (50nM). As summarised in Figure 14C, ocadaic acid did not influence VL30 expression, precluding PP2A as the responsible phosphatase involved in VL30 regulation.

Finally we want to suggest the following model for VL30 regulation, which integrates many of the previous findings about VL30 induction: external stimuli activate the p38 (stress) or the ERK (growth signal) pathway leading to activation of the downstream kinase MSK1/2 which is recruited to VL30 elements *via* DNA response elements. This results in phosphorylation of H3S10. Together with the induction of hyperacetylation a phosphoacetylation mark is created leading to full transcriptional activation. An alternative, independent pathway is mediated by the binding of RAR/RXR to the RAR-RXR binding site upon retinoic acid treatment and induction of hyperacetylation (Figure 15).

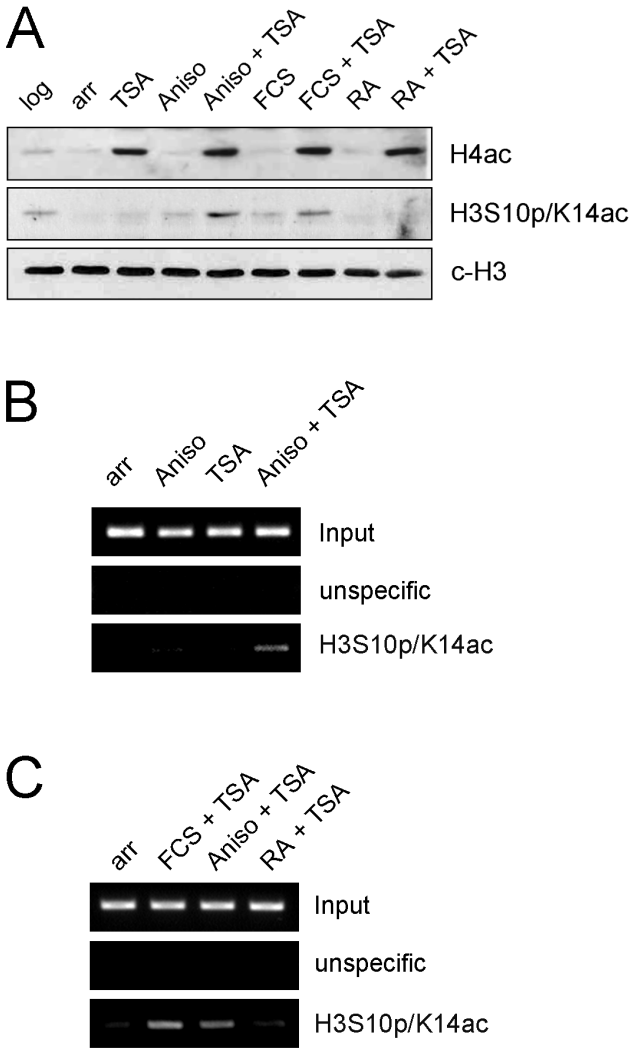

Figure 12. Activation of the p38 or ERK MAP kinase pathway together with HDAC inhibition creates phosphoacetylated histones.
(A) Swiss 3T3 fibroblasts were grown in DMEM containing 10% FCS (log) or arrested in DMEM containing 0.1% FCS for 72h (arr) and subsequently treated for 2h with 166nM TSA (TSA), 189nM Anisomycin (Aniso), TSA and Anisomycin (TSA + Aniso), 20% FCS (FCS), FCS and TSA (FCS + TSA), 10nM all-trans-Retinoic acid (RA) or RA and TSA (RA + TSA). Histones were isolated and histone modification levels were surveyed *via* Western Blot analysis. Antibodies were directed against pan-acetylated histone H4 (H4ac), S10p/K14ac double modified histone H3 (H3S10p/H3K14ac) and the c-terminal part of histone H3 (c-H3) which served as loading control. Acetylation levels of histone H4 were higher in logarithmically growing cells, than in arrested cells. HDAC inhibition by TSA increased H4ac in arrested cells; Anisomycin, and Retinoic acid had no influence. Phosphoacetylated histone H3 (H3S10p/H3K14ac) was present at low abundance upon stimulation of the p38 pathway with Anisomycin (Aniso) or the ERK pathway with FCS (log; FCS). Additional incubation with TSA lead to efficient creation of double modified histones; Retinoic acid showed no impact on phosphoacetylation of bulk histones.
(B) Arrested Swiss 3T3 fibroblasts were treated for 1h with 166nM TSA (TSA), 189nM Anisomycin (Aniso) or both compounds (Aniso + TSA), chromatin was harvested and subjected to ChIP experiments. To survey the levels of phosphoacetylated histones associated with VL30 elements, an antibody against H3S10/K14ac was used for precipitation and primers annealing at VL30 LTRs were used to estimate the amount of associated VL30 DNA *via* semi-quantitative PCR. An unspecific IgG was used as control. Phosphoacetylated histones were associated with VL30 LTRs specifically upon treatment with Anisomycin together with TSA.
(C) Treatment of arrested Swiss 3T3 fibroblasts for 3h with chemicals as in (A). ChIP experiments using unspecific IgGs and an antibody recognising phosphoacetylated histones showed association of double modified histones with VL30 LTRs upon FCS and TSA treatment, Aniso and TSA treatment, but not upon RA and TSA treatment.

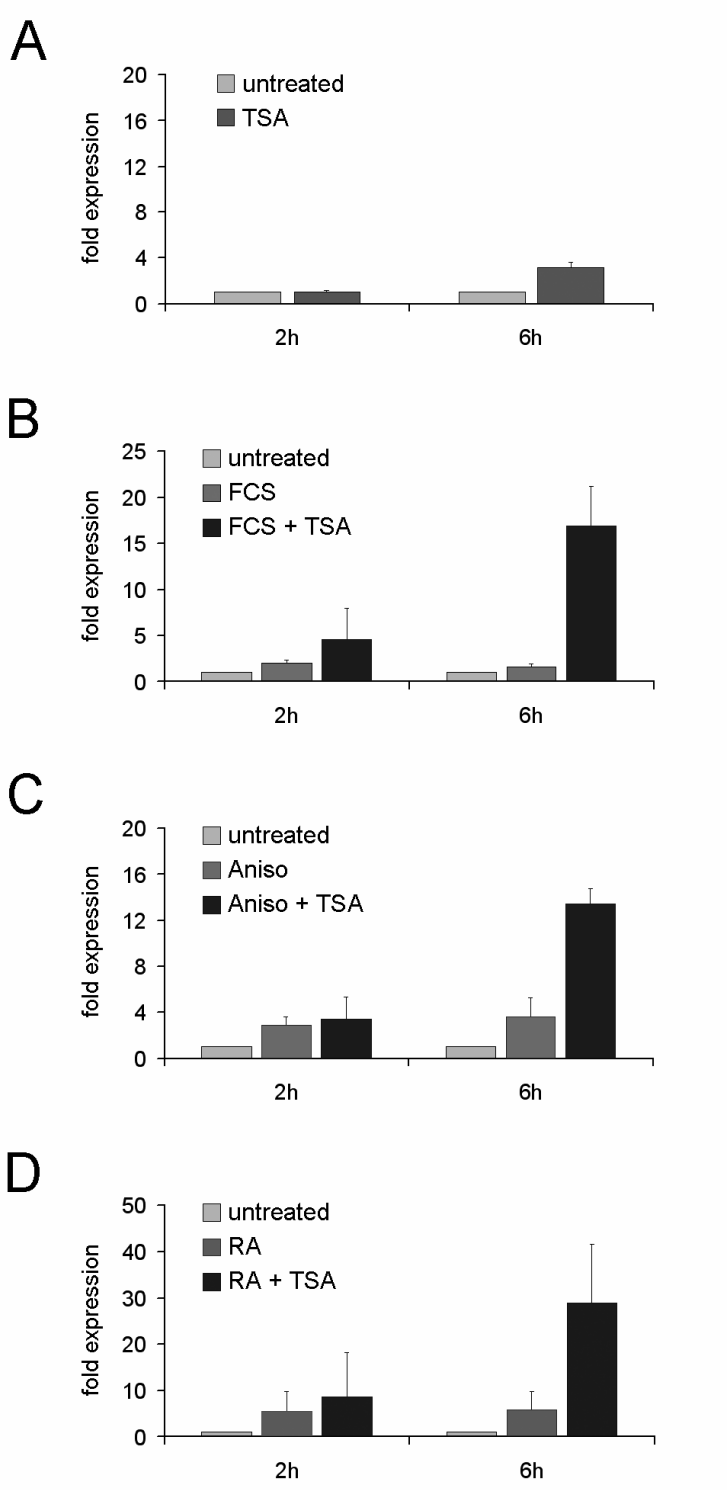

Figure 13. Expression levels of VL30 elements upon p38, ERK or retinoic acid receptor activation and HDAC inhibition.
Arrested Swiss 3T3 fibroblasts were treated for 2 or 6h with the indicated chemicals at concentration as in Figure 11A. To survey VL30 mRNA levels, mRNA was isolated, reversely transcribed and quantified *via* Real Time PCR. Values obtained with VL30 specific primers were normalised to levels of the housekeeping gene HPRT. Values represent the mean of three independent experiments. ± SD. n=3.
VL30 transcript levels were moderately increased upon treatment with either TSA, FCS, Aniso or RA ((A – D) dark grey bars) but showed a marked increase upon combined treatment with FCS, Aniso and RA together with TSA for 6h ((B – D) black bars).

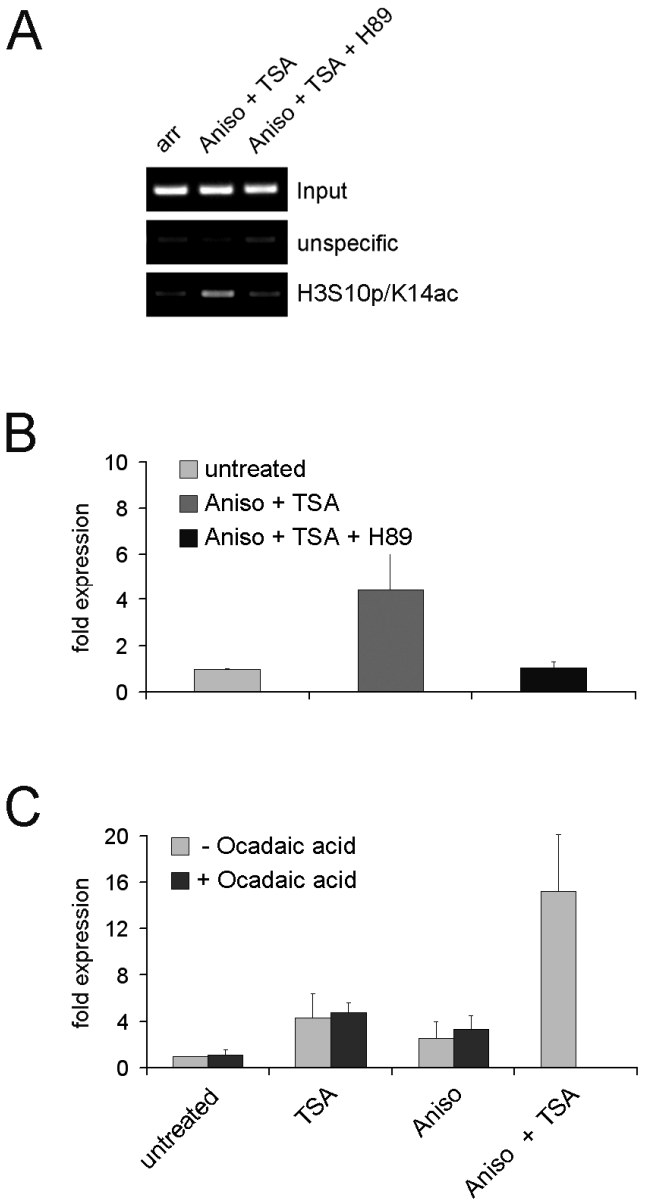

Figure 14. MSK1/2 is most likely the kinase responsible for H3 phosphorylation of VL30 elements; PP2A seems not to be the relevant phosphatase to remove the phospho-mark.
(A) To test if MSK1/2 might be the relevant kinase for phosphorylation of VL30 associated chromatin, we compared phosphoacetylation levels in untreated, Aniso + TSA treated (1h) and Aniso + TSA treated (1h) Swiss 3T3 cells which have been incubated with 10µM H89 15min prior to addition of Aniso + TSA. ChIP experiments were performed as in Figure 11. Inhibition of MSK1/2 with H89 prohibited the creation of a phosphoacetylation mark upon Aniso + TSA treatment.
(B) Treatment of cells is in (A), quantification of VL30 mRNA levels as in Figure 12. Precluding phosphoacetylation of VL30 elements with H89 also abolished transcriptional induction of VL30 elements upon Aniso + TSA treatment. ± SD. n=3.
(C) Logarithmically growing Swiss 3T3 fibroblasts were incubated with TSA, Aniso or Aniso + TSA alone (grey bars) or together with 50nM Okadaic acid (black bars) for 5h. VL30 transcript levels were determined as in Figure 12. n=3, ± SD. TSA and Aniso moderately increased VL30 transcription, Aniso + TSA further enhanced expression. Additional administration of Ocadaic acid had no influence.

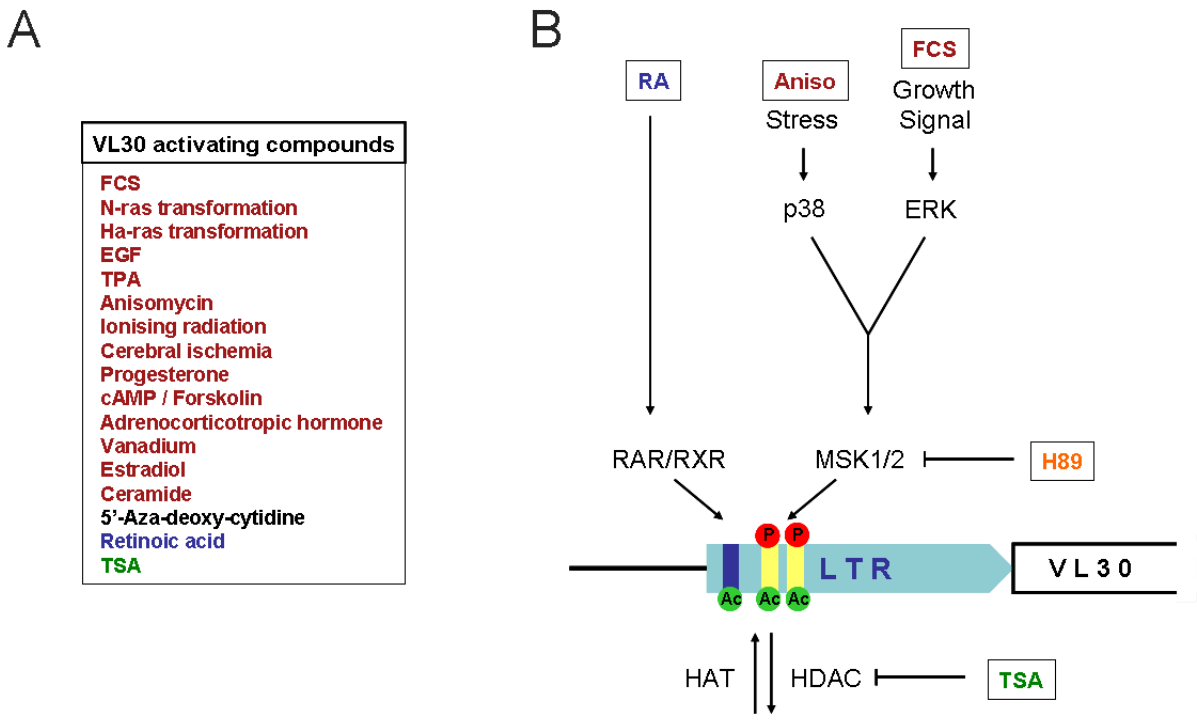

Figure 15. Model for transcriptional activation of VL30 elements.
(A) Numerous stimuli can activate VL30 expression. Notably most of the compounds identified so far can activate the MAPK pathway (dark red).
(B) Model for the induction of VL30 expression. Activation of the p38 or ERK MAPK signaling pathway leads to phosphorylation of VL30 associated chromatin (red circle) mediated by MSK1/2. Induction of hyperacetylation (green circle) creates a phosphoacetylation mark, triggering full transcriptional activation. RAR/RXR binding to the LTR induced by retinoic acid together with induction of hyperacetylation is an alternative mechanism to activate VL30 expression.

4.6. The influence of HDAC inhibition on transposition frequency

Regulating the expression of a transposable element is one way to regulate its activity. However, transposition is a complex process including many more steps and each of them can be targeted by regulatory mechanisms. After transcription, RNA has to be exported to the cytoplasm, translated, the gene product has to be shuttled into the nucleus and finally a reversely transcribed mRNA has to be integrated into the genomic DNA. That way, altering RNA stability, translation, nuclear shuttling, editing template RNA or effecting integration efficiency has severe impact on the rate of successful transposition.

We could show in Chapter 3.1. that treatment of cells with the HDAC inhibitor TSA had severe effects on the chromatin state including changes in histone acetylation and methylation patterns. As the chromatin state is not only regulating gene transcription but also constitutes the substrate for the last step of transposition – integration – we raised the hypothesis that changed histone modification patterns might influence the efficiency of transposition independent of TE transcription. In the simplest model, opening of the chromatin might render the DNA more accessible and susceptible for the integration machinery. To test this hypothesis we took advantage of an experimental system recently used to investigate the influence of the RNA editing APOBEC enzymes on transposition efficiency (Esnault, 2005). Different retroelements carrying its set of functional genes essential for autonomous retrotransposition were marked with a neo reporter gene placed in reverse orientation. Upon transfection, TEs were transcribed and spliced, removing the intron located inside the neo gene in forward orientation. The mRNA served as source for reverse transcription and integration into the genome resulted in the creation of a genomic retroelement interrupted by a functional neo gene. This was used as selection marker and that way we could select for cells with successful transposition of a transposable element delivered from an episome (Figure 17A). To test the influence of histone modifying enzymes on this process, we transfected U2OS cells with different marked transposable elements or a control plasmid (MusD and IAP as representatives for LTR elements; L1.Md and L1.2B as representatives for LINEs; pEGFP-N2 as control plasmid) and treated them with TSA for 24h after transfection. For quantification of transposition frequency we followed the protocol presented in Figure 17B. Concomitantly we performed control experiments to determine the effect of TSA on (1) the transfection efficiency of cells and (2) the expression of the marked TEs after transfection. Figure 16 shows that TSA treatment for 24 or 48h after transfection was connected to a modest increase in the percentage of GFP positive cells, when U2OS cells were transfected with a plasmid containing EGPF driven by the CMV immediate early promoter (Figure 16A and C). However, the detected increase was rather small and also might originate from the enhanced expression of EGPF when cells were treated with TSA

(Figure 16B and D). This lead us to the conclusion, that TSA treatment did not have a major impact on transfection efficiency. The expression of the marked TEs was surveyed as described in Figure 17C: after transfection, cells were treated with TSA for 24h, RNA was isolated, reversely transcribed and subjected to Real Time PCR analysis. Using primers directed against the neo gene of the marked TE we measured the abundance of TE derived transcripts. In the case of the marked IAP, we also used IAP specific primers, leading to identical results (data not shown). Additionally, untransfected cells were included in the analysis, where we could not detect any transcripts (data not shown). Values obtained with the neo-specific primers were then normalised to expression of the housekeeping gene GAPDH.

As presented in Figure 17D, treatment of TSA lead to an increase in marked TE mRNA abundance of about two to three times. The increase in mRNA abundance is accompanied with a two to four fold increase in transposition events (Figure 17D, compare black to grey bars). These data suggest that TSA treatment leads to enhanced expression of marked TEs, which in turn results in increased transposition rates. Therefore, changes on histone modification patterns as induced by TSA seem not sufficient to influence TE transposition rates.

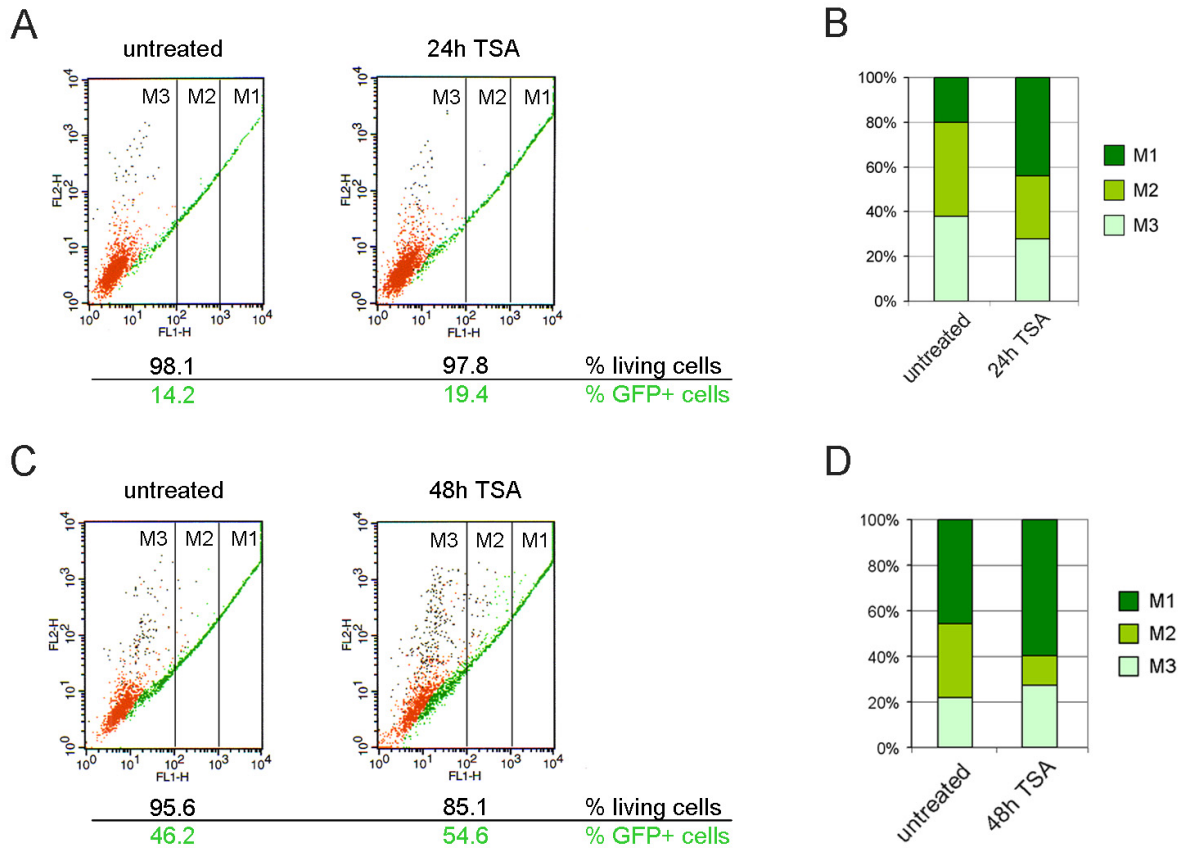

Figure 16. Effect of HDAC inhibition on transfection efficiency.
To test the impact of HDAC inhibition on transfection efficiency, U20S cells were transfected with the pEGFP-N2 plasmid containing a cassette encoding the EGFP gene driven by the CMV immediate early promoter. After transfection, cells were incubated with 66nM TSA for 24 or 48h, harvested, fixed with 85% ethanol and subjected to fluorescent-activated cell sorting (FACS) analysis. (A) and (C) show FACS blots of untreated cells and cells incubated for 24 or 48h with TSA after transfection. The portion of GFP positive cells is 27% increased upon TSA treatment 24h post transfection and 15% 48h post transfection. Green dots: GFP positive cells; red dots: GFP negative cells; black dots: dead cells. Classification of GFP positive cells into lowly (M3), medium (M2) and highly expressing (M3) subpopulations revealed that TSA administration lead to elevated expression of the EGFP protein ((B) and (D)) in transfected cells.

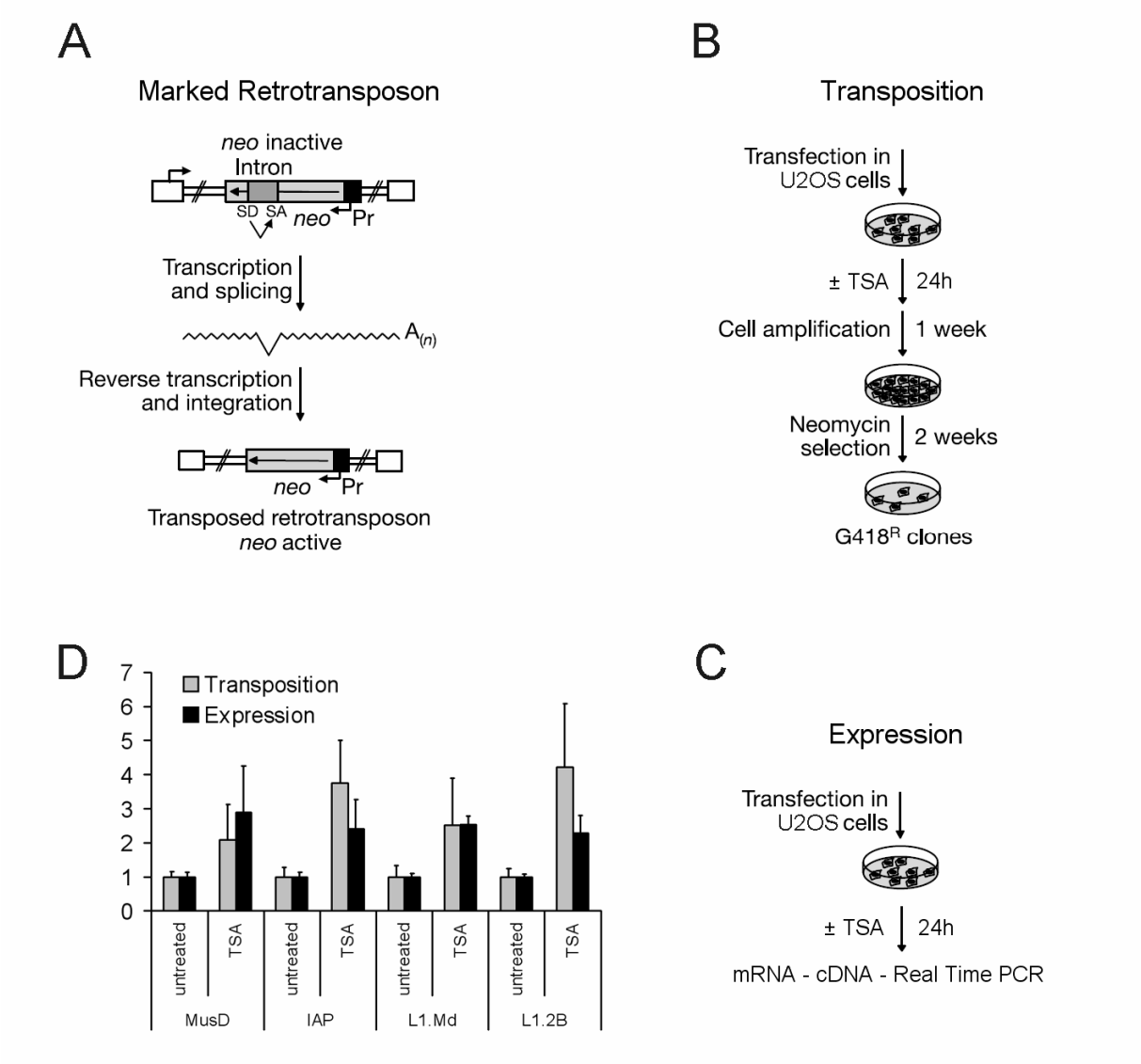

Figure 17. TSA treatment has no major impact on the transposition frequency of retrotransposons.
(A) Representation of a retroelement marked with the *neo* reporter gene placed in reverse orientation with its own promoter (Pr). Besides the *neo* cassette, each marked retroelement carries its set of functional genes, allowing autonomous retrotransposition. Only upon retrotransposition including the steps of transcription, splicing, reverse transcription and integration the *neo* gene becomes functional. (B) Experimental procedure for the detection of retrotransposition. After transfection, cells were treated with 66nM TSA for 24h to determine the effect of HDAC inhibition on transposition frequency determined by quantification of G418 resistant clones. (C) To monitor the influence of HDAC inhibition on the expression of transfected plasmids, mRNA abundance was measured *via* Real Time PCR. Primers were directed against the *neo* gene cassette and values were normalised against levels of the housekeeping gene GAPDH. (D) Analysis of the activity of murine LTR elements MusD and IAP, the murine non-LTR element L1.Md and the human non-LTR element L1.2B in U2OS cells upon TSA treatment. Grey bars represent transposition events as determined by counting G418 resistant clones. The numbers of clones in TSA treated cells are given relative to the numbers of clones determined in untreated cells. Black bars display the abundance of mRNA derived from transfected plasmids. Values for mRNA levels upon TSA treatment are given as relative numbers based on the mRNA levels determined in untreated cells. Values represent mean values of at least three independent experiments. ± SD. TSA treatment is enhancing transposition frequencies as well as transcription of tested retrotransposons.

5. Discussion

5.1. Different epigenetic modifications are interconnected

The goal of this work was to define the role of histone acetylation in the regulation of TEs in murine somatic cells. It is well known that histone acetylation is generally correlated with gene transcription; this has been demonstrated on the genome wide level (Kurdistani, 2004; Koch, 2007; Fischer, 2008) as well as for numerous individual genes and LTR retroviruses such as e.g. HIV (He, 2002; Lusic, 2003). Altering histone acetylation levels either *via* genetic inactivation of individual HATs and HDACs or *via* chemical inhibition of HDACs leads to changes in the expression pattern of defined genes in a cell type specific manner (Zhang, 1998; Howe, 2001; Foglietti, 2006; Zupkovitz, 2006; Senese, 2007; Knutson, 2008). This is of clinical relevance, since cancer cells seem to be more sensitive to such changes than normal cells and application of HDACi has been demonstrated to induce cell cycle arrest or apoptosis in cancer cells (Marks, 2005). However, the exact mode of action is only poorly understood; although some important genes for cell cycle progression (e.g. p21) or apoptosis are often targeted upon HDACi treatment, effects also seem to be cell type specific.

The vast majority of work on histone acetylation and transcription throughout the last years has been dedicated to gene regulation in different cancer cells (Yang, 2007), throughout development (Kalkhoven, 2004; Brunmeir, 2008) or to the silencing of retroviruses such as HIV (He, 2002; Lusic, 2003); to our knowledge no extensive study has been performed so far to analyse the interrelation between histone acetylation and regulation of endogenous retroelements. As already mentioned above, tight regulation of TE expression is crucial for genomic integrity and exploring the impact of histone acetylation on TE regulation is highly relevant: HDACis are already in clinical trials as anti-cancer drugs and they are also promising agents for the treatment of patients with HIV, bipolar disorders or neurodegenerative diseases (Lehrman 2005; Sharma 2006; Sadri-Vakili 2006; Hahnen 2008). Therefore possible side effects have to be studied carefully.

To perform this study, we exploited an experimental system where histone acetylation was altered in murine fibroblasts; either by the knock out of the major histone deacetylase HDAC1 or by chemical inhibition of all class I and II HDACs *via* TSA. For comparison, Aza-dC treated cells with decreased DNA methylation levels were included in the analysis. Before we specifically addressed questions dealing with the effects of those perturbations on TE regulation, we wanted to monitor global effects on histone modification patterns and the expression of the targeted proteins. This analysis lead to some general conclusions: (1) HDAC1 function is not essential for the maintenance of most chromatin modification patterns analysed. (2) General HDAC and DNMT inhibition has far reaching consequences on the

cellular chromatin and DNA modification landscape, influencing not only directly targeted modifications, but also interfering with histone methylation patterns.

Ad (1) Although HDAC1 is the major histone deacetylase in fibroblasts delivering more than 30% of total HDAC activity (see also J. Jurkin, diploma thesis), the knock out shows only a very mild phenotype including the hyperacetylation of the single lysine residue H4K8 and the deregulation of few target genes (Y. Zhang, FMI Basel). Most likely HDAC2, the close homologue present in the same multiprotein complexes as HDAC1 and which is upregulated upon HDAC1 knock out, can take over the vast majority of functions. This is consistent with the finding that the knock out of HDAC1 or HDAC2 in several tissues does not result in obvious phenotypes, most likely due to redundancy between the two homologues. In contrast, deletion of both genes leads to severe phenotypes in all analysed cell types (Brunmeir, 2008). Still, under several circumstances the loss of HDAC1 alone is sufficient to cause phenotypic changes: loss of HDAC1 during embryogenesis leads to embryonic lethality before day E10.5 (Lagger, 2002), ES cells and primary fibroblasts without HDAC1 show reduced proliferation rates (Lagger, 2002; R. Grausenburger, PhD thesis, 2006) and loss of HDAC1 in a teratocarcinoma or epithelial cancer model system affects cancerogenesis and cellular differentiation (D. Meunier, S. Lagger, unpublished observation, G. Machat, diploma thesis, 2008). This points towards a model, where most cellular tasks (including all basic cellular functions) are redundantly fulfilled by HDAC1 and HDAC2, but certain cell type specific functions are only properly executed when both homologues are present.

Ad (2) Inhibition of all class I and II HDACs with TSA leads to major changes in chromatin modification patterns: acetylation levels are increased at histone H3 and H4 proteins, as a secondary effect H3K4m4 and H3K27m3 are enriched. Models to mechanistically explain this phenomenon have been mentioned above. A decrease in DNA methylation as caused by Aza-dC treatment procures even more complex changes: histone acetylation as well as the activating histone methylation mark H3K4m3 and the repressive marks H3K9m3, H3K27m3, H4K29m2 and H4K20m3 are enriched. Notably these are only the changes we detected with our limited number of antibodies; unbiased techniques such as mass spectrometry would certainly disclose additional deformations in chromatin modification patterns. However, with these quantitative methods we do not gain information about qualitative changes as for example the genomic distribution of chromatin modifications. ChIP-chip experiments, which are currently conducted in several laboratories are addressing this open question and might be helpful to better understand the crosstalk between different histone modifications as well as DNA methylation.

5.2. TE expression and histone acetylation

Having monitored global changes mediated by TSA and Aza-dC treatment on a variety of histone modifications, we went on and narrowed our focus on the initial topic of interest i.e. the interrelation between histone acetylation and TE regulation. Determining histone acetylation levels of a representative selection of TEs in a HDAC$^{-/-}$ background, upon TSA and Aza-dC treatment and correlating these data with the expression of TEs revealed the following findings: (1) only a limited number of TEs can be activated by either TSA or Aza-dC treatment. In the prevalent model of TE silencing, transcription in somatic cells is restrained by DNA methylation (Yoder, 1997; Walsh, 1998) with some contribution of histone methylation (Martens, 2005) and small RNAs (Kanellopoulou, 2005), in germ cells by DNA methylation and piRNA related mechanisms (Bourc'his, 2004; Carmell, 2007; Aravin, 2007). Relieving DNA methylation in somatic fibroblasts strongly enhances the expression of IAP and VL30 LTR elements demonstrating that losing repression is sufficient to activate transcription of some, but not all TEs. Activating factors for other TEs might be absent in this cell type, impeding high expression; alternatively other repressive mechanisms could still be present. (2) Enhanced expression correlates with increased acetylation levels. This is obvious for VL30 elements, which are highly expressed upon TSA and Aza-dC treatment, and IAP elements which are highly expressed after treatment with Aza-dC: both LTR elements exhibit hyperacetylation when transcribed. SINEs are also hyperacetylated in TSA treated fibroblasts, but this comes along with only mild effects on transcription; therefore we want to suggest that SINEs are acetylated as parts of genes, which are under the influence of histone acetylation. (3) TSA treatment leads to hyperacetylation of H4 proteins independent of transcriptional activity. H4 specific HATs seem to readily acetylate lysine residues of H4 when the dominant HDACs are inhibited, suggesting their regular presence at TEs and silent genes. In contrast, acetylation of H3 seems coupled with transcription, pointing towards a model where H3 acetylation might stimulate the recruitment of the transcription machinery or alternatively H3 specific HATs are recruited together with the transcription machinery. Interestingly Koch and colleagues recently showed that although H4ac and H3ac are both enriched around the transcriptional start site, only H3ac can be used as a highly predictive marker for gene activity (Koch, 2008). One might speculate that differential HAT recruitment reflects a functional difference between H3 and H4 acetylation. In addition to their role in transcription where both modifications act synergistically, H4 acetylation / deacetylation could have other biological tasks.

5.3. DNA sequence does matter

The TEs activated by TSA or Aza-dC are derived from several genomic loci. Examining IAP and VL30 transcripts in untreated and treated fibroblasts clearly shows that expressed TEs originate from numerous loci dispersed throughout the genome. However, upon different stimuli, certain groups of elements are preferentially expressed. We could show that elements preferentially expressed harbour characteristic DNA sequence features within the LTR, the regulatory region of the element. IAPs are more efficiently activated with Aza-dC, when they carry additional binding sites for the transcription factor C/EBPalpha. Strikingly, Ishihara and colleagues, who characterised IAP elements active upon irradiation of mouse acute myeloid leukaemia (AML) cells, isolated elements with especially long stretches of C/EBPalpha binding sites (Ishihara, 2004) (Table 3, AB099818). In contrast, IAP elements responsible for recent integration events in the mouse germline (Maksakova, 2006) harbour only one TF binding site (Table 3, X04120 and AxinFu).

VL30 elements treated with Aza-dC or TSA are preferentially expressed when driven by a LTR with a subtype I U3 region. Several years ago Nilsson and Bohm already proposed a model that the enhancer design of VL30 elements determines tissue specific expression and the response to external stimuli (Nilsson, 1994). Our data clearly support this model.

In summary, upon release of silencing, expression is mainly determined by intrinsic features of the elements, e.g. transcription factor binding sites and external factors e.g. the availability of corresponding transcription factors. The impact of cellular components on expression is exemplified by the finding that VL30 elements expressed upon TSA are distinct in different fibroblasts cell lines: whereas in logarithmically growing fibroblasts subtype I elements are especially responsive to external stimuli, in arrested Swiss 3T3 we found predominant transcription of elements with LTR subtype IV U3 region (data not shown).

5.4. VL30 – a special case

In mammals, transcriptional release in TE silencing has been reported repeatedly: loss of proteins involved in DNA methylation, the siRNA and piRNA pathways and to a certain degree histone methylation lead to a deregulation of TEs expression. SINE elements can be activated *via* stress and Adenovirus infection (Panning, 1993; Liu, 1995), LINEs by benzo(a) pyrene (Stribinskis, 2006). In cancer cells, TE silencing is impaired probably due to altered DNA methylation patterns (Rauch, 2008; Wilson, 2007) and several human diseases are associated with a relaxation of TE repression (Colmegna, 2006).

Still, the regulation of VL30 expression is unique among mammalian retrotransposons; a multitude of stimuli is able to highly induce transcription in several cell systems such as

fibroblasts, keratinocytes, haematopoietic and neuronal cells (French, 1997; Tzavaras, 2003; Noutsopoulos, 2007). Furthermore VL30 elements are the first mammalian TEs responsive to HDAC inhibition. Freshly integrated retroelements including retroviruses and LINEs have been reported to exhibit sensitivity to HDAC inhibition; however this responsiveness is lost after few generations when other, HDAC insensitive mechanisms (most likely DNA methylation) take over the silencing function (Pannell, 2000). Derepression of endogenous, not recently integrated TE elements with HDACis has not been reported so far to our knowledge. VL30 elements seem to exist in a default state which is “ready for transcription” and external stimuli can easily flip the switch to “active transcription”.

Why does the host not antagonise this loose repression more vehemently? Why does it allow VL30 expression, but is tightly controlling expression of other TEs? One possible answer is that VL30 elements are simply ahead in the arms race between host and parasite. Alternatively, the evolutionary pressure on the host is relatively low: as long as other TEs, which are required for intracellular mobility of VL30 elements – VL30 elements are absolutely dependent the enzymatic machinery of other LTR elements as they do not encode functional proteins – are efficiently silenced, VL30 elements do not constitute a danger to the host and therefore expression does not have to be tightly controlled.

Finally, a third scenario is plausible: Song and colleagues recently showed that VL30 RNA can interact with the PSF protein and modulate PSF mediated repression of target genes (Song, 2004; Song, 2005). Therefore VL30 elements have acquired physiological functions in murine cells and might be necessary for the regulation of certain host genes. This finding suggests that VL30 could be a symbiont rather than a parasite to the host.

5.5. VL30 expression is synergistically regulated by histone acetylation and phosphorylation

Another novel and important finding of our study is the positive impact of histone H3 phosphorylation on VL30 transcription. Since several years, mechanistic links between histone acetylation and histone phosphorylation caused by different stimuli, including stress and growth factors, have been established. For example, immediate early genes such as c-myc, c-fos, c-jun (Cheung, 2000; Clayton, 2000; L,i 2001), but also an increasing number of others (Hauser, 2002; Winter, 2008; E. Simboeck, PhD thesis, 2008) depend on the induction of histone H3 phosphoacetylation. Simultaneous H3 phosphorylation and acetylation provides a recognition mark for 14-3-3 proteins which translate this histone code into a biological outcome i.e. gene transcription (Winter, 2008; Walter, 2008).

In a series of experiments we could show that VL30 expression is synergistically activated by stimuli leading to histone phosphorylation (FCS, anisomycin) and histone acetylation (TSA); full transcriptional activity is correlated with the creation of phosphoacetylated histone

proteins at the VL30 LTR. Usage of the inhibitor of the nucleosomal response H89 indicates that the creation of this dual histone mark is necessary for activation caused by FCS/TSA or Anisomycin/TSA and that MSK1/2 might be the responsible kinase responsible for phosphorylation. The phosphatase counteracting MSK1/2 activity in the non-induced state is not identified yet, first experiments with the inhibitor ocadaic acid indicate, that it is a different phosphatase than PP2A. We also do not know by now which HAT is responsible for histone acetylation. The contribution of the different HDACs in the maintenance an inactive state is also unclear. However, results from several experiments suggest the involvement of other HDACs beside HDAC1 and HDAC2. First, loss of HDAC1 in fibroblasts does not change VL30 transcript levels. Second, RNAi mediated knock down of HDAC1, HDAC2 or HDAC1 and HDAC2 in primary fibroblasts has no influence on VL30 transcript levels as determined *via* RT-Real Time PCR (preliminary result, data not shown). Third, treatment of fibroblasts with MS-275 (5µM; 24h), an HDI with limited specificity against HDAC1 (Khan, 2008), results in an only 2 fold enrichment of VL30 transcripts, a modest increased as compared to the 30 fold enrichment we observed when cells were treated with the general HDI TSA (data not shown).

In summary we collected data supporting a model that VL30 transposable elements are novel phosphoacetylation target genes. Transcriptional activation can be mediated *via* stress or growth factor induced activation of the p38 or ERK MAPK pathway and subsequent phosphorylation of promoter associated histone proteins by MSK1/2 together with acetylation of histones. This pathway is one of at least two possible ways to activate VL30 elements; phosphoacetylation independent mechanisms involving retinoic acid receptor signalling exist in parallel.

Still many details about the exact mechanism of VL30 regulation *via* dual histone modification are unclear. As mentioned above, we do not know the responsible HAT(s), HDAC(s) and phosphatase(s) and if the phosphoacetylation mark is read by 14-3-3 proteins as it is the case for the HDAC1 and p21 genes.

Activation of specific VL30 subtypes in different cell lines could originate from differential enhancer design of elements. We speculate that the availability of transcription factors necessary for the recruitment of factors (kinase, HAT, phosphatase, HDAC) to the regulatory regions might be the determining factor for the different regulation of VL30 subgroups in different cell lines. This is a testable hypothesis.

5.6. Transposition rates of several TEs are not influenced by HDAC inhibition in mouse fibroblasts

The link between increased transcription and transposition is evident; production of an adequate amount of mRNA is an essential premise for all subsequent steps in the lifecycle of a TE. Similar to expression, upcoming events such as mRNA processing, export, translation, reverse transcription, nuclear import, integration including DNA cleavage and repair of the double strand brake, greatly depend on host factors. This delivers the host additional points of action to encounter transposon activity. An example for post-transcriptional regulation is the deamination of cytidine residues of nascent DNA molecules during reverse transcription leading to hypermutation of retroviruses and TEs (Mangeat, 2003; Esnault, 2005; Dutko, 2005; Chiu, 2006). Genetic screens in yeast have uncovered numerous other host factors either restricting or enhancing transposon activity (Scholes, 2001; Griffith, 2003; Aye, 2004; Irwin, 2005; Nyswaner, 2008). Strikingly, a substantial fraction of the genes identified has a role in chromatin biology; for instance, members of the PAF1 complex involved in histone H2B ubiquitination, the histone chaperone ASF1 and most importantly SIN3 and RPD3, major components of the yeast HDAC complex were found to restrict Ty1 activity. Interestingly, SIN3/RPD3 do not act at the transcriptional level as they have no influence on Ty1 mRNA levels. In addition to increasing transposition rates, they also change target site selection of the LTR retrotransposon (Nyswaner 2008).

In an experimental setup, where we monitored retrotransposition of tagged IAPs, MusD and L1 LINE elements from episomes into the genome, we detect only minor differences in the frequency of retrotransposition events when cells were treated with TSA. Transposition events were increased between two and four times upon TSA treatment, however we also observed a two to three fold enrichment of the transcript. Therefore we think that the increase in retrotransposition events is due to enhanced transcription. The finding that TSA treatment does not have a major influence on the retrotransposition frequency of murine LTR and non LTR retroelements is quite surprising considering the finding described above that HDAC complexes greatly influence TE activity in yeast. In addition to complex changes in the histone modification landscape, TSA treatment of cancer cells also results in the deregulation of a multitude of genes, presumably including several host factors important for retrotransposition. Therefore it is still possible that TSA treatment leads to qualitative changes of TE activity (i.e. target site selection); this aspect could be analysed *via* cloning of integration sites; or HDAC inhibition leads to an equal deregulation of activating and restricting histone modifications / host factors.

6. References

Agalioti T, Chen G, Thanos D. Deciphering the transcriptional histone acetylation code for a human gene. Cell. 2002 Nov 1;111(3):381-92.

Akhtar A, Becker PB. Activation of transcription through histone H4 acetylation by MOF, an acetyltransferase essential for dosage compensation in Drosophila. Mol Cell. 2000 Feb;5(2):367-75.

Allan J, Cowling GJ, Harborne N, Cattini P, Craigie R, Gould H. Regulation of the higher-order structure of chromatin by histones H1 and H5. J Cell Biol. 1981 Aug;90(2):279-88.

Allfrey VG, Mirsky AE. Structural Modifications of Histones and their Possible Role in the Regulation of RNA Synthesis. Science. 1964 May 1;144(3618):559

Allis CD, Chicoine LG, Richman R, Schulman IG. Deposition-related histone acetylation in micronuclei of conjugating Tetrahymena. Proc Natl Acad Sci U S A. 1985 Dec;82(23):8048-52.

Aravin AA, Hannon GJ, Brennecke J. The Piwi-piRNA pathway provides an adaptive defense in the transposon arms race. Science. 2007 Nov 2;318(5851):761-4. Review.

Aye M, Irwin B, Beliakova-Bethell N, Chen E, Garrus J, Sandmeyer S. Host factors that affect Ty3 retrotransposition in Saccharomyces cerevisiae. Genetics. 2004 Nov;168(3):1159-76.

Bannister AJ, Kouzarides T. Reversing histone methylation. Nature. 2005 Aug 25;436(7054):1103-6. Review.

Becker PB. Nucleosome sliding: facts and fiction. EMBO J. 2002 Sep 16;21(18):4749-53. Review.

Benson G. Tandem repeats finder: a program to analyze DNA sequences. Nucleic Acids Res. 1999 Jan 15;27(2):573-80.

Bhaskara S, Chyla BJ, Amann JM, Knutson SK, Cortez D, Sun ZW, Hiebert SW. Deletion of histone deacetylase 3 reveals critical roles in S phase progression and DNA damage control. Mol Cell. 2008 Apr 11;30(1):61-72.

Birchler JA, Kavi HH. Molecular biology. Slicing and dicing for small RNAs. Science. 2008 May 23;320(5879):1023-4. Epub 2008 May 8.

Bourc'his D, Bestor TH. Meiotic catastrophe and retrotransposon reactivation in male germ cells lacking Dnmt3L. Nature. 2004 Sep 2;431(7004):96-9. Epub 2004 Aug 18.

Bradbury EM. Reversible histone modifications and the chromosome cell cycle. Bioessays. 1992 Jan;14(1):9-16. Review.

Branciforte D, Martin SL. Developmental and cell type specificity of LINE-1 expression in mouse testis: implications for transposition. Mol Cell Biol. 1994 Apr;14(4):2584-92.

Brownell JE, Allis CD. Special HATs for special occasions: linking histone acetylation to chromatin assembly and gene activation. Curr Opin Genet Dev. 1996 Apr;6(2):176-84. Review.

Brunmeir R, Lagger S, Seiser C. HDAC1/HDAC2-controlled embryonic development and cell differentiation. Int. J. Developmental Biology. In Press. Review

Butler PJ, Thomas JO. Changes in chromatin folding in solution. J Mol Biol. 1980 Jul 15;140(4):505-29.

Cano E, Hazzalin CA, Kardalinou E, Buckle RS, Mahadevan LC. Neither ERK nor JNK/SAPK MAP kinase subtypes are essential for histone H3/HMG-14 phosphorylation or c-fos and c-jun induction. J Cell Sci. 1995 Nov;108 (Pt 11):3599-609.

Carmell MA, Girard A, van de Kant HJ, Bourc'his D, Bestor TH, de Rooij DG, Hannon GJ. MIWI2 is essential for spermatogenesis and repression of transposons in the mouse male germline. Dev Cell. 2007 Apr;12(4):503-14. Epub 2007 Mar 29.

Cheung P, Tanner KG, Cheung WL, Sassone-Corsi P, Denu JM, Allis CD.
Synergistic coupling of histone H3 phosphorylation and acetylation in response to epidermal growth factor stimulation.
Mol Cell. 2000 Jun;5(6):905-15.

Chiu YL, Witkowska HE, Hall SC, Santiago M, Soros VB, Esnault C, Heidmann T, Greene WC. High-molecular-mass APOBEC3G complexes restrict Alu retrotransposition. Proc Natl Acad Sci U S A. 2006 Oct 17;103(42):15588-93. Epub 2006 Oct 9.

Clayton AL, Rose S, Barratt MJ, Mahadevan LC. Phosphoacetylation of histone H3 on c-fos- and c-jun-associated nucleosomes upon gene activation. EMBO J. 2000 Jul 17;19(14):3714-26.
Colmegna I, Garry RF. Role of endogenous retroviruses in autoimmune diseases. Infect Dis Clin North Am. 2006 Dec;20(4):913-29. Review.
Costain WJ, Rasquinha I, Graber T, Luebbert C, Preston E, Slinn J, Xie X, MacManus JP. Cerebral ischemia induces neuronal expression of novel VL30 mouse retrotransposons bound to polyribosomes. Brain Res. 2006 Jun 13;1094(1):24-37. Epub 2006 May 30.
Davies SP, Reddy H, Caivano M, Cohen P. Specificity and mechanism of action of some commonly used protein kinase inhibitors. Biochem J. 2000 Oct 1;351(Pt 1):95-105
Davis CM, Constantinides PG, van der Riet F, van Schalkwyk L, Gevers W, Parker MI. Activation and demethylation of the intracisternal A particle genes by 5-azacytidine. Cell Differ Dev. 1989 Jul;27(2):83-93.
Denslow SA, Wade PA. The human Mi-2/NuRD complex and gene regulation. Oncogene. 2007 Aug 13;26(37):5433-8. Review.
Dewannieux M, Dupressoir A, Harper F, Pierron G, Heidmann T. Identification of autonomous IAP LTR retrotransposons mobile in mammalian cells. Nat Genet. 2004 May;36(5):534-9. Epub 2004 Apr 25.
Dormann HL, Tseng BS, Allis CD, Funabiki H, Fischle W. Dynamic regulation of effector protein binding to histone modifications: the biology of HP1 switching. Cell Cycle. 2006 Dec;5(24):2842-51. Epub 2006 Dec 15.
Dupressoir A, Heidmann T. Germ line-specific expression of intracisternal A-particle retrotransposons in transgenic mice. Mol Cell Biol. 1996 Aug;16(8):4495-503.
Dutko JA, Schäfer A, Kenny AE, Cullen BR, Curcio MJ. Inhibition of a yeast LTR retrotransposon by human APOBEC3 cytidine deaminases. Curr Biol. 2005 Apr 12;15(7):661-6.
Eickbush TH. Telomerase and retrotransposons: which came first? Science. 1997 Aug 15;277(5328):911-2.
Esnault C, Heidmann O, Delebecque F, Dewannieux M, Ribet D, Hance AJ, Heidmann T, Schwartz O. APOBEC3G cytidine deaminase inhibits retrotransposition of endogenous retroviruses. Nature. 2005 Jan 27;433(7024):430-3.
Fennelly J, Harper K, Laval S, Wright E, Plumb M. Co-amplification to tail-to-tail copies of MuRVY and IAPE retroviral genomes on the Mus musculus Y chromosome. Mamm Genome. 1996 Jan;7(1):31-6.
Finnin MS, Donigian JR, Cohen A, Richon VM, Rifkind RA, Marks PA, Breslow R, Pavletich NP. Structures of a histone deacetylase homologue bound to the TSA and SAHA inhibitors. Nature. 1999 Sep 9;401(6749):188-93.
Fischer JJ, Toedling J, Krueger T, Schueler M, Huber W, Sperling S. Combinatorial effects of four histone modifications in transcription and differentiation. Genomics. 2008 Jan;91(1):41-51. Epub 2007 Nov 8.
Fischle W, Wang Y, Allis CD. Binary switches and modification cassettes in histone biology and beyond. Nature. 2003 Oct 2;425(6957):475-9.
Fodor BD, Kubicek S, Yonezawa M, O'Sullivan RJ, Sengupta R, Perez-Burgos L, Opravil S, Mechtler K, Schotta G, Jenuwein T. Jmjd2b antagonizes H3K9 trimethylation at pericentric heterochromatin in mammalian cells. Genes Dev. 2006 Jun 15;20(12):1557-62. Epub 2006 May 31.
Foglietti C, Filocamo G, Cundari E, De Rinaldis E, Lahm A, Cortese R, Steinkühler C. Dissecting the biological functions of Drosophila histone deacetylases by RNA interference and transcriptional profiling. J Biol Chem. 2006 Jun 30;281(26):17968-76. Epub 2006 Apr 21.
Fraga MF, Ballestar E, Paz MF, Ropero S, Setien F, Ballestar ML, Heine-Suñer D, Cigudosa JC, Urioste M, Benitez J, Boix-Chornet M, Sanchez-Aguilera A, Ling C, Carlsson E, Poulsen P, Vaag A, Stephan Z, Spector TD, Wu YZ, Plass C, Esteller M. Epigenetic differences arise during the lifetime of monozygotic twins. Proc Natl Acad Sci U S A. 2005 Jul 26;102(30):10604-9. Epub 2005 Jul 11.
French NS, Norton JD. Structure and functional properties of mouse VL30 retrotransposons. Biochim Biophys Acta. 1997 May 2;1352(1):33-47. Review.

Fuks F, Burgers WA, Brehm A, Hughes-Davies L, Kouzarides T. DNA methyltransferase Dnmt1 associates with histone deacetylase activity. Nat Genet. 2000 Jan;24(1):88-91.
Gaudet F, Rideout WM 3rd, Meissner A, Dausman J, Leonhardt H, Jaenisch R. Dnmt1 expression in pre- and postimplantation embryogenesis and the maintenance of IAP silencing. Mol Cell Biol. 2004 Feb;24(4):1640-8.
Ghoshal K, Datta J, Majumder S, Bai S, Kutay H, Motiwala T, Jacob ST. 5-Aza-deoxycytidine induces selective degradation of DNA methyltransferase 1 by a proteasomal pathway that requires the KEN box, bromo-adjacent homology domain, and nuclear localization signal. Mol Cell Biol. 2005 Jun;25(11):4727-41.
Giet R, Prigent C. The non-catalytic domain of the Xenopus laevis auroraA kinase localises the protein to the centrosome. J Cell Sci. 2001 Jun;114(Pt 11):2095-104.
Girard A, Hannon GJ. Conserved themes in small-RNA-mediated transposon control. Trends Cell Biol. 2008 Mar;18(3):136-48. Epub 2008 Feb 20. Review.
Gonzalgo ML, Jones PA. Rapid quantitation of methylation differences at specific sites using methylation-sensitive single nucleotide primer extension (Ms-SNuPE). Nucleic Acids Res. 1997 Jun 15;25(12):2529-31.
Goto H, Tomono Y, Ajiro K, Kosako H, Fujita M, Sakurai M, Okawa K, Iwamatsu A, Okigaki T, Takahashi T, Inagaki M. Identification of a novel phosphorylation site on histone H3 coupled with mitotic chromosome condensation. J Biol Chem. 1999 Sep 3;274(36):25543-9.
Griffith JL, Coleman LE, Raymond AS, Goodson SG, Pittard WS, Tsui C, Devine SE. Functional genomics reveals relationships between the retrovirus-like Ty1 element and its host Saccharomyces cerevisiae. Genetics. 2003 Jul;164(3):867-79.
Grunstein M. Histone acetylation in chromatin structure and transcription. Nature. 1997 Sep 25;389(6649):349-52. Review.
Hauser C, Schuettengruber B, Bartl S, Lagger G, Seiser C. Activation of the mouse histone deacetylase 1 gene by cooperative histone phosphorylation and acetylation. Mol Cell Biol. 2002 Nov;22(22):7820-30.
Hahnen E, Hauke J, Tränkle C, Eyüpoglu IY, Wirth B, Blümcke I. Histone deacetylase inhibitors: possible implications for neurodegenerative disorders. Expert Opin Investig Drugs. 2008 Feb;17(2):169-84. Review.
Haigis MC, Guarente LP. Mammalian sirtuins--emerging roles in physiology, aging, and calorie restriction. Genes Dev. 2006 Nov 1;20(21):2913-21. Review.
He G, Margolis DM. Counterregulation of chromatin deacetylation and histone deacetylase occupancy at the integrated promoter of human immunodeficiency virus type 1 (HIV-1) by the HIV-1 repressor YY1 and HIV-1 activator Tat. Mol Cell Biol. 2002 May;22(9):2965-73.
Horie K, Saito ES, Keng VW, Ikeda R, Ishihara H, Takeda J. Retrotransposons influence the mouse transcriptome: implication for the divergence of genetic traits. Genetics. 2007 Jun;176(2):815-27. Epub 2007 Apr 15.
Howard G, Eiges R, Gaudet F, Jaenisch R, Eden A. Activation and transposition of endogenous retroviral elements in hypomethylation induced tumors in mice. Oncogene. 2008 Jan 10;27(3):404-8. Epub 2007 Jul 9.
Howe L, Auston D, Grant P, John S, Cook RG, Workman JL, Pillus L. Histone H3 specific acetyltransferases are essential for cell cycle progression. Genes Dev. 2001 Dec 1;15(23):3144-54.
Huang J, Fan T, Yan Q, Zhu H, Fox S, Issaq HJ, Best L, Gangi L, Munroe D, Muegge K. Lsh, an epigenetic guardian of repetitive elements. Nucleic Acids Res. 2004 Sep 24;32(17):5019-28. Print 2004.
Inoue T, Hiratsuka M, Osaki M, Oshimura M. The molecular biology of mammalian SIRT proteins: SIRT2 in cell cycle regulation. Cell Cycle. 2007 May 2;6(9):1011-8. Epub 2007 May 30. Review.
Irwin B, Aye M, Baldi P, Beliakova-Bethell N, Cheng H, Dou Y, Liou W, Sandmeyer S. Retroviruses and yeast retrotransposons use overlapping sets of host genes. Genome Res. 2005 May;15(5):641-54. Epub 2005 Apr 18.
Ishihara H, Tanaka I, Wan H, Nojima K, Yoshida K. Retrotransposition of limited deletion type of intracisternal A-particle elements in the myeloid leukemia Clls of C3H/He mice. J Radiat Res (Tokyo). 2004 Mar;45(1):25-32.

Jackson-Grusby L, Beard C, Possemato R, Tudor M, Fambrough D, Csankovszki G, Dausman J, Lee P, Wilson C, Lander E, Jaenisch R. Loss of genomic methylation causes p53-dependent apoptosis and epigenetic deregulation. Nat Genet. 2001 Jan;27(1):31-9.
Jaenisch R, Schnieke A, Harbers K. Treatment of mice with 5-azacytidine efficiently activates silent retroviral genomes in different tissues. Proc Natl Acad Sci U S A. 1985 Mar;82(5):1451-5.
Januchowski R, Dabrowski M, Ofori H, Jagodzinski PP. Trichostatin A down-regulate DNA methyltransferase 1 in Jurkat T cells. Cancer Lett. 2007 Feb 8;246(1-2):313-7. Epub 2006 Apr 19.
Jenuwein T, Allis CD. Translating the histone code. Science. 2001 Aug 10;293(5532):1074-80. Review.
Jiang L, Smith JN, Anderson SL, Ma P, Mizzen CA, Kelleher NL. Global assessment of combinatorial post-translational modification of core histones in yeast using contemporary mass spectrometry. LYS4 trimethylation correlates with degree of acetylation on the same H3 tail. J Biol Chem. 2007 Sep 21;282(38):27923-34. Epub 2007 Jul 24.
Jurka, J., Kapitonov, V.V., Pavlicek, A., Klonowski, P., Kohany, O., Walichiewicz, J. Repbase Update, a database of eukaryotic repetitive elements. Cytogenetic and Genome Research 110:462-467
Lusic M, Marcello A, Cereseto A, Giacca M. Regulation of HIV-1 gene expression by histone acetylation and factor recruitment at the LTR promoter. EMBO J. 2003 Dec 15;22(24):6550-61.
Kalkhoven E. CBP and p300: HATs for different occasions. Biochem Pharmacol. 2004 Sep 15;68(6):1145-55. Review.
Kanellopoulou C, Muljo SA, Kung AL, Ganesan S, Drapkin R, Jenuwein T, Livingston DM, Rajewsky K. Dicer-deficient mouse embryonic stem cells are defective in differentiation and centromeric silencing. Genes Dev. 2005 Feb 15;19(4):489-501.
Kazazian HH Jr. Mobile elements and disease. Curr Opin Genet Dev. 1998 Jun;8(3):343-50. Review.
Kimura A, Matsubara K, Horikoshi M. A decade of histone acetylation: marking eukaryotic chromosomes with specific codes. J Biochem. 2005 Dec;138(6):647-62.
Khan N, Jeffers M, Kumar S, Hackett C, Boldog F, Khramtsov N, Qian X, Mills E, Berghs SC, Carey N, Finn PW, Collins LS, Tumber A, Ritchie JW, Jensen PB, Lichenstein HS, Sehested M. Determination of the class and isoform selectivity of small-molecule histone deacetylase inhibitors. Biochem J. 2008 Jan 15;409(2):581-9.
Koshland D, Strunnikov A. Mitotic chromosome condensation. Annu Rev Cell Dev Biol. 1996;12:305-33.
Knutson SK, Chyla BJ, Amann JM, Bhaskara S, Huppert SS, Hiebert SW. Liver-specific deletion of histone deacetylase 3 disrupts metabolic transcriptional networks. EMBO J. 2008 Apr 9;27(7):1017-28. Epub 2008 Mar 20.
Koch CM, Andrews RM, Flicek P, Dillon SC, Karaöz U, Clelland GK, Wilcox S, Beare DM, Fowler JC, Couttet P, James KD, Lefebvre GC, Bruce AW, Dovey OM, Ellis PD, Dhami P, Langford CF, Weng Z, Birney E, Carter NP, Vetrie D, Dunham I. The landscape of histone modifications across 1% of the human genome in five human cell lines. Genome Res. 2007 Jun;17(6):691-707.
Korber P, Luckenbach T, Blaschke D, Hörz W. Evidence for histone eviction in trans upon induction of the yeast PHO5 promoter. Mol Cell Biol. 2004 Dec;24(24):10965-74.
Kuff EL, Lueders KK. The intracisternal A-particle gene family: structure and functional aspects. Adv Cancer Res. 1988;51:183-276. Review.
Kurdistani SK, Tavazoie S, Grunstein M. Mapping global histone acetylation patterns to gene expression. Cell. 2004 Jun 11;117(6):721-33.
Lagger G, O'Carroll D, Rembold M, Khier H, Tischler J, Weitzer G, Schuettengruber B, Hauser C, Brunmeir R, Jenuwein T, Seiser C. Essential function of histone deacetylase 1 in proliferation control and CDK inhibitor repression. EMBO J. 2002 Jun 3;21(11):2672-81.
Lander ES, Linton LM, Birren B, Nusbaum C, Zody MC, Baldwin J, Devon K, Dewar K, Doyle M, FitzHugh W, Funke R, Gage D, Harris K, Heaford A, Howland J, Kann L, Lehoczky J, LeVine R, McEwan P, McKernan K, Meldrim J, Mesirov JP, Miranda C, Morris W, Naylor J,

Raymond C, Rosetti M, Santos R, Sheridan A, Sougnez C, Stange-Thomann N, Stojanovic N, Subramanian A, Wyman D, Rogers J, Sulston J, Ainscough R, Beck S, Bentley D, Burton J, Clee C, Carter N, Coulson A, Deadman R, Deloukas P, Dunham A, Dunham I, Durbin R, French L, Grafham D, Gregory S, Hubbard T, Humphray S, Hunt A, Jones M, Lloyd C, McMurray A, Matthews L, Mercer S, Milne S, Mullikin JC, Mungall A, Plumb R, Ross M, Shownkeen R, Sims S, Waterston RH, Wilson RK, Hillier LW, McPherson JD, Marra MA, Mardis ER, Fulton LA, Chinwalla AT, Pepin KH, Gish WR, Chissoe SL, Wendl MC, Delehaunty KD, Miner TL, Delehaunty A, Kramer JB, Cook LL, Fulton RS, Johnson DL, Minx PJ, Clifton SW, Hawkins T, Branscomb E, Predki P, Richardson P, Wenning S, Slezak T, Doggett N, Cheng JF, Olsen A, Lucas S, Elkin C, Uberbacher E, Frazier M, Gibbs RA, Muzny DM, Scherer SE, Bouck JB, Sodergren EJ, Worley KC, Rives CM, Gorrell JH, Metzker ML, Naylor SL, Kucherlapati RS, Nelson DL, Weinstock GM, Sakaki Y, Fujiyama A, Hattori M, Yada T, Toyoda A, Itoh T, Kawagoe C, Watanabe H, Totoki Y, Taylor T, Weissenbach J, Heilig R, Saurin W, Artiguenave F, Brottier P, Bruls T, Pelletier E, Robert C, Wincker P, Smith DR, Doucette-Stamm L, Rubenfield M, Weinstock K, Lee HM, Dubois J, Rosenthal A, Platzer M, Nyakatura G, Taudien S, Rump A, Yang H, Yu J, Wang J, Huang G, Gu J, Hood L, Rowen L, Madan A, Qin S, Davis RW, Federspiel NA, Abola AP, Proctor MJ, Myers RM, Schmutz J, Dickson M, Grimwood J, Cox DR, Olson MV, Kaul R, Raymond C, Shimizu N, Kawasaki K, Minoshima S, Evans GA, Athanasiou M, Schultz R, Roe BA, Chen F, Pan H, Ramser J, Lehrach H, Reinhardt R, McCombie WR, de la Bastide M, Dedhia N, Blöcker H, Hornischer K, Nordsiek G, Agarwala R, Aravind L, Bailey JA, Bateman A, Batzoglou S, Birney E, Bork P, Brown DG, Burge CB, Cerutti L, Chen HC, Church D, Clamp M, Copley RR, Doerks T, Eddy SR, Eichler EE, Furey TS, Galagan J, Gilbert JG, Harmon C, Hayashizaki Y, Haussler D, Hermjakob H, Hokamp K, Jang W, Johnson LS, Jones TA, Kasif S, Kaspryzk A, Kennedy S, Kent WJ, Kitts P, Koonin EV, Korf I, Kulp D, Lancet D, Lowe TM, McLysaght A, Mikkelsen T, Moran JV, Mulder N, Pollara VJ, Ponting CP, Schuler G, Schultz J, Slater G, Smit AF, Stupka E, Szustakowski J, Thierry-Mieg D, Thierry-Mieg J, Wagner L, Wallis J, Wheeler R, Williams A, Wolf YI, Wolfe KH, Yang SP, Yeh RF, Collins F, Guyer MS, Peterson J, Felsenfeld A, Wetterstrand KA, Patrinos A, Morgan MJ, de Jong P, Catanese JJ, Osoegawa K, Shizuya H, Choi S, Chen YJ; International Human Genome Sequencing Consortium.** Initial sequencing and analysis of the human genome. Nature. 2001 Feb 15;409(6822):860-921

Lee KK, Workman JL. Histone acetyltransferase complexes: one size doesn't fit all. Nat Rev Mol Cell Biol. 2007 Apr;8(4):284-95. Review.

Lee MG, Wynder C, Cooch N, Shiekhattar R. An essential role for CoREST in nucleosomal histone 3 lysine 4 demethylation. Nature. 2005 Sep 15;437(7057):432-5. Epub 2005 Aug 3.

Lee MG, Wynder C, Bochar DA, Hakimi MA, Cooch N, Shiekhattar R. Functional interplay between histone demethylase and deacetylase enzymes. Mol Cell Biol. 2006 Sep;26(17):6395-402.

Lehrman G, Hogue IB, Palmer S, Jennings C, Spina CA, Wiegand A, Landay AL, Coombs RW, Richman DD, Mellors JW, Coffin JM, Bosch RJ, Margolis DM. Depletion of latent HIV-1 infection in vivo: a proof-of-concept study. Lancet. 2005 Aug 13-19;366(9485):549-55.

Li E, Bestor TH, Jaenisch R. Targeted mutation of the DNA methyltransferase gene results in embryonic lethality. Cell. 1992 Jun 12;69(6):915-26.

Liang G, Chan MF, Tomigahara Y, Tsai YC, Gonzales FA, Li E, Laird PW, Jones PA. Cooperativity between DNA methyltransferases in the maintenance methylation of repetitive elements. Mol Cell Biol. 2002 Jan;22(2):480-91.

Liu CL, Kaplan T, Kim M, Buratowski S, Schreiber SL, Friedman N, Rando OJ. Single-nucleosome mapping of histone modifications in S. cerevisiae. PLoS Biol. 2005 Oct;3(10):e328. Epub 2005 Aug 30.

Liu WM, Chu WM, Choudary PV, Schmid CW. Cell stress and translational inhibitors transiently increase the abundance of mammalian SINE transcripts. Nucleic Acids Res. 1995 May 25;23(10):1758-65.

Lorch Y, Zhang M, Kornberg RD. Histone octamer transfer by a chromatin-remodeling complex. Cell. 1999 Feb 5;96(3):389-92.

Luger K, Mäder AW, Richmond RK, Sargent DF, Richmond TJ. Crystal structure of the nucleosome core particle at 2.8 A resolution. Nature. 1997 Sep 18;389(6648):251-60.
Macdonald N, Welburn JP, Noble ME, Nguyen A, Yaffe MB, Clynes D, Moggs JG, Orphanides G, Thomson S, Edmunds JW, Clayton AL, Endicott JA, Mahadevan LC. Molecular basis for the recognition of phosphorylated and phosphoacetylated histone h3 by 14-3-3. Mol Cell. 2005 Oct 28;20(2):199-211.
Mahadevan LC, Willis AC, Barratt MJ. Rapid histone H3 phosphorylation in response to growth factors, phorbol esters, okadaic acid, and protein synthesis inhibitors. Cell. 1991 May 31;65(5):775-83.
Mangeat B, Turelli P, Caron G, Friedli M, Perrin L, Trono D. Broad antiretroviral defence by human APOBEC3G through lethal editing of nascent reverse transcripts. Nature. 2003 Jul 3;424(6944):99-103. Epub 2003 May 28.
Maksakova IA, Romanish MT, Gagnier L, Dunn CA, van de Lagemaat LN, Mager DL. Retroviral elements and their hosts: insertional mutagenesis in the mouse germ line. PLoS Genet. 2006 Jan;2(1):e2.
Marks PA, Jiang X. Histone deacetylase inhibitors in programmed cell death and cancer therapy. Cell Cycle. 2005 Apr;4(4):549-51. Epub 2005 Apr 28. Review.
Martens JH, O'Sullivan RJ, Braunschweig U, Opravil S, Radolf M, Steinlein P, Jenuwein T. The profile of repeat-associated histone lysine methylation states in the mouse epigenome. EMBO J. 2005 Feb 23;24(4):800-12. Epub 2005 Jan 27.
Mietz JA, Grossman Z, Lueders KK, Kuff EL. Nucleotide sequence of a complete mouse intracisternal A-particle genome: relationship to known aspects of particle assembly and function. J Virol. 1987 Oct;61(10):3020-9.
Milutinovic S, D'Alessio AC, Detich N, Szyf M. Valproate induces widespread epigenetic reprogramming which involves demethylation of specific genes. Carcinogenesis. 2007 Mar;28(3):560-71. Epub 2006 Sep 28.
Miller WJ, McDonald JF, Nouaud D, Anxolabéhère D. Molecular domestication--more than a sporadic episode in evolution. Genetica. 1999;107(1-3):197-207.
Montgomery RL, Davis CA, Potthoff MJ, Haberland M, Fielitz J, Qi X, Hill JA, Richardson JA, Olson EN. Histone deacetylases 1 and 2 redundantly regulate cardiac morphogenesis, growth, and contractility. Genes Dev. 2007 Jul 15;21(14):1790-802.
Muotri AR, Chu VT, Marchetto MC, Deng W, Moran JV, Gage FH. Somatic mosaicism in neuronal precursor cells mediated by L1 retrotransposition. Nature. 2005 Jun 16;435(7044):903-10.
Narlikar GJ, Fan HY, Kingston RE. Cooperation between complexes that regulate chromatin structure and transcription. Cell. 2002 Feb 22;108(4):475-87. Review.
Nilsson M, Bohm S. Inducible and cell type-specific expression of VL30 U3 subgroups correlate with their enhancer design. J Virol. 1994 Jan;68(1):276-88.
Noutsopoulos D, Markopoulos G, Koliou M, Dova L, Vartholomatos G, Kolettas E, Tzavaras T. Vanadium induces VL30 retrotransposition at an unusually high level: a possible carcinogenesis mechanism. J Mol Biol. 2007 Nov 16;374(1):80-90. Epub 2007 Sep 11.
Nyswaner KM, Checkley MA, Yi M, Stephens RM, Garfinkel DJ. Chromatin-associated genes protect the yeast genome from Ty1 insertional mutagenesis. Genetics. 2008 Jan;178(1):197-214.
Okano M, Bell DW, Haber DA, Li E. DNA methyltransferases Dnmt3a and Dnmt3b are essential for de novo methylation and mammalian development. Cell. 1999 Oct 29;99(3):247-57.
Ou JN, Torrisani J, Unterberger A, Provençal N, Shikimi K, Karimi M, Ekström TJ, Szyf M. Histone deacetylase inhibitor Trichostatin A induces global and gene-specific DNA demethylation in human cancer cell lines. Biochem Pharmacol. 2007 May 1;73(9):1297-307. Epub 2007 Jan 5.
Pannell D, Osborne CS, Yao S, Sukonnik T, Pasceri P, Karaiskakis A, Okano M, Li E, Lipshitz HD, Ellis J. Retrovirus vector silencing is de novo methylase independent and marked by a repressive histone code. EMBO J. 2000 Nov 1;19(21):5884-94.

Panning B, Smiley JR. Activation of RNA polymerase III transcription of human Alu repetitive elements by adenovirus type 5: requirement for the E1b 58-kilodalton protein and the products of E4 open reading frames 3 and 6. Mol Cell Biol. 1993 Jun;13(6):3231-44.
Peaston AE, Evsikov AV, Graber JH, de Vries WN, Holbrook AE, Solter D, Knowles BB. Retrotransposons regulate host genes in mouse oocytes and preimplantation embryos. Dev Cell. 2004 Oct;7(4):597-606.
Peters AH, O'Carroll D, Scherthan H, Mechtler K, Sauer S, Schöfer C, Weipoltshammer K, Pagani M, Lachner M, Kohlmaier A, Opravil S, Doyle M, Sibilia M, Jenuwein T. Loss of the Suv39h histone methyltransferases impairs mammalian heterochromatin and genome stability. Cell. 2001 Nov 2;107(3):323-37.
Prak ET, Kazazian HH Jr. Mobile elements and the human genome. Nat Rev Genet. 2000 Nov;1(2):134-44. Review.
Puschendorf M, Stein P, Oakeley EJ, Schultz RM, Peters AH, Svoboda P. Abundant transcripts from retrotransposons are unstable in fully grown mouse oocytes. Biochem Biophys Res Commun. 2006 Aug 18;347(1):36-43. Epub 2006 Jun 27.
Ramakrishnan V. Histone H1 and chromatin higher-order structure. Crit Rev Eukaryot Gene Expr. 1997;7(3):215-30. Review.
Rauch TA, Zhong X, Wu X, Wang M, Kernstine KH, Wang Z, Riggs AD, Pfeifer GP. High-resolution mapping of DNA hypermethylation and hypomethylation in lung cancer. Proc Natl Acad Sci U S A. 2008 Jan 8;105(1):252-7. Epub 2007 Dec 27.
Ribet D, Harper F, Dupressoir A, Dewannieux M, Pierron G, Heidmann T. An infectious progenitor for the murine IAP retrotransposon: emergence of an intracellular genetic parasite from an ancient retrovirus. Genome Res. 2008 Apr;18(4):597-609. Epub 2008 Feb 6.
Ringrose L, Paro R. Epigenetic regulation of cellular memory by the Polycomb and Trithorax group proteins. Annu Rev Genet. 2004;38:413-43. Review.
Rougeulle C, Chaumeil J, Sarma K, Allis CD, Reinberg D, Avner P, Heard E. Differential histone H3 Lys-9 and Lys-27 methylation profiles on the X chromosome. Mol Cell Biol. 2004 Jun;24(12):5475-84.
Sadri-Vakili G, Cha JH. Histone deacetylase inhibitors: a novel therapeutic approach to Huntington's disease (complex mechanism of neuronal death). Curr Alzheimer Res. 2006 Sep;3(4):403-8. Review.
Saito ES, Keng VW, Takeda J, Horie K. Translation from nonautonomous type IAP retrotransposon is a critical determinant of transposition activity: implication for retrotransposon-mediated genome evolution. Genome Res. 2008 Jun;18(6):859-68. Epub 2008 May 2.
Sarg B, Helliger W, Talasz H, Koutzamani E, Lindner HH. Histone H4 hyperacetylation precludes histone H4 lysine 20 trimethylation. J Biol Chem. 2004 Dec 17;279(51):53458-64. Epub 2004 Sep 28.
Scholes DT, Banerjee M, Bowen B, Curcio MJ. Multiple regulators of Ty1 transposition in Saccharomyces cerevisiae have conserved roles in genome maintenance. Genetics. 2001 Dec;159(4):1449-65.
Schotta G, Lachner M, Sarma K, Ebert A, Sengupta R, Reuter G, Reinberg D, Jenuwein T. A silencing pathway to induce H3-K9 and H4-K20 trimethylation at constitutive heterochromatin. Genes Dev. 2004 Jun 1;18(11):1251-62. Epub 2004 May 14.
Seifarth W, Frank O, Zeilfelder U, Spiess B, Greenwood AD, Hehlmann R, Leib-Mösch C. Comprehensive analysis of human endogenous retrovirus transcriptional activity in human tissues with a retrovirus-specific microarray. J Virol. 2005 Jan;79(1):341-52.
Senese S, Zaragoza K, Minardi S, Muradore I, Ronzoni S, Passafaro A, Bernard L, Draetta GF, Alcalay M, Seiser C, Chiocca S. Role for histone deacetylase 1 in human tumor cell proliferation. Mol Cell Biol. 2007 Jul;27(13):4784-95. Epub 2007 Apr 30.
Sharif J, Muto M, Takebayashi S, Suetake I, Iwamatsu A, Endo TA, Shinga J, Mizutani-Koseki Y, Toyoda T, Okamura K, Tajima S, Mitsuya K, Okano M, Koseki H. The SRA protein Np95 mediates epigenetic inheritance by recruiting Dnmt1 to methylated DNA. Nature. 2007 Dec 6;450(7171):908-12. Epub 2007 Nov 11.

Sharma RP, Rosen C, Kartan S, Guidotti A, Costa E, Grayson DR, Chase K. Valproic acid and chromatin remodeling in schizophrenia and bipolar disorder: preliminary results from a clinical population. Schizophr Res. 2006 Dec;88(1-3):227-31. Epub 2006 Sep 25.
Shi Y, Lan F, Matson C, Mulligan P, Whetstine JR, Cole PA, Casero RA, Shi Y. Histone demethylation mediated by the nuclear amine oxidase homolog LSD1. Cell. 2004 Dec 29;119(7):941-53.
Smit AF. Identification of a new, abundant superfamily of mammalian LTR-transposons. Nucleic Acids Res. 1993 Apr 25;21(8):1863-72.
Smit AF. Interspersed repeats and other mementos of transposable elements in mammalian genomes. Curr Opin Genet Dev. 1999 Dec;9(6):657-63. Review.
Sobel RE, Cook RG, Perry CA, Annunziato AT, Allis CD. Conservation of deposition-related acetylation sites in newly synthesized histones H3 and H4. Proc Natl Acad Sci U S A. 1995 Feb 14;92(4):1237-41.
Soloaga A, Thomson S, Wiggin GR, Rampersaud N, Dyson MH, Hazzalin CA, Mahadevan LC, Arthur JS. MSK2 and MSK1 mediate the mitogen- and stress-induced phosphorylation of histone H3 and HMG-14. EMBO J. 2003 Jun 2;22(11):2788-97.
Song X, Wang B, Bromberg M, Hu Z, Konigsberg W, Garen A. Retroviral-mediated transmission of a mouse VL30 RNA to human melanoma cells promotes metastasis in an immunodeficient mouse model. Proc Natl Acad Sci U S A. 2002 Apr 30;99(9):6269-73. Epub 2002 Apr 16.
Song X, Sui A, Garen A. Binding of mouse VL30 retrotransposon RNA to PSF protein induces genes repressed by PSF: effects on steroidogenesis and oncogenesis. Proc Natl Acad Sci U S A. 2004 Jan 13;101(2):621-6. Epub 2004 Jan 2.
Song X, Sun Y, Garen A. Roles of PSF protein and VL30 RNA in reversible gene regulation. Proc Natl Acad Sci U S A. 2005 Aug 23;102(34):12189-93. Epub 2005 Aug 3.
Strahl BD, Allis CD. The language of covalent histone modifications. Nature. 2000 Jan 6;403(6765):41-5.
Stribinskis V, Ramos KS. Activation of human long interspersed nuclear element 1 retrotransposition by benzo(a)pyrene, an ubiquitous environmental carcinogen. Cancer Res. 2006 Mar 1;66(5):2616-20.
Suka N, Luo K, Grunstein M. Sir2p and Sas2p opposingly regulate acetylation of yeast histone H4 lysine16 and spreading of heterochromatin. Nat Genet. 2002 Nov;32(3):378-83. Epub 2002 Oct 15.
Takabatake T, Ishihara H, Ohmachi Y, Tanaka I, Nakamura MM, Fujikawa K, Hirouchi T, Kakinuma S, Shimada Y, Oghiso Y, Tanaka K. Microarray-based global mapping of integration sites for the retrotransposon, intracisternal A-particle, in the mouse genome. Nucleic Acids Res. 2008 Jun;36(10):e59. Epub 2008 May 1.
Taunton J, Hassig CA, Schreiber SL. A mammalian histone deacetylase related to the yeast transcriptional regulator Rpd3p. Science. 1996 Apr 19;272(5260):408-11.
Thomson S, Clayton AL, Hazzalin CA, Rose S, Barratt MJ, Mahadevan LC. The nucleosomal response associated with immediate-early gene induction is mediated via alternative MAP kinase cascades: MSK1 as a potential histone H3/HMG-14 kinase. EMBO J. 1999 Sep 1;18(17):4779-93.
Thorne AW, Kmiciek D, Mitchelson K, Sautiere P, Crane-Robinson C. Patterns of histone acetylation. Eur J Biochem. 1990 Nov 13;193(3):701-13.
Trewick SC, McLaughlin PJ, Allshire RC. Methylation: lost in hydroxylation? EMBO Rep. 2005 Apr;6(4):315-20.
Turner BM. Decoding the nucleosome. Cell. 1993 Oct 8;75(1):5-8. Review.
Turner BM. Histone acetylation and an epigenetic code. Bioessays. 2000 Sep;22(9):836-45. Review.
Tzavaras T, Eftaxia S, Tavoulari S, Hatzi P, Angelidis C. Factors influencing the expression of endogenous reverse transcriptases and viral-like 30 elements in mouse NIH3T3 cells. Int J Oncol. 2003 Oct;23(4):1237-43.
van der Vlag J, Otte AP. Transcriptional repression mediated by the human polycomb-group protein EED involves histone deacetylation. Nat Genet. 1999 Dec;23(4):474-8.

Walsh CP, Chaillet JR, Bestor TH. Transcription of IAP endogenous retroviruses is constrained by cytosine methylation. Nat Genet. 1998 Oct;20(2):116-7.
Walter W, Clynes D, Tang Y, Marmorstein R, Mellor J, Berger SL. 14-3-3 interaction with histone H3 involves a dual modification pattern of phosphoacetylation. Mol Cell Biol. 2008 Apr;28(8):2840-9. Epub 2008 Feb 11.
Waterston RH, Lindblad-Toh K, Birney E, Rogers J, Abril JF, Agarwal P, Agarwala R, Ainscough R, Alexandersson M, An P, Antonarakis SE, Attwood J, Baertsch R, Bailey J, Barlow K, Beck S, Berry E, Birren B, Bloom T, Bork P, Botcherby M, Bray N, Brent MR, Brown DG, Brown SD, Bult C, Burton J, Butler J, Campbell RD, Carninci P, Cawley S, Chiaromonte F, Chinwalla AT, Church DM, Clamp M, Clee C, Collins FS, Cook LL, Copley RR, Coulson A, Couronne O, Cuff J, Curwen V, Cutts T, Daly M, David R, Davies J, Delehaunty KD, Deri J, Dermitzakis ET, Dewey C, Dickens NJ, Diekhans M, Dodge S, Dubchak I, Dunn DM, Eddy SR, Elnitski L, Emes RD, Eswara P, Eyras E, Felsenfeld A, Fewell GA, Flicek P, Foley K, Frankel WN, Fulton LA, Fulton RS, Furey TS, Gage D, Gibbs RA, Glusman G, Gnerre S, Goldman N, Goodstadt L, Grafham D, Graves TA, Green ED, Gregory S, Guigó R, Guyer M, Hardison RC, Haussler D, Hayashizaki Y, Hillier LW, Hinrichs A, Hlavina W, Holzer T, Hsu F, Hua A, Hubbard T, Hunt A, Jackson I, Jaffe DB, Johnson LS, Jones M, Jones TA, Joy A, Kamal M, Karlsson EK, Karolchik D, Kasprzyk A, Kawai J, Keibler E, Kells C, Kent WJ, Kirby A, Kolbe DL, Korf I, Kucherlapati RS, Kulbokas EJ, Kulp D, Landers T, Leger JP, Leonard S, Letunic I, Levine R, Li J, Li M, Lloyd C, Lucas S, Ma B, Maglott DR, Mardis ER, Matthews L, Mauceli E, Mayer JH, McCarthy M, McCombie WR, McLaren S, McLay K, McPherson JD, Meldrim J, Meredith B, Mesirov JP, Miller W, Miner TL, Mongin E, Montgomery KT, Morgan M, Mott R, Mullikin JC, Muzny DM, Nash WE, Nelson JO, Nhan MN, Nicol R, Ning Z, Nusbaum C, O'Connor MJ, Okazaki Y, Oliver K, Overton-Larty E, Pachter L, Parra G, Pepin KH, Peterson J, Pevzner P, Plumb R, Pohl CS, Poliakov A, Ponce TC, Ponting CP, Potter S, Quail M, Reymond A, Roe BA, Roskin KM, Rubin EM, Rust AG, Santos R, Sapojnikov V, Schultz B, Schultz J, Schwartz MS, Schwartz S, Scott C, Seaman S, Searle S, Sharpe T, Sheridan A, Shownkeen R, Sims S, Singer JB, Slater G, Smit A, Smith DR, Spencer B, Stabenau A, Stange-Thomann N, Sugnet C, Suyama M, Tesler G, Thompson J, Torrents D, Trevaskis E, Tromp J, Ucla C, Ureta-Vidal A, Vinson JP, Von Niederhausern AC, Wade CM, Wall M, Weber RJ, Weiss RB, Wendl MC, West AP, Wetterstrand K, Wheeler R, Whelan S, Wierzbowski J, Willey D, Williams S, Wilson RK, Winter E, Worley KC, Wyman D, Yang S, Yang SP, Zdobnov EM, Zody MC, Lander ES.; Mouse Genome Sequencing Consortium. Initial sequencing and comparative analysis of the mouse genome. Nature. 2002 Dec 5;420(6915):520-62.
Wilson AS, Power BE, Molloy PL. DNA hypomethylation and human diseases. Biochim Biophys Acta. 2007 Jan;1775(1):138-62. Epub 2006 Sep 1. Review.
Winter S, Simboeck E, Seiser C. Open Chromatin (Review). Genes, Genomes and Genomics. 2007; 209-225
Winter S, Simboeck E, Fischle W, Zupkovitz G, Dohnal I, Mechtler K, Ammerer G, Seiser C. 14-3-3 proteins recognize a histone code at histone H3 and are required for transcriptional activation. EMBO J. 2008 Jan 9;27(1):88-99. Epub 2007 Dec 6.
Xing J, Witherspoon DJ, Ray DA, Batzer MA, Jorde LB. Mobile DNA elements in primate and human evolution. Am J Phys Anthropol. 2007;Suppl 45:2-19. Review.
Yamamoto Y, Verma UN, Prajapati S, Kwak YT, Gaynor RB. Histone H3 phosphorylation by IKK-alpha is critical for cytokine-induced gene expression. Nature. 2003 Jun 5;423(6940):655-9.
Yang XJ, Seto E. HATs and HDACs: from structure, function and regulation to novel strategies for therapy and prevention. Oncogene. 2007 Aug 13;26(37):5310-8. Review.
Yang XJ, Seto E. The Rpd3/Hda1 family of lysine deacetylases: from bacteria and yeast to mice and men. Nat Rev Mol Cell Biol. 2008 Mar;9(3):206-18. Review.
Ymer S, Tucker WQ, Sanderson CJ, Hapel AJ, Campbell HD, Young IG. Constitutive synthesis of interleukin-3 by leukaemia cell line WEHI-3B is due to retroviral insertion near the gene. Nature. 1985 Sep 19-25;317(6034):255-8.
Yoder JA, Walsh CP, Bestor TH. Cytosine methylation and the ecology of intragenomic parasites. Trends Genet. 1997 Aug;13(8):335-40. Review.

You JS, Kang JK, Lee EK, Lee JC, Lee SH, Jeon YJ, Koh DH, Ahn SH, Seo DW, Lee HY, Cho EJ, Han JW. Histone deacetylase inhibitor apicidin downregulates DNA methyltransferase 1 expression and induces repressive histone modifications via recruitment of corepressor complex to promoter region in human cervix cancer cells. Oncogene. 2008 Feb 28;27(10):1376-86. Epub 2007 Sep 10.
Yu F, Zingler N, Schumann G, Strätling WH. Methyl-CpG-binding protein 2 represses LINE-1 expression and retrotransposition but not Alu transcription. Nucleic Acids Res. 2001 Nov 1;29(21):4493-501.
Zhang W, Bone JR, Edmondson DG, Turner BM, Roth SY. Essential and redundant functions of histone acetylation revealed by mutation of target lysines and loss of the Gcn5p acetyltransferase. EMBO J. 1998 Jun 1;17(11):3155-67.
Zupkovitz G, Tischler J, Posch M, Sadzak I, Ramsauer K, Egger G, Grausenburger R, Schweifer N, Chiocca S, Decker T, Seiser C. Negative and positive regulation of gene expression by mouse histone deacetylase 1. Mol Cell Biol. 2006 Nov;26(21):7913-28. Epub 2006 Aug 28.

CURRICULUM VITAE

Name:	Reinhard Brunmeir
Date of Birth:	18.05.1977
Place of Birth:	Wels, Austria
Nationality:	Austrian

Education:

2004 – 2007	PhD thesis at the Max F. Perutz Laboratories, Department of Medical Biochemistry, Medical University of Vienna, Vienna Biocenter, Austria. Supervisor: Prof. Dr. Christian Seiser (Prof. Dr. Manuela Baccarini)
2002	Diploma thesis at the Max F. Perutz Laboratories, Department of Medical Biochemistry, Medical University of Vienna, Vienna Biocenter, Austria. Supervisor: Prof. Dr. Christian Seiser
1996 – 2003	Studies of Genetics, University of Vienna
1995 – 1996	Military Service
1987 – 1995	Stiftsgymnasium Wilhering
1983 – 1987	Primary School Stroheim

Scholarship:

2004 – 2005	Schering Stiftung scholarship for PhD students

Publications:

Lagger G, O'Carroll D, Rembold M, Khier H, Tischler J, Weitzer G, Schuettengruber B, Hauser C, Brunmeir R, Jenuwein T, Seiser C.
Essential function of histone deacetylase 1 in proliferation control and CDK inhibitor repression.
EMBO J. 2002 Jun 3;21(11):2672-81.

Brunmeir R*, Lagger S*, Seiser C.
HDAC1/HDAC2-controlled embryonic development and cell differentiation.
Int. J. Developmental Biology. 2008. In Press. Review.
*equal contribution